LINEAR ANALYSIS FOR STABILITY THRESHOLD FOR A FINITE FLEXIBLY SUPPORTED JOURNAL BEARINGS LUBRICATED WITH MICROPOLAR FLUIDS

A

Thesis

Submitted in partial fulfillment of the requirement for the award of degree

MASTER OF ENGINEERING
IN
CAD/CAM & ROBOTICS

Submitted By

Mahesh Kumar

Roll No. 800881012

Under the Guidance of

Dr. A.K.CHATTOPADHYAY
Professor & HOD
Mechanical Engg. Deppt.
Mody Institute of Technology and Science ,
Lakshmangarh, Rajasthan.

Mr. R.K. DUVEDI
Assistant Professor
Mechanical Engg. Deppt
Thapar University ,
Patiala

DEPARTMENT OF MECHANICAL ENGINEERING
THAPAR UNIVERSITY
PATIALA-147004, INDIA

CERTIFICATE

This is to certify that the work which is being presented in this thesis report entitled "Linear Analysis for Stability Threshold for a Finite Flexibly Supported Journal Bearings Lubricated with Micropolar Fluids" in partial fulfilment of requirement for the award of the Master Degree in CAD/CAM and Robotics, submitted in the Mechanical Engineering Department, Thapar University, Patiala, is an authentic record of the initial work carried out by under the guidance of **Dr. A.K.CHATTOPADHYAY**, Professor & Head of Department, Mechanical Engineering Department, Mody Institute of Technology and Science, Lakshmangarh, Rajasthan and **Mr. R.K. DUVEDI ,** Assistant Professor Mechanical Engg. Deppt Thapar University, Patiala

The matter embodied in this report has not been submitted in part or full to any other university or institute for the award of any degree.

DATED: 6/oct/2010

MAHESH KUMAR

This is to certify that above declaration made by the student concerned is correct to the best of our knowledge & belief.

Dr. A.K.CHATTOPADHYAY
Professor & HOD
Mechanical Engg. Deppt.
Mody Institute of Technology and Science ,
Lakshmangarh, Rajasthan.

Mr. R.K. DUVEDI
Assistant Professor
Mechanical Engg. Deppt
Thapar University ,
Patiala

Countersigned by

Dr. S.K. MOHAPATRA
Head MED, and Dean Academic Affairs
Thapar University, Patiala

ACKNOWLEDEGEMENT

'Acknowledgement'-although a light surrounding term contains the deepest sense of gratitude, that not only services within the boundary line of a few calculations oriented papers, but also it denotes an extensive range of emotional aspects in the mind of person concerned. Especially, who is grateful for a praiseworthy remuneration, of course, remuneration does not exist on the logic of financial benefit, but it brings forth only personal satisfaction. It sincerest implication goes into the farthest core of my heart, being fully aware of the fact, that this thesis would never attain successful completion, but for the kind and direct guidance of **Dr. A.K.CHATTOPADHYAY,** which is exclusively fathomless indeed, existing vividly in the procedure as well as the relevant steps formulated by the author.

I am highly grateful to the authorities of Thapar University, Patiala for providing this opportunity to carry out the research work.

I am especially thankful to **Mr. R.K. DUVEDI,** Assistant Professor, Mechanical Engineering Department for his invaluable guidance.

I am also thankful to other faculty members of Mechanical Engineering Department, TU, Patiala for their intellectual support. My special thanks are due to my family members and friends who constantly encouraged me to complete this research.

MAHESH KUMAR

ABSTRACT

The aim of the present thesis is to investigate and predict theoretically the static and dynamic characteristics including the stability of hydrodynamic journal bearing lubricated with micropolar flied. The static characteristics examined for finite flexibly supported journal bearing are load carrying capacity and steady state attitude angle, and dynamic characteristics evaluated are non-dimensional stiffness and damping coefficients, critical mass parameter, whirl ratio and Geometric parameter considered for FDM analysis of flexibly supported finite journal bearing are l_m, L/D, and mass ratio.

The theoretical prediction of hydrodynamic pressure in the bearing is obtained by the solution of modified Reynolds equation satisfying the appropriate boundary conditions. The steady state pressure profile has been obtained by FDM. For dynamic pressure, using liberalized analysis, first order perturbation of eccentricity ratio and attitude angle are used, and the resulting equations are solved by finite difference method with successive over relaxation scheme.

LIST OF FIGURES

NOTATIONS

C	Radial clearance (m)
C_B	Body couple per unit mass of micropolar fluid (m^2/s^2)
D	Journal diameter (m)
D_{ij}	Damping co-efficients of micropolar fliud film, for i=R,φ and j=R,φ (Ns/m)
$\overline{D}_{ij}$	Dimensionless damping co-efficient of micropolar fluid film
F_B	Body force per unit mass of micropolar fluid (m/s^2)
F_i	Force component along the R and φ direction
h	Local film thickness (m)
$\overline{h}$	Non-dimensional film thickness =h/C
l_m	Non-dimensional characteristic length of the micropolar fluid=Λ/C
M	Mass parameter (kg)
$\overline{M}$	Non-dimensional parameter =$MC\omega^2/W_0$
$\overline{M}_C$	Critical value of non-dimensional parameter
N	Coupling number= $[\chi/(2\mu+\chi)]^{1/2}$
P	Micropolar film pressure in the film region in the non-linear analysis (Pa)
$\overline{p}$	Non-dimensional micropolar film pressure in the film region in the non-linear analysis.
p_i	Local micropolar film pressure in the film region , i=0,1 and 2 for the steady State & first order perturbed film pressure along the ε_0 and φ directions (Pa)
$\overline{p}_i$	Non-dimensional local micropolar film pressure in the film region , i=0,1 and 2 for the steady state and first Order perturbed film pressure along the ε_0 and φ directions (Pa)
S_{ij}	Stiffness of the micropolar fluid film for i=R,φ and j=R, φ (N/m)
$\overline{S}_{ij}$	Dimensionless damping co-efficient of the micropolar fluid film = $2C^3S_{ij}/(\mu\omega R^3L)$ For i=R , φ and j=R , φ
t	Time (s)

U	Velocity of journal=ωR (m/s)
v	Microrotational velocity vector
V	Velocity vector (m/s)
W_0	Steady state load in the bearing (N)
$\overline{W_0}$	Non-dimensional steady state load in the bearing = $2C^2W_0/(\mu\omega R^3 L)$
x	Cartesian coordinate axis along the circumferential direction= $R\theta$ (m)
z	Cartesian coordinate axis along the bearing axis (m)
$\bar{z}$	Non-dimensional Cartesian coordinate axis along the bearing axis = $2z/L$
α, β, γ	Viscosity co-efficient of the micropolar fluid (kg m/s)
ε_i	Perturbed eccentricity for i=R and φ
ε_0	Steady state eccentricity ratio
θ	Circumferential coordinate (rad)
λ_R	Whirl ratio
Λ	Characteristic length of the micropolar fluid= $[\gamma/(4\mu)]^{1/2}$ (m)
μ, λ	Newtonian viscocity co-efficient (Pa s)
μ_V	Effective viscosity coefficient of the micropolar fluid = $(2\mu+\chi)/2$ (Pa s)
π^*	Thermodynamic pressure
ρ	Mass density (kg/m^3)
τ	Non-dimensional time = ωt
Φ	Attitude angle (rad)
Φ_0	Steady state attitude angle (rad)
χ	Spin viscosity coefficients of the micropolar fluid (Pa s)
ω	Angular velocity of the journal (rad/s)
ω_p	Angular velocity of the orbital motion of the journal centre (rad/s)

ABBREVIATION USED

SRR — Stiffness in r-direction due to disturbance in r-direction — S_{rr}

SPP — Stiffness in φ-direction due to disturbance in φ-direction — $S_{\varphi\varphi}$

SRP — Stiffness in r direction due to disturbance in φ -direction — $S_{r\varphi}$

SPR — Stiffness in φ -direction due to disturbance in r-direction — $S_{\varphi r}$

DRR — Damping co-efficient in r-direction due to disturbance in r-direction — D_{rr}

DPP — Damping co-efficient in φ-direction due to disturbance in φ-direction — $D_{\varphi\varphi}$

DRP — Damping co-efficient in r-direction due to disturbance in φ -direction — $D_{r\varphi}$

DPR — Damping co-efficient in φ -direction due to disturbance in r-direction — $D_{\varphi r}$

INDEX

CHAPTER 1 INTRODUCTION

1.1 Introduction

The use of bearings is in vogue for centuries, but the recent developments in science and technology demands critical designs of bearings with high precision and optimum performance even in the most adverse working conditions.

The rapid developments in the fields of rocketry and missile technology, cryogenics, aeronautics and space engineering, nuclear engineering, electronics, computer sciences and technologies, bio-medical engineering and a lot more fields in science and technology make the aspects of designing bearings more and more challenging and innovative. Moreover, the mode, time and place of operations demand exploration of new materials, lubricants and even lubrication theories and technologies.

1.2 Classification of Bearing

Bearing are basically of two types

1. Rolling contact bearings and
2. Sliding contact bearings.

As the name suggests the rolling contact bearings use rolling elements at the points of contact of the surfaces in relative motion and thus reduce the friction. They consist of different ball bearings and roller bearings.

The sliding friction bearings are based upon two concepts of lubrication:

(a) Sliding friction thin film lubrication or boundary film lubrication and

(b) Sliding friction thick film lubrication.

The sliding friction thick film lubrication is further categorized into two different groups, namely, Self-acting or hydrodynamic lubrication, and externally pressurized or hydrostatic lubrication.

1.3 Principle of Hydrodynamic Lubrication

1. In hydrodynamic lubrication, the load supporting high pressure fluid film is created due to the shape and relative motion between the two surfaces.

2. The moving surface pulls the lubricant into a wedge-shaped zone, at a velocity sufficiently high to create the high pressure film necessary to separate the two surfaces against the load.

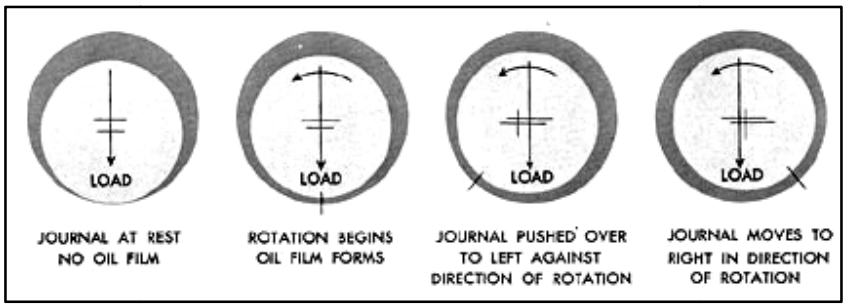

Figure: 1.1 Principle of Hydrodynamic Lubrication

1.4 Mechanisms of Load Supporting Pressure

The load supporting pressure is developed due to the following mechanisms:

1. Formation of a convergent wedge-shaped film due to the dragging of fluid into such a clearance space owing to the shape and mode of operation of the bearing. These types of bearings are particularly known as wedge film bearings.

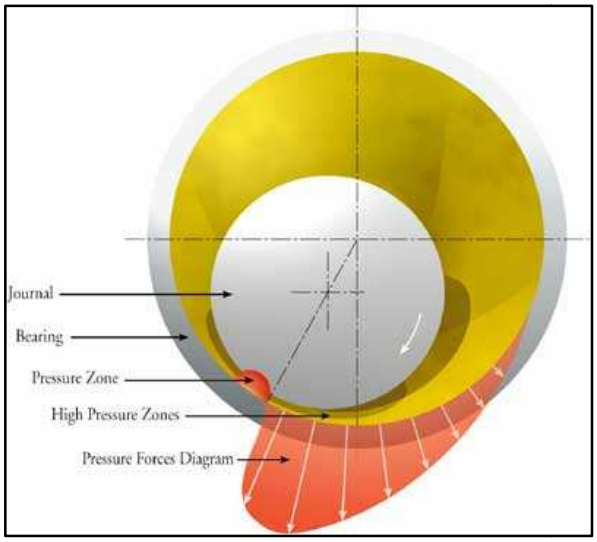

Figure 1.2: Variation of Pressure in the Converging Film

2. The resistance of the viscous fluid being squeezed out from the space between two surfaces relatively approaching or oscillating with relative normal motion. The bearings operating under this principle are known as squeeze film bearings.

Hydrodynamic bearings are generally used:

1. When the relative velocities are high enough.
2. Speeds of the rotating machinery or
3. Due to use of fluids having kinematic viscosity, the oil film close in the bearings frequently become turbulent.

As the magnitude of hydrodynamic pressure depends upon the relative tangential or normal velocity, sometimes the developed pressure may not be sufficient for obtaining the desired load carrying capacity, particularly at the low relative velocity and thereby demands external supply of pressurized lubricants. This type of lubrication is called externally pressurized or hydrostatic lubrication. These bearings are also known as hybrid bearings as their operational principle includes both self-acting and external pressurization.

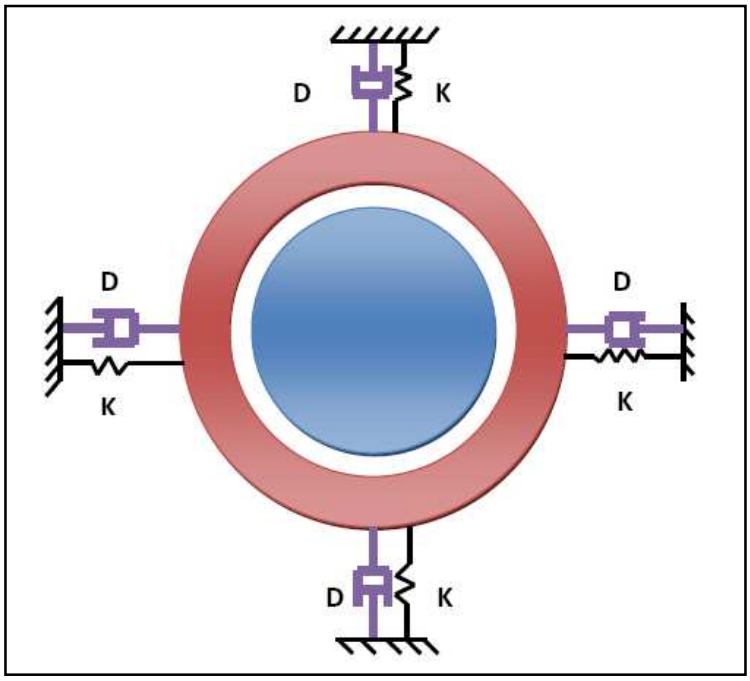

Figure.1.3: Hydrodynamic journal Bearing on Flexible Support

However, it has been observed that the hydrodynamic journal bearings can show excellent performances in withstanding static load, but fail easily under dynamic conditions if not critically designed for the specific purpose.

Though dry lubrication like lubrication with graphite, molybdenum disulphide etc. are used in some cases, *e.g.* in extrusion processes in cold and hot working, most of the above types of bearings are lubricated with fluids *i.e.* with liquids and gases. Under the general industrial

operating conditions such Newtonian lubricating fluids become contaminated with microstructures like dust and worn out metal particles. As the classical continuum theory becomes erroneous in the analysis of such lubrication, microcontinuum approach seems to be more appropriate.

Based upon the microcontinuum approach, the first consistent theory of fluid microcontinua, was presented by Eringen [41]. The microfluid was considered to contain microstructures having individual mass and velocity, in as much as the macrovolume element contains the microvolume elements and those microstructures can translate, rotate and deform independently of the motion of the macrovolume. The theory included the mechanism to support the local stress moments and body moments and to consider the influence of the spin inertia of each microelement. But this theory of microfluid is too complicated and the mathematical model is not so acquiescent to the solution of the non-trivial problems. Eringen [45],therefore again simplified the theory postulating a subclass of the microfluids, called micropolar fluids, considering the microrotational effects and ignoring the microdeformation effects of the substructures and permitting the surface and the body couples. The theory included two independent kinematic vector fields representing the translation velocities and the angular or spin velocities of the microstructures *i.e.* translation velocity vector and microrotational velocity vector. Although contemporary theories of fluid microcontinua were also presented by various authors, the basic field equations, however, remained similar to those of Eringen [41].

Physically the fluid consisting of bar like elements may be represented as micropolar fluid. The theory of micropolar fluid, thus, may be a satisfactory model for analyzing the flow behaviors of real fluid suspensions, polymeric fluids and fluid consisting of polymeric additives as is mixed with the engine oil for enhancing lubricating effectiveness, certain anisotropic fluids, *e.g.* liquid crystals consisting of dumbbell shaped molecules and possibly animal blood. Hence the theory of micropolar fluid has found its application as a refined model for studying the behavior of such fluid flows as in the field of lubrication, where the clearance in a bearing is comparable to the average grain size or molecular size of a non-Newtonian fluid *viz.* a polymeric fluid or in the practical usage where the lubricants under general operating conditions become fluid suspensions after being contaminated with dirt and worn out metal particles. For an important practical example, in the area of nuclear power plant, where sodium, which is used in a dual role of a heat transfer agent and a lubricant in the journal bearing supporting the mixing screw in the batch mixers exhibits the non-

Newtonian micropolar characteristics. The microcontinuum theory finds another worth-mentioning application in the study of blood rheology because the sizes of the blood cells are comparable to the diameters of the arteries and thus, there may exist the possible rotation and deformation of each blood cell while flowing through arteries.

Hydrodynamic bearings are generally used in cases when the relative velocity are high enough as a result of continuous increase in the sizes and speeds of the rotating machinery or due to use of fluids having kinematic viscosity, the oil film close in the bearings frequently becomes turbulent.

Again keeping in mind the extremely small radial clearance to facilitate case of alignment flexibly supported bearings have come into vogue. Therefore, it is important to do a study on stability of such flexibly supported journal bearing.

1.5 Present Work

In the present work is to theoretically investigate the static and dynamic characteristics including the stability of finite self-acting oil journal bearings lubricated with the micropolar fluids. The basic 3D Reynolds equation has been modified considering the equations of continuity of mass, equation for the linear momentum and the balance of angular momentum, which are coupled together due to the existence of two kinematic vector fields of the microstructures and characterizing the micropolar fluid,.

The theoretical prediction of hydrodynamic pressures in the bearing has been obtained by the solution of modified Reynolds equation satisfying the appropriate boundary conditions. The steady state pressure profile has been obtained easily by Finite Difference Technique with successive over-relaxation scheme. The steady state parameters like load carrying capacity, attitude angle has been obtained using the pressure profile over the entire bearing surface.

For dynamic pressure, using liberalized analysis, first order perturbations of eccentricity ratio and attitude angle has been used, and the resulting equations has been solved by Finite Difference Method with successive over-relaxation scheme Dynamic characteristics in terms of the components of stiffness and damping coefficients has been found using perturbed pressures profile in the hydrodynamic journal bearing. Also the threshold stability and whirl ratio have been examined for the fixed value of geometric and operating bearing characteristics with respect to stiffness and damping coefficients to predict the bearing behavior in better manner.

In addition the linearized stability analysis have also been considered in the rotor bearing system to get actual threshold of stability and the values of various characteristics obtained in the parametric study have been obtained at different operating parameter to check the stability.

CHAPTER 2 LITERATURE SURVEY

In the following section the literature relating the studies of finite hydrodynamic flexibly supported journal bearing operating with micropolar fluids have been systematically presented. Tribology is the science and engineering of interacting surfaces in relative motion. It includes the study and application of the principles of friction, lubrication and wear. Human interest in the constituent parts of tribology probably started with the aim of reducing their physical labor in moving heavy loads.

2.1 Lubrication for Friction

The first formulation of a hypothesis regarding the force necessary to overcome the viscous resistance of a fluid was derived by Newton [1], and Petroff [2], have reported first significant contribution theoretically in 1883 with his consideration of the effect of viscous force in the fluid film lubrication.

Tower, B. [3], Beruchamp Tower's experiments for the determination of suitable methods of lubricating railway axle bearings, which were partial bearings lubricated from an oil bath, were the first significant experimental studies and the developed pressure distribution in the bearing clearance under the loaded condition as measured through a number of pressure gauges at the midplane in the circumferential direction was found to exhibit a peak, which was several times higher than the mean pressure calculated on the basis of the projected area.

Reynolds, O. [4], Just after three years of Tower's first experiments, Reynolds presented a theoretical study to justify the experimental results of Tower. The experiments of Tower and the analysis of Reynolds may be considered as the entrance to the concept of hydrodynamic lubrication and the field of Tribology.

Since the development of the concept of the hydrodynamic lubrication about 120 years ago with the experiments of Tower and theoretical study of Reynolds lot of theoretical, experimental and analytical studies were presented by a number of authors. A few of them considered as benchmark work are only briefly reported.

Kingsbury, A. [5], extended the concept of hydrodynamic lubrication to the gasses by using air as lubricant, and also developed an experimental set up to study the behaviors of gas bearings based on the concept of electrical analogy. Sommerfeld, A. [6], has presented the first exact solution of Reynolds equation for pressure distribution for a full journal bearing using full film boundary condition along with the load and friction characteristics in terms of

eccentricity ratio. Harrison, W. J. [7], enriched the hydrodynamic lubrication through his experiments with special reference to air as lubricant.

Rayleigh [8], has investigated the effect of film shape on the operating characteristics of a bearing using the calculus of variations and Christopherson [9], pioneered in establishing the suitability of the Southwell's relaxation method for the lubrication problems and using the relaxation method Cameron and Wood [10], have obtained the solution of finite bearings and presented bearing characteristics for two slenderness ratios using realistic boundary conditions and during the same time Vogelpohl [11], developed an approximate solution based on infinite series.

Ocvirk [12], presented the solution of the Reynolds equation using narrow bearing approximation and Theoretical research on the dynamic characteristics of impervious self-acting oil bearing was initiated by Harrison [13], has showed that hydrodynamic equations for a light rigid rotor, supported by a pair of infinitely long bearings with full film, are satisfied by an orbital motion of the journal axis under a constant load. Kahlert [14], Osterle and Saibel [15], are always cited for their pioneering studies. However, the derivation of Reynolds equation was based upon the assumptions relating to cavitation, fluid inertia forces and non-linear flow effects among the studies of the effect of the convective inertia forces on the hydrodynamic lubrication.

Coles and Hughes [16], have investigated the cavitation in the lubricating film was initiated with the experiments, which shown that the end of the pressure curve was coinciding with the position of zero pressure gradient, which however, conflicted with the experimental results of Jacobson and Floberg [17], which indicated that the pressure cavitated somewhere beyond the point observed. Pinkus [18], Raimondi and Boyd [19], in 1958, have been used digital computers for the numerical solution of bearing characteristics.

2.2 Stability of Journal Bearing

Majumder [20] has presented the perturbation solution for the torque produced due to misalignment for gas lubricated porous journal bearings, The torque was found to decrease with the increase in the bushing thickness, but was increased with the increase in the slenderness ratio, whereas torque angle was found to increase at lower speeds and then decreased as speed increased.

Pinkus and Bupara [21], have presented a comprehensive analysis to the solution of the Reynolds equation for grooved misaligned journal bearings of finite lengths and with any number of grooves located at any arbitrary angular positions.

Guha S. K. [22], has presented the steady-state characteristics to study the isotropic roughness effect on hydrodynamic journal bearings of finite width, considering two types of misalignment *viz.* axial (vertical displacement) and twisting (horizontal displacement) with an isoviscous incompressible lubricant.

Holmes [23], has investigated the use of external damping against the oil-whirl instability and its usefulness for achieving stability control were studied and discussed by in the context of rigid and flexible rotor systems.

Marsh [24], and Kerr [25], has shown that the stability characteristic of this system are affected by both the stiffness and damping of the bearing support, based on the assumption that a local linearization may be applied to the pressure field generated by small dynamic motions to successfully predict all modes of half speed whirl onset. Dynamic analyses were made leading to the formation of translational and conical dynamic stiffness matrices, which in turn, were utilized to derive stability criteria for translation and conical modes of whirl in both single and double bearing systems

Holmes [26], utilized the values of bearing coefficients for finite bearings as given by Smith [27], to calculate stability limits and frequency response of a symmetrical rigid rotor.

Akers [28], has represented the time transient analysis, equations of motion, for a finite journal bearing for various slenderness ratios were solved, which showed that the stability was non-uniform with the addition of out of balance loads, and improved with the increase in viscosity of oil, but is found to be unaffected by the initial disturbances imparted on the shaft.

Experimental evidences since the early years of last century put forward the realization of the existence of a separate lubrication theory for fluid suspension and the effort for establishing a theory was intensified since mid of the last century. The early studies on such theories of fluid micro-continua have no concern with the research works of bearings. The theory was later simplified to an acceptable fluid film lubrication theory, called micropolar lubrication theory and in subsequent years this simplified micropolar lubrication theory was introduced in the analyses of bearings.

2.3 Micropolar Fluid Theories

The development of the theory of micropolar fluid was initiated with the development of the theory on micro-continuum approach. For the application of the classical continuum theory in the field of film lubrication, the most practical importance is whether the deep molecular orientation results in any rheological abnormalities in the vicinity of the solid surfaces; and

the significant differences in the behavior of the molecules of the liquid in intimate contact with and adhering to the surfaces or to absorbed layers on the surface from the behavior of the adjacent molecules of the fluid in the bulk are found obvious and the experimental evidences may be worth mentioning herein.

Kingsbury, A. [29], observed that such rheological abnormalities that varied from a small enhancement of viscosity to rigidity in the adhering layer ranging from 10^{-3} mm to 10^{-7} mm and attributed this difference in the behavior of the molecules to a possible intensified viscosity in that part of the fluid within the range of the attraction of the surface molecules of the metal. Cosserat, E. and Cosserat, F [30], have developed the theories of oriented media in which there existed three directors at each point. Jeffery [31], has studied the effect of the behavior of the Newtonian fluid of infinite extent in presence of a single ellipsoidal particle and the result indicated the enhancement of the viscosity of such fluid suspension than its base fluid.

Hardy and Nottage [32], have concluded that to be beyond the range of surface influence, the liquid film must be between 0.00762 to 0.01015 mm. in thickness and Buckley's [33], experimently shown the total loss of rigidity in clean liquid at a distance of 0.3 x 10-4 mm from a solid boundary. Anzelius [34], in 1931 the unexpected behavior of the fluid containing oblong molecules in a shear field and dependence of the stress and moment at each point of the fluid was expressed by him as a function of the usual rate of strain tensor and the orientation of the substructure.

Needs [35], has represented through a series of experiments of the boundary surface influences on the viscosity of thin lubricating films squeezed in between two optically plane parallel circular disks approaching each other with no tangential velocity and film thickness down to 0.000635 mm, found an increasing time lag for the plates in their time of approach than that predicted by classical Newtonian theory for the film thickness below 0.00127 mm, indicating the increase in the effective viscosity of the film in that zone. He found the evidences where the effective viscosity in the boundary film increased nearly five times than that in the bulk

Henniker [36], has experimently represented of the Couette type flow performed on leuben oil containing additives of aluminum napthenate up to 2%, he found an extensive tenfold increase in the viscosity within 50000A of the surface. Fuks [37,38], has been presented later by squeeze film experiments of various fluids between two plates submerged in the fluid and by measuring the gap between the plates as a function of time, Fuks found the existence of a

residual film between the plates even after squeezing for a very long time, similar to those obtained by Needs[35] observed that the thickness of such residual film increased with the increase in fatty acid concentration, the chain length of the hydrocarbon in both solvent and fatty acid and the surface energy of the solid substrate.

A few more experiments by Hoyt and Fabula [39], and Vogel and Patterson [40], have shown that the mixing of some extremely small amount of polymeric additives in the lubricating fluid reduced the skin friction near a rigid body than in such a fluid to an extent of 30-35%.Earlier the additives were considered to be beneficial in the boundary lubrication not in hydrodynamic lubrication, but the experiments also had shown evidences of favorable effects in the thin film hydrodynamic lubrication by their usages.Eringen, A. C. [41], have proposed a similar theory, the basic equations, jump conditions and constitutive equations of 'simple microfluent' media, exhibiting similar micro-effects. These fluids, named as 'simple microfluids' are considered to be a fluent medium and a generalization of the Stokesian fluids whose properties and behavior are affected by the local motions of the material particles contained in each of its volume element. Non-linear Stokesian fluids are considered to be a special class of simple micro-fluids. As these fluids possess local inertia, Eringen extended continuum theory considering Conservation of micro-inertia moments and Balance of first stress moments

The auther developed and discussed the concepts of inertial spin, body moments, gyration tensors, stress moments, wherein the stresses and stress moments were expressed as the functions of deformation rate tensor and various microdeformation rate tensors. A simple microfluid in its simplest form has as many as twenty two viscosity coefficients and the fluids in which gyrational effects are important, such as anistropic fluids, vortex fluids and fluid having surface tensions are guessed to fall in this group.Eringen, A. C. [42], presented the theory of micromorphic material. As even the linear theory was too complicated for engineering application, Eringen [43], has simplified the consideration of a subclass of micromorphic materials, named as micropolar media. The study however presented the discussions on deformation and motion, laws of motion, constitutive equations, theory of micropolar media, micropolar viscoelasticity, micropolar materials with attenuating neighbourhood and the problem of micropolar channel flow, with the assumptions of linear constitutive equations, microisotropic medium and negligible heat conduction.

As an extension of the above study, the linear theory with basic equations, theory of micropolar elasticity, couple stress theory, non-negative internal energy and the Uniqueness theorem of micropolar elasticity were presented by Eringen [44], in the same year.

Eringen [45], presented the laws of motion, constitutive equations of microfluids, the definition of micropolar fluids— the theories of its thermodynamics and field equations and the study of such a fluid flow in a circular pipe.

2.4 Bearings with Micropolar Lubrication

Eringen, A. C. [45], Based on the theory of micropolar lubrication the first application of the theory was presented by himself for the steady motion of micropolar fluids in a circular channel in which the profiles for the velocity, microrotational velocity, shear stress difference and the couple stress on the fluid surface adjacent to the wall were presented graphically. The velocity profile was found to lose its parabolic nature and was smaller than that of classical Navier-Stokes fluid. Though the shearing stress remained the same as that determined by classical theory, the surface shear was found to be reduced by an amount equivalent to the effect of the distributed couples aroused on the fluid surface in a thin layer adjacent to the surface thus, indicating the development of a boundary layer phenomenon not present in the Navier-Stokes theory.

Ariman and Cakmak [46], have couple stress and micropolar theories were first applied by to the Couette and Poiseuille types of flow problems for one-dimensional fully developed and steady flow of an incompressible fluid between two parallel plates. The equations for the velocity distribution and the mass flux were presented. The results for the velocity profiles for both types of flow and the mass flux were shown in comparative graphical forms for couple stress and micropolar fluids.

Allen and Kline [47], gave an approximate analytical solution for the two-dimensional slider bearing with micropolar lubrication containing rigid spherical substructure and using order-of-magnitude arguments reduced the governing equations into a set of coupled, linear, ordinary differential equations. Datta [48], presented a theoretical study of a pivoted slider bearing with convex pad surface in micropolar fluid. The modified Reynolds equation was derived and the parametric study showing the effects of pad surface curvature on the pressure, load capacity, centre of pressure and friction coefficient were presented and discussed. It was concluded that the micropolar fluid resulted in higher load carrying capacity than the Newtonian fluid.

Agrawal, Ganju, and Jethi [49], have theoretical represented squeeze films between two infinitely long rectangular plates, circular plates and externally pressurized bearings with micropolar lubricant showed that in micropolar lubricants the squeeze film bearings exhibited larger time of approaches and for a given flow rate the externally pressurized bearing under micropolar lubrication showed a higher load carrying capacity than those with the Newtonian fluid. Balaram [50], presented an analysis of micropolar squeeze films between two rectangular plates of infinite length along with the expressions for the pressure, the load carrying capacity of the squeeze film and the relationship of film thickness with time. The results showed an improvement in load carrying capacity with the increase in the density of the macromolecular volume but a decrease in load capacity with an increase in substructure particle size.

Prakash, J. And Christensen, H. [51], though his work developed the hydrodynamic theory for the two-dimensional micropolar lubrication of a rigid cylinder on a plane surface in order to make critical analysis of micropolar effects revealed in the results of Fuks [37,38].

Prakash and Sinha [52], have been presented a paper on the application of the micropolar fluid to a journal bearing considering a two-dimensional incompressible steady laminar flow between two eccentric cylinders in relative rotary motion. The governing equations were reduced into a system of coupled, ordinary differential equations and non-dimensional form of various bearing characteristics— velocity distributions, pressure distribution, load capacity, and coefficient of friction were presented under this type of lubrication. The two parameters characterizing the micropolarity in a combined manner were considered separately by them rather than to use their product as were considered by Eringen [45], and other authors. The authors again published an analytical study [53],have been obtain the Reynolds equation from the field equations of the micropolar fluids and presented the non-dimensional forms of load and the time for a steady laminar incompressible micropolar squeeze flow for both parallel circular plates and parallel rectangular plates when the upper plate was moving towards the stationary lower plate without having any relative tangential velocity of the plates. The results were found to have excellent qualitative agreement with Needs' [35] experimental results.

Prakash, J. and Sinha, P. [54], also presented a theoretical analysis of squeeze films in both full and half journal bearings with a steady, laminar, incompressible flow of micropolar fluid between two eccentric cylinders in relative normal motion along with the expressions for Reynolds equation, nondimensional pressure distribution, load capacity and response time.

The results supported the experimental results [35, 36] of increase in the effective viscosity in narrow passages.

Prakash and Sinha [55], presented the Reynolds equation and the expressions for various bearing characteristics of squeeze films for the general case of dynamically loaded infinitely long journal bearing for steady incompressible two-dimensional micropolar fluid flow under a sinusoidal load with no journal rotation. The graphical representation of results exhibited decreasing velocity of approach with increasing micropolar effect.

Zaheeruddin and Isa, Md. [56],have analytically provided the expressions for different hydrodynamic characteristics such as the load carrying capacity, the volume flow flux and the frictional force, of one dimensional journal bearings, both infinitely long and infinitely short, with micropolar lubrication, and the results showed that an increase in the equivalent viscosity of the micropolar fluid increased the load carrying capacity and the time of approach, but decreases the coefficient of friction.Tipei, N [57], obtained similar results in his analysis of short bearing problem with micropolar lubrication. For constant viscosity and other micropolar coefficients, he presented simplified generalised expressions for the velocity field, friction torque and side flow. The fluid pressure was found to increase in comparison to that in the Newtonian flow and was represented by a surface depending on two groups of micropolar parameters. The general bearing characteristics except the coefficient of friction, which showed the lower values, were found to exhibit improved results than those in Newtonian lubricants.

Zaheeruddin, Kh. [58], has reported the another paper that the generalized Reynolds equation in dynamically loaded one-dimensional, both infinitely long and infinitely short types of porous journal bearings operating under a cyclic load and lubricated with micropolar fluids. The analysis was to show the effects of microstructures present in the lubricants, the permeability of the bearing material and the bearing wall thickness on the operating eccentricity ratio. Singh and Sinha [59], The Three-Dimensional Reynolds Equation for Micropolar Fluid Lubricated Bearings first presented by Singh and Sinha though which the authors solved to yield the expressions for the velocity distribution, microrotational velocities flow flux and frictional torques. Huang *et al.* [60], presented an analysis of finite width journal bearings in three-dimensional steady flow of incompressible micropolar fluid for the cases of width to diameter ratio 1.0 and $\pi/10$ .The analysis showed that the micropolar fluid exhibited higher load carrying capacity and lower frictional coefficient than the Newtonian fluid, which were more pronounced at higher eccentricity ratio and lower width-to-diameter

ratio; whereas volumetric side flow rate was found marginally differing in either types of lubrication.

Khonsari and Brewe [61], have reported lubricating effectiveness in micropolar fluid for a journal bearing of finite length and the non-dimensional expressions were developed for the load capacity, leakage flow rate and friction force. The results showed the achievements of higher load carrying capacity and frictional force, but lower frictional parameter in comparison with those in Newtonian fluid. Huang and Weng [62], studied the dynamic characteristics of finite width journal bearing with micropolar lubrication using linear stability theory and graphically presented the stiffness, damping coefficients and the critical stability parameter of the journal bearings for width to diameter 30 ratio 1.0 and 10 under both Newtonian and micropolar lubrication. The micropolar fluids exhibited larger normal stiffness coefficient but smaller normal damping coefficient, and comparatively narrower stable region of the journal. The features of increasing effective viscosity and load capacity under micropolar lubrication resulted in lower limit values of the Sommerfeld number for completely stable operation. A long journal was found to exhibit significant difference in the values of critical mass parameter for the Newtonian and micropolar fluids, whereas the short bearing was found to be almost equally stable in both types of lubrication.

The steady flow of a micropolar fluid between two rotating disks of finite radius rotating at different same speeds was investigated by Chaturani and Narasimman [63], and the equations of motion were reduced to a set of ordinary non-linear coupled differential equations, which were then linearized by quasilinearisation technique. The numerical solutions were obtained using fourth order Runga-Kutta method via orthonormalisation.

Qiu and Zhang [64], reported the field equation of micropolar fluid with general lubrication theory assumptions is simplified into two systems of coupled ordinary differential equation. The analytical solutions of velocity and microrotation velocity are obtained. Micropolar fluid lubrication Reynolds equation is deduced. By means of numerical method, the characteristics of a -finitely long journal bearing under various dynamic parameters, geometrical parameters and micropolar parameters are shown in curve form.D.A.Boefey [65], examined the stability characteristics of a bearing on a flexible damped support using a purely analytical approach. His analysis was based on the linearized solution to the time dependent Reynolds equation. Castelli, Stevenson and Gunter [66] have reported the Steady-state Characteristics of Gaslubricated Self-acting Partial-arc Journal Bearings of Finite Width.

The theoretical analysis is presented by Chattopadhyay, A.K., Karmakar, S., [67], investigating the stability of a symmetrical, rigid rotor on a flexibly supported journal bearingin which oil-film flow in the bearing is assumed to be turbulent and the dynamics of the system is studied by calculating the components of the fluid film force by solving the generalized Reynolds equation modified to include the effect of turbulence and using these in the non-linear equation of motion of the journal and the bearing. The modified Reynolds equation is solved for pressure distribution by using finite difference method with S.O.R. scheme. Chattopadhyay, A.K. [68], have presented a paper is to studied theoretically, using finite difference techniques, the stability characteristics of hydrodynamic journal bearings lubricated with micropolar fluids. The theoretical study has been presented using both the linear analysis based on the perturbation method and non-linear analysis using Runge-Kutta method.

Parametric studies have been conducted and stability characteristics have been obtained and a comparison of the results of linear and non-linear analyses for different parameters have been compared and presented. A modified Reynolds equation has been obtained using micropolar lubrication theory and the solution of pressure obtained from this equation is used in the governing differential equations of motion to arrive at a stability threshold.

The present work has, therefore, been aimed at studying the lubrication effectiveness of flexibly supported hydrodynamic journal bearings using micropolar lubrication under the abovementioned operational situations

CHAPTER 3 CONCLUSION OF LITERATURE SURVEY AND OUTLINE OF THESIS WORK

From the literature revised it has been found that a lot of work in the area of hydrodynamic journal bearing have been done but very less research work has been reported which demonstrated the use of micropolar lubricant in flexibly supported hydrodynamic journal bearing. The literature revised especially the dynamic performance of bearings including linear stability analysis deserves special attention and very less work have been reported in this area.

The objective of this work is to investigate both the steady state and dynamic characteristics including the stability of a flexibly supported finite hydrodynamic journal bearing lubricated with micropolar fluid.

3.1 Steps Followed In the Organization of the Present Work

1. Review of literature.
2. Derivation the basic governing equation for modified Reynolds equation.
3. Theoretical analysis of steady state characteristic of the finite journal bearing lubricated with micropolar fluids.
4. Dynamic analysis of the finite journal bearing lubricated with micropolar fluids has been studied, which are, Perturbed pressure equation, Stiffness and Damping coefficients and derived the Equation of Motions and stability parameter.
5. Solution of governing steady state equation by analytical method
6. Solution of Governing equation with FDM method.
7. Finally numerical computations have been performed to plot the results for various static and dynamic characteristics and logical conclusions have been drawn.

CHAPTER 4 BASIC EQUATION

4.1 Introduction

In this chapter, starting from the basic field equation and using certain assumptions, modified Reynolds equation has been derived and a brief discussion of the various non-dimensional parameters related to micropolar fluid has been made.

As the presence of the microstructures in the lubricating fluid, particularly in the hydrodynamic lubrication, imparts the microrotation and microdeformation of the particles with the attendant enhancement of the viscosity of the fluid, the analysis with such lubricants requires the concepts of conservation of the micro-inertia moments and the balance of the first stress moments in addition to the basic principle of the continuous media

The basic field equations of the micropolar fluid were developed by Eringen [45], and later adopted by Prakash and Sinha [52] followed by the model of Singh and Sinha [59].

4.2 Field Equations

The field equations for micropolar fluids in vectorial form are [52]:
Principle of conservation of mass

$$\frac{\partial \rho}{\partial t} + \nabla \bullet (\rho V) = 0 \qquad \textbf{... (4.1)}$$

Conservation of linear momentum:

$$(\lambda + 2\mu)\nabla(\nabla \cdot \vec{V}) - \frac{(2\mu + \chi)}{2}\nabla \times \nabla \times \vec{V} + \chi \nabla \times v - \nabla \pi^* + \rho F_B = \rho \frac{D\vec{V}}{Dt} \qquad \textbf{… (4.2)}$$

Conservation of angular momentum:

$$(\alpha + \beta + \gamma)\nabla(\nabla \cdot v) - \gamma \nabla \times \nabla \times v + \chi \nabla \times \vec{V} - 2\chi v + \rho C_B = \rho j \frac{Dv}{Dt} \qquad \textbf{… (4.3)}$$

Where; **ρ** =mass density;

V = velocity vector and

v = microrotational velocity vector **… (4.4)**

π^* is the thermodynamic pressure and is to be replaced by the hydrodynamic film pressure**,** p

since, $\pi^* = -\left[\frac{\partial E}{\partial \rho^{-1}}\right] = p$ **… (4.5)**

where E = internal energy [45,61] and p is to be determined by the boundary conditions.

μ and λ are the familiar viscosity coefficients of the classical fluid mechanics

while $\boldsymbol{\alpha}$,$\boldsymbol{\beta}$ and $\boldsymbol{\gamma}$ are the new viscosity coefficients derived as the combinational effects of the gyroviscosities for micropolar fluid as defined by Eringen [45].

$\boldsymbol{\chi}$ = new viscosity coefficient for micropolar fluid, termed as spin viscosity, which establishes the link between the velocity vector, V and the microrotational velocity vector, v

F_B = body force per unit mass,

C_B = body couple (moment) per unit mass and

j = microinertia constant.

λ, μ and $\boldsymbol{\chi}$ are all of dimension $\left[ML^{-1}T^{-1}\right]$,

$\boldsymbol{\alpha}$, and$\boldsymbol{\gamma}$ are all of dimension $\left[ML\,T^{-1}\right]$and

j is of dimension $[L^2]$.

If microrotation velocity and local fluid vorticity are considered to be identically equal and is imposed as a possible solution of the balance equations, which seems to be a natural solution and is desirable in reducing the number of constitutive coefficients,it can be shown that
$j = \Lambda^2$.

$\frac{D}{Dt}$ indicates the material differentiation.

Constitutive equations for the stress tensor t_{kl} and the couple stress tensor m_{kl} are [52]:

$$t_{kl} = \left(-\pi^* + \lambda \overline{V}_{r,r}\right)\delta_{k1} + \left(\mu - \frac{1}{2}\chi\right)\left(\overline{V}_{k,1} + \overline{V}_{1,k}\right) + \chi\left(\overline{V}_{1,k} - \eta_{k1r}v_r\right) \quad \textbf{… (4.6)}$$

$$m_{k1} = \alpha v_{r,r}\delta_{k1} + \beta v_{k,1} + \gamma v_{1,k} \quad \textbf{… (4.7)}$$

Where, η_{k1r} is an alternating tensor. An index followed by a comma represents partial differentiation with respect to the space variable x_k.

4.3 Modified Reynolds Equation's Derivation

The above micropolar effects are then incorporated into the lubrication problem for a journal bearing to derive the modified Reynolds equation with certain simplifications.

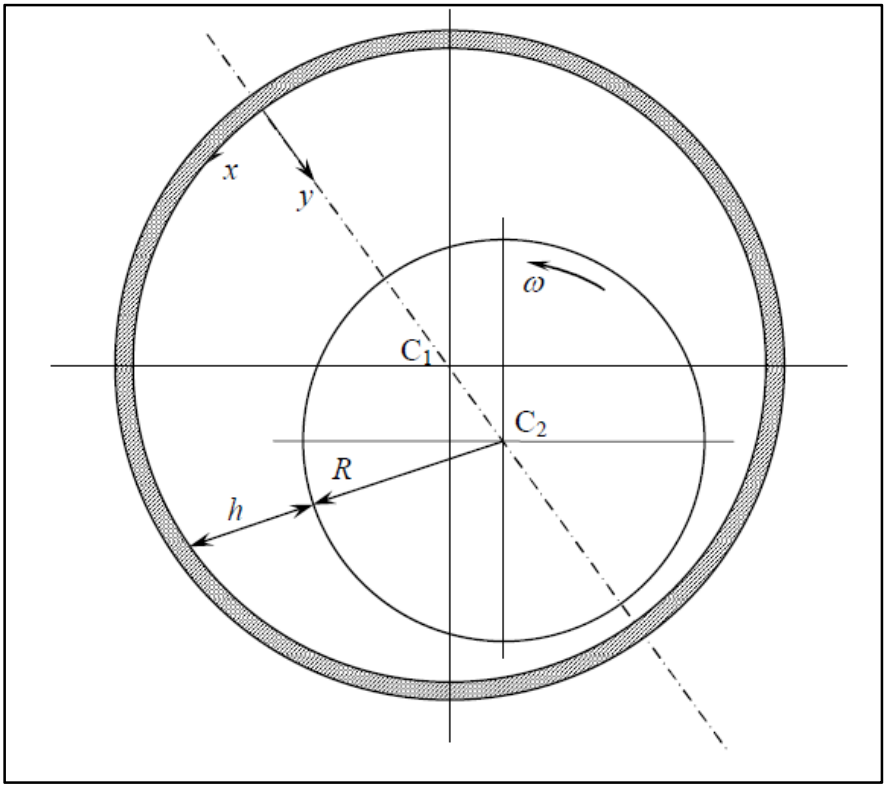

Figure 4.1: Bearing Configuration for the Derivation of Reynolds Equation

4.3.1 Basic Assumptions

The basic assumptions in micropolar lubrication to a journal bearing include the usual lubrication assumptions in deriving Reynolds equation and the assumptions to generalize the micropolar effects [59]:

a. The flow is laminar *i.e.* free of vortices and turbulences.

b. Body forces and body couples are negligible, *i.e.* $F_B = 0$ and $C_B = 0$.

c. No slip occurs at the bearing surfaces.

d. The flow is incompressible and steady, *i.e.* $\boldsymbol{\rho}$ = constant and $\frac{\partial \rho}{\partial t} = 0$

e. Bearing surfaces are smooth, non-porous and rigid *i.e.* no effects of surface roughness or porosity and the surface can withstand infinite pressure and stress theoretically without having any deformation.

f. No fluid flow exists across the fluid film, *i.e.* the lubrication characteristics are independent of *y*-direction.

g. The micropolar properties are also independent of *y*-direction.

h. The film is very thin in comparison to the length and the span of the bearing. Thus, the curvature effect of the fluid film may be ignored and the rotational velocities may be replaced by the translatory velocities.

The velocity vector, the microrotational velocity vector and the fluid film pressure are given as:

$$\vec{V} = \left[\vec{V}_X(x,y,z), \vec{V}_y(x,y,z), \vec{V}_Z(x,y,z)\right] \quad \textbf{... (4.8)}$$

$$v = \left[v_1(x,y,z), v_2(x,y,z), v_3(x,y,z)\right] \quad \textbf{... (4.9)}$$

$$p = p(x,y,z) \quad \textbf{... (4.10)}$$

Note that for $\boldsymbol{\alpha} = \boldsymbol{\beta} = \boldsymbol{\gamma} = \boldsymbol{\chi} = 0$ and for negligible body couple per unit mass equation (4.3) yields $v = 0$ and so, equation (4.2) reduces to the classical Navier-Stokes equation. For $\boldsymbol{\chi} = 0$ the velocity vector and the microrotational velocity vector are uncoupled and the global motion of the fluid becomes free of the microrotation and their effects.

4.3.2 Directional Flow Equations:

With the above assumptions (4.1) reduces to

$$\left.\begin{aligned} \nabla \cdot \vec{V} &= 0 \\ \frac{\partial \vec{V}_X}{\partial x} + \frac{\partial \vec{V}_y}{\partial y} + \frac{\partial \vec{V}_Z}{\partial z} &= 0 \end{aligned}\right\} \quad \textbf{… (4.11)}$$

It can also be considered that,

$$\nabla . \boldsymbol{v} = 0 \quad \textbf{... (4.12)}$$

The explanation for equation (4.12) can be given following Tipei [57] as:

In case of a flow in thin layers bounded by solid surfaces, as in lubrication problem, the component of $\boldsymbol{v}$ perpendicular to the boundaries becomes negligible with respect to the other two components. Since the derivatives with respect to the normal *y*-direction are much larger

than the other derivatives, *i.e.* $\frac{\partial}{\partial y} >> \frac{\partial}{\partial x} or \frac{\partial}{\partial z}$, hence $\nabla(\nabla.v) = \frac{\partial^2 v_1}{\partial x \partial y} + \frac{\partial^2 v_3}{\partial z \partial y}$, while the other components are much smaller. The component of $(\nabla \times v)$ upon *y*-coordinate *i.e.* & $\left[\frac{\partial v_1}{\partial z} - \frac{\partial v_3}{\partial x}\right]$ is an order of magnitude smaller and may be neglected and hence equation (4.3) as projected upon *y*-axis yields $\nabla(\nabla.\boldsymbol{v}) \approx 0$. This result can be obtained directly under usual approximations in lubrication theory [70] by considering $\nabla^2 v >> \nabla\ (\nabla.\ v)$. Now from the vector calculus $(\nabla \times \nabla \times V)$ and $(\nabla \times \nabla \times \mathrm{v})$ can be written as:

$$\nabla \times \nabla \times \mathrm{V} = \nabla(\nabla.\mathrm{V}) - \nabla^2 \mathrm{V} \quad \text{and} \quad \nabla \times \nabla \times \mathbf{v} = \nabla(\nabla.\mathbf{v}) - \nabla^2 \mathbf{v} \qquad \textbf{... (4.13)}$$

With the basic assumptions and equation (4.13), equation (4.2) yields the following three equations along *x*-, *y*- and *z*-directions respectively:

$$\frac{(2\mu+\chi)}{2}\left(\frac{\partial^2 \vec{V}_X}{\partial x^2} + \frac{\partial^2 \vec{V}_X}{\partial y^2} + \frac{\partial^2 \vec{V}_X}{\partial z^2}\right) + \chi\left(\frac{\partial v_3}{\partial y} - \frac{\partial v_2}{\partial z}\right) - \frac{\partial p}{\partial x} = \rho\left(\vec{V}_X \frac{\partial \vec{V}_X}{\partial x} + \vec{V}_Y \frac{\partial \vec{V}_X}{\partial y} + \vec{V}_Z \frac{\partial \vec{V}_X}{\partial z}\right) \qquad \textbf{… (4.14)}$$

$$\frac{(2\mu+\chi)}{2}\left(\frac{\partial^2 \vec{V}_Y}{\partial x^2} + \frac{\partial^2 \vec{V}_Y}{\partial y^2} + \frac{\partial^2 \vec{V}_Y}{\partial z^2}\right) + \chi\left(\frac{\partial v_1}{\partial y} - \frac{\partial v_3}{\partial x}\right) - \frac{\partial p}{\partial y} = \rho\left(\vec{V}_X \frac{\partial \vec{V}_Y}{\partial x} + \vec{V}_Y \frac{\partial \vec{V}_Y}{\partial y} + \vec{V}_Z \frac{\partial \vec{V}_Y}{\partial z}\right) \qquad \textbf{… (4.15)}$$

$$\frac{(2\mu+\chi)}{2}\left(\frac{\partial^2 \vec{V}_Z}{\partial x^2} + \frac{\partial^2 \vec{V}_Z}{\partial y^2} + \frac{\partial^2 \vec{V}_Z}{\partial z^2}\right) + \chi\left(\frac{\partial v_2}{\partial x} - \frac{\partial v_1}{\partial y}\right) - \frac{\partial p}{\partial z} = \rho\left(\vec{V}_X \frac{\partial \vec{V}_Z}{\partial x} + \vec{V}_Y \frac{\partial \vec{V}_Z}{\partial y} + \vec{V}_Z \frac{\partial \vec{V}_Z}{\partial z}\right) \qquad \textbf{… (4.16)}$$

Similarly, with the basic assumptions and equation (4.13), equation (4.3) yields the following three equations along *x*-, *y*- and *z*-directions respectively:

$$\gamma\left(\frac{\partial^2 v_1}{\partial x^2} + \frac{\partial^2 v_1}{\partial y^2} + \frac{\partial^2 v_1}{\partial z^2}\right) + \chi\left(\frac{\partial \vec{V}_Z}{\partial y} - \frac{\partial \vec{V}_Y}{\partial z}\right) - 2\chi v_1 = \rho j\left(\vec{V}_X \frac{\partial v_1}{\partial x} + \vec{V}_Y \frac{\partial v_1}{\partial y} + \vec{V}_Z \frac{\partial v_1}{\partial z}\right) \qquad \textbf{… (4.17)}$$

$$\gamma\left(\frac{\partial^2 v_2}{\partial x^2} + \frac{\partial^2 v_2}{\partial y^2} + \frac{\partial^2 v_2}{\partial z^2}\right) + \chi\left(\frac{\partial \vec{V}_X}{\partial z} - \frac{\partial \vec{V}_Z}{\partial x}\right) - 2\chi v_2 = \rho j\left(\vec{V}_X \frac{\partial v_2}{\partial x} + \vec{V}_Y \frac{\partial v_2}{\partial y} + \vec{V}_Z \frac{\partial v_2}{\partial z}\right) \qquad \textbf{… (4.18)}$$

$$\gamma\left(\frac{\partial^2 v_3}{\partial x^2} + \frac{\partial^2 v_3}{\partial y^2} + \frac{\partial^2 v_3}{\partial z^2}\right) + \chi\left(\frac{\partial \vec{V}_Y}{\partial x} - \frac{\partial \vec{V}_X}{\partial y}\right) - 2\chi v_3 = \rho j\left(\vec{V}_X \frac{\partial v_3}{\partial x} + \vec{V}_Y \frac{\partial v_3}{\partial y} + \vec{V}_Z \frac{\partial v_3}{\partial z}\right) \qquad \textbf{… (4.19)}$$

4.3.3 Non-Dimensional Scheme for Equation

Equations (4.14) to (4.19) when non-dimensionalised with the following substitutions

$$\bar{x} = \frac{x}{R}; \quad \bar{y} = \frac{y}{R}; \quad \bar{z} = \frac{z}{L/2}; \quad \delta_1 = \frac{C}{R}; \quad \delta_2 = \frac{C}{L/2}; \quad \delta_3 = \frac{h_{\min}}{R}; \quad \delta_4 = \frac{L/2}{R};$$

$$\bar{V}_i = \frac{V_i}{U}, \text{ where i = x, y, z,} \quad \bar{v}_i = v_i \frac{C}{U}, \text{ where i = 1, 2, 3;} \quad \xi = \frac{h_{\min}}{C}$$

$$\bar{p} = \frac{p h^2{}_{\min}}{\left(\mu + \frac{\chi}{2}\right) UR}, \quad R_e = \frac{2\rho CU}{(2\mu + \chi)}, \quad R_R = \frac{\rho j U h}{4\mu\Lambda}, \quad N = \left(\frac{\chi}{2\mu + \chi}\right)^{1/2} \quad \text{… (4.20)}$$

$$l_m = \frac{C}{\Lambda}; L_R = \frac{h_{\min}}{\Lambda}; \text{ where } \Lambda = \left(\frac{\gamma}{4\mu}\right)^{1/2} \text{ and is of dimension of length.}$$

The following equations will result:

$$\left(\delta_1^2 \frac{\partial^2 \bar{V}_X}{\partial \bar{x}^2} + \frac{\partial^2 \bar{V}_X}{\partial \bar{y}^2} + \delta_2^2 \frac{\partial^2 \bar{V}_X}{\partial \bar{z}^2}\right) + 2N^2 \left(\frac{\partial \bar{v}_3}{\partial \bar{y}} - \delta_2 \frac{\partial \bar{v}_2}{\partial \bar{z}}\right) - \frac{1}{\xi^2} \frac{\partial \bar{p}}{\partial \bar{x}}$$
$$= R_e \left(\delta_1 \bar{V}_X \frac{\partial \bar{V}_X}{\partial \bar{x}} + \bar{V}_Y \frac{\partial \bar{V}_X}{\partial \bar{y}} + \delta_2 \bar{V}_Z \frac{\partial \bar{V}_X}{\partial \bar{z}}\right) \quad \text{… (4.21)}$$

$$\xi\delta_3 \left(\delta_1^2 \frac{\partial^2 \bar{V}_Y}{\partial \bar{x}^2} + \frac{\partial^2 \bar{V}_Y}{\partial \bar{y}^2} + \delta_2^2 \frac{\partial^2 \bar{V}_Y}{\partial \bar{z}^2}\right) + 2\xi\delta_3 N^2 \left(\delta_2 \frac{\partial \bar{v}_1}{\partial \bar{z}} - \delta_1 \frac{\partial \bar{v}_3}{\partial \bar{x}}\right) - \frac{\partial \bar{p}}{\partial \bar{y}}$$
$$= \xi\delta_3 R_e \left(\delta_1 \bar{V}_X \frac{\partial \bar{V}_Y}{\partial \bar{x}} + \bar{V}_Y \frac{\partial \bar{V}_Y}{\partial \bar{y}} + \delta_2 \bar{V}_Z \frac{\partial \bar{V}_Y}{\partial \bar{z}}\right) \quad \text{… (4.22)}$$

$$\xi^2\delta_4 \left(\delta_1^2 \frac{\partial^2 \bar{V}_Z}{\partial \bar{x}^2} + \frac{\partial^2 \bar{V}_Z}{\partial \bar{y}^2} + \delta_2^2 \frac{\partial^2 \bar{V}_Z}{\partial \bar{z}^2}\right) + 2\xi^2\delta_4 N^2 \left(\delta_1 \frac{\partial \bar{v}_2}{\partial \bar{x}} - \frac{\partial \bar{v}_1}{\partial \bar{y}}\right) - \frac{\partial \bar{p}}{\partial \bar{z}}$$
$$= \xi^2\delta_4 R_e \left(\delta_1 \bar{V}_X \frac{\partial \bar{V}_Z}{\partial \bar{x}} + \bar{V}_Y \frac{\partial \bar{V}_Z}{\partial \bar{y}} + \delta_2 \bar{V}_Z \frac{\partial \bar{V}_Z}{\partial \bar{z}}\right) \quad \text{… (4.23)}$$

$$\left(\delta_1^2 \frac{\partial^2 \bar{v}_1}{\partial \bar{x}^2} + \frac{\partial^2 \bar{v}_1}{\partial \bar{y}^2} + \delta_2^2 \frac{\partial^2 \bar{v}_1}{\partial \bar{z}^2}\right) + \frac{N^2 L_R^2}{2(1-N^2)\xi^2} \left(\frac{\partial \bar{V}_Z}{\partial \bar{y}} - \delta_2 \frac{\partial \bar{V}_Z}{\partial \bar{z}}\right) - \frac{N^2 L_R^2}{(1-N^2)\xi^2} \bar{v}_1$$
$$= R_R \left(\delta_1 \bar{V}_X \frac{\partial \bar{v}_1}{\partial \bar{x}} + \bar{V}_Y \frac{\partial \bar{v}_1}{\partial \bar{y}} + \delta_2 \bar{V}_Z \frac{\partial \bar{v}_1}{\partial \bar{z}}\right) \quad \text{… (4.24)}$$

$$\left(\delta_1^2\frac{\partial^2\bar{v}_2}{\partial\bar{x}^2}+\frac{\partial^2\bar{v}_2}{\partial\bar{y}^2}+\delta_2^2\frac{\partial^2\bar{v}_2}{\partial\bar{z}^2}\right)+\frac{N^2L_R^2}{2\left(1-N^2\right)\xi^2}\left(\delta_2\frac{\partial\bar{V}_X}{\partial\bar{z}}-\delta_1\frac{\partial\bar{V}_Z}{\partial\bar{x}}\right)-\frac{N^2L_R^2}{\left(1-N^2\right)\xi^2}\bar{v}_2$$
$$=R_R\left(\delta_1\bar{V}_X\frac{\partial\bar{v}_2}{\partial\bar{x}}+\bar{V}_Y\frac{\partial\bar{v}_2}{\partial\bar{y}}+\delta_2\bar{V}_Z\frac{\partial\bar{v}_2}{\partial\bar{z}}\right) \quad \text{… (4.25)}$$

$$\left(\delta_1^2\frac{\partial^2\bar{v}_3}{\partial\bar{x}^2}+\frac{\partial^2\bar{v}_3}{\partial\bar{y}^2}+\delta_2^2\frac{\partial^2\bar{v}_3}{\partial\bar{z}^2}\right)+\frac{N^2L_R^2}{2\left(1-N^2\right)\xi^2}\left(\delta_1\frac{\partial\bar{V}_Y}{\partial\bar{x}}-\frac{\partial\bar{V}_X}{\partial\bar{y}}\right)-\frac{N^2L_R^2}{\left(1-N^2\right)\xi^2}\bar{v}_3$$
$$=R_R\left(\delta_1\bar{V}_X\frac{\partial\bar{v}_3}{\partial\bar{x}}+\bar{V}_Y\frac{\partial\bar{v}_3}{\partial\bar{y}}+\delta_2\bar{V}_Z\frac{\partial\bar{v}_3}{\partial\bar{z}}\right) \quad \text{… (4.26)}$$

4.3.4 Non Dimensional Parameters Study

In this section the interpretations of the non-dimensional parameters are given briefly. As the current analysis is aimed at showing the micropolar effects on the hydrodynamic journal bearings, a separate importance is given in discussion of the micropolar properties at the end of this section

Micropolar Parameters (N and Λ): N and Λ are two parameters distinguishing a micropolar fluid from a Newtonian fluid. N is a non-dimensional parameter called the *coupling number*, which couples the linear and angular momentum equations arising out of the microrotational effect of the suspended particles in the fluid. Λ, a dimensional parameter represents the interaction between the micropolar fluid and the film gap. Λ is termed as the *characteristic length* of the micropolar fluid and has the dimension of the length. l_m is a non-dimensional quantity and is termed as the *non-dimensional characteristic length* of the micropolar fluid. For $\chi = 0$, $N = 0$ the equations representing linear and angular momentums are uncoupled and equation (4.2) reduces to that of classical Navier-Stokes equation. On the other hand the strong micropolar effect is exhibited with the increase in the value of Λ or decrease in clearance in between the journal and bearing *i.e.* when non-dimensional characteristic length *l*m decreases. The second case is most likely here as C is usually very small in lubrication theory. Hence for $N \longrightarrow 0$ or for $l_m \longrightarrow \infty$, (*i.e.* characteristic length of the microstructure is small), the micropolar characteristic is lost and the lubrication problem reduces to that of the classical hydrodynamic lubrication. Again, as the gradient of the microrotational velocity across the film thickness is very small, when $l_m \longrightarrow 0$, the velocity and other flow characteristics will reduce to their equivalents in the Newtonian theory with μ everywhere replaced by $\left(\mu+\frac{1}{2}\chi\right)$Hence$\left(\mu+\frac{1}{2}\chi\right)$ togetherly may be considered as the

effective viscosity, μ_e, which arises due to the microrotational effect. The thermodynamic restrictions require that $0 \leq N \leq 1$. *j*, the microinertia constant is evolved due to the microrotational effects.

Other Non-Dimensional Parameters and Order Analysis: L_R, a non-dimensional quantity, may be termed as *length ratio*. During the initial stage of the application of the micropolar theory to the lubrication flow problems, researchers [45, 57] used either NL_R or Nl_m as the parameter in discussing the micropolar fluid; but as these products characterize the combinational effects, later N and l_m were considered separately to study their effects as can be found in Prakash and Sinha [52]. R_e may be considered as the modified Reynolds number, where μ has been replaced by effective viscosity, μ_e, i.e. $\left(\mu + \frac{1}{2}\chi\right)$ and this number is always less than the classical Reynolds number. Generally for lubrication problem, Re << 1 and is usually of the order of 10^{-3}. As j is the square of a length typical of the microstructure as discussed earlier, it is reasonable to consider $R_R << 1$.

Also with the assumptions that δ_1, δ_2,δ_3 are of the order of 10^{-3} and δ_4, ξ, L_R are of the order of 1, equations (4.21) to (4.26) will reduce to

$$\frac{\partial^2 \bar{V}_X}{\partial \bar{y}^2} + 2N^2 \frac{\partial \bar{v}_3}{\partial \bar{y}} - \frac{1}{\xi^2}\frac{\partial \bar{p}}{\partial \bar{x}} = 0 \qquad \text{… (4.27)}$$

$$\frac{\partial \bar{p}}{\partial \bar{y}} = 0 \qquad \text{… (4.28)}$$

$$\frac{\partial^2 \bar{V}_Z}{\partial \bar{y}^2} - 2N^2 \frac{\partial \bar{v}_1}{\partial \bar{y}} - \frac{1}{\xi^2 \delta_4}\frac{\partial \bar{p}}{\partial \bar{z}} = 0 \qquad \text{… (4.29)}$$

$$\frac{\partial^2 \bar{v}_1}{\partial \bar{y}^2} + \frac{N^2 L_R^2}{2\left(1-N^2\right)\xi^2}\frac{\partial \bar{V}_Z}{\partial \bar{y}} - \frac{N^2 L_R^2}{\left(1-N^2\right)\xi^2}\bar{v}_1 = 0 \qquad \text{… (4.30)}$$

$$\frac{\partial^2 \bar{v}_2}{\partial \bar{y}^2} - \frac{N^2 L_R^2}{\left(1-N^2\right)\xi^2}\bar{v}_2 = 0 \qquad \text{… (4.31)}$$

$$\frac{\partial^2 \bar{v}_3}{\partial \bar{y}^2} - \frac{N^2 L_R^2}{2\left(1-N^2\right)\xi^2}\frac{\partial \bar{V}_X}{\partial \bar{y}} - \frac{N^2 L_R^2}{\left(1-N^2\right)\xi^2}\bar{v}_3 = 0 \qquad \text{… (4.32)}$$

4.3.5 Velocity and Microrotational Velocity Vectors

Now to solve the velocity components and the microrotational velocity components equations (4.27) to (4.32) are returned to their dimensional forms as follows:

$$\frac{(2\mu+\chi)}{2}\frac{\partial^2 \vec{V}_X}{\partial y^2}+\chi\frac{\partial v_3}{\partial y}-\frac{\partial p}{\partial x}=0 \quad \text{… (4.33)}$$

$$\frac{\partial p}{\partial y}=0 \quad \text{… (4.34)}$$

$$\frac{(2\mu+\chi)}{2}\frac{\partial^2 \vec{V}_Z}{\partial y^2}-\chi\frac{\partial v_1}{\partial y}-\frac{\partial p}{\partial z}=0 \quad \text{… (4.35)}$$

$$\gamma\frac{\partial v_1}{\partial y^2}+\chi\frac{\partial \vec{V}_Z}{\partial y}-2\chi v_1=0 \quad \text{… (4.36)}$$

$$\gamma\frac{\partial^2 v_2}{\partial y^2}-2\chi v_2=0 \quad \text{… (4.37)}$$

$$\gamma\frac{\partial^2 v_3}{\partial y^2}-\chi\frac{\partial \vec{V}_X}{\partial y}-2\chi v_3=0 \quad \text{… (4.38)}$$

As $x = R\theta$, equation (4.33) reduces to

$$\frac{(2\mu+\chi)}{2}\frac{\partial^2 \vec{V}_X}{\partial y^2}+\chi\frac{\partial v_3}{\partial y}-\frac{1}{R}\frac{\partial p}{\partial \theta}=0 \quad \text{… (4.39)}$$

Solving equations (4.35) and (4.36) the expressions for v_1 and V_Z are evaluated as follows

$$v_1=A_1+A_2e^{ay}+A_3e^{-ay}+\left(\frac{1}{2\mu}\frac{\partial p}{\partial z}\right)y \quad \text{… (4.40)}$$

$$\vec{V}_Z=2A_1y+2A_2\frac{N^2}{a}e^{ay}-2A_3\frac{N^2}{a}e^{-ay}+A_4+\left(\frac{1}{2\mu}\frac{\partial p}{\partial z}\right)y^2 \quad \text{… (4.41)}$$

Where, A_1, A_2, A_3 and A_4 are four constants to be evaluated from the boundary conditions and a is a non-dimensional quantity given by, $a=\frac{N}{\Lambda}=\sqrt{\frac{4\mu N^2}{\gamma}}$

Boundary conditions for v_1 and V_Z are:

(i).At y=0 $v_1=0$ and $V_z=0$

(ii).At y=h $v_1=0$ and $V_z=0$ **… (4.42)**

Using the above boundary conditions in equations (4.40) and (4.41) A_1, A_2, A_3 and A_4 are evolved as

$$A_1=-\frac{h}{4\mu}\frac{\partial p}{\partial z};\qquad A_2=-\frac{h}{4\mu}\frac{\partial p}{\partial z}\frac{1}{\left(e^{ah}-1\right)}$$

$$A_3=\frac{h}{4\mu}\frac{\partial p}{\partial z}\frac{1}{\left(1-e^{-ah}\right)}\qquad A_4=\frac{hN^2}{2\mu a}\frac{\partial p}{\partial z}\frac{\left(1+e^{-ah}\right)}{\left(1-e^{-ah}\right)}$$ **… (4.43)**

With the substitutions of A_1, A_2, A_3 and A_4 the expressions for v_1 and V_z become

$$v_1=\frac{h}{4\mu}\left(\sinh ay\right)\left\{\frac{\left(\cosh ay-1\right)}{\sinh ay}-\frac{\left(\cosh ah+1\right)}{\sinh ah}\right\}\frac{\partial p}{\partial z}+\frac{y}{2\mu}\frac{\partial p}{\partial z}$$ **… (4.44)**

$$\vec{V}_Z=\frac{y\left(y-h\right)}{2\mu}\frac{\partial p}{\partial z}+\frac{h}{2\mu}\frac{N^2}{a}\left\{\sinh ay-\frac{\left(\cosh ay-1\right)\left(\cosh ah+1\right)}{\sinh ah}\right\}\frac{\partial p}{\partial z}$$ **… (4.45)**

Similarly, solving equations (4.38) and (4.39) with the following boundary conditions

(i).At y=0 $v_3=0$ and $V_x=0$

(ii).At y=h $v_3=0$ and $V_x=U$ **… (4.46)**

The previous equations will result:

$$v_3=-\frac{h}{4\mu R}\left(\sinh ay\right)\left\{\frac{\left(\cosh ay-1\right)}{\sinh ay}-\frac{\left(\cosh ah+1\right)}{\sinh ah}\right\}\frac{\partial p}{\partial\theta}-\frac{y}{2\mu R}\frac{\partial p}{\partial\theta}$$
$$+\frac{U}{2\left[\frac{2N^2}{a}-h\frac{\left(\cosh ah+1\right)}{\sinh ah}\right]}\left\{\sinh ay-\frac{\left(\cosh ay-1\right)\left(\cosh ah+1\right)}{\sinh ah}\right\}$$ **… (4.47)**

$$\vec{V}_X=\frac{y\left(y-h\right)}{2\mu R}\frac{\partial p}{\partial\theta}+\frac{h}{2\mu R}\frac{N^2}{a}\left\{\sinh ay-\frac{\left(\cosh ay-1\right)\left(\cosh ah+1\right)}{\sinh ah}\right\}\frac{\partial p}{\partial\theta}-$$
$$\frac{U}{2\left[\frac{2N^2}{a}-h\frac{\left(\cosh ah+1\right)}{\sinh ah}\right]}\left[\frac{2y\left(\cosh ah+1\right)}{\sinh ah}+\frac{2N^2}{a}\left(\sinh ay\right)\left\{\frac{\left(\cosh ay-1\right)}{\sinh ay}-\frac{\left(\cosh ah+1\right)}{\sinh ah}\right\}\right]$$

… (4.48)

Now, from the principle of conservation of mass as stated in equation (4.1), it follows that

$$\frac{\partial\left(\rho\vec{V}_Y\right)}{\partial y}=-\frac{\partial\rho}{\partial t}-\frac{\partial\left(\rho\vec{V}_X\right)}{\partial x}-\frac{\partial\left(\rho\vec{V}_Z\right)}{\partial z} \qquad \text{… (4.49)}$$

Integrating both sides with respect to *y* within the limit 0 and *h*, equation (4.48) becomes:

$$\rho\left(\vec{V}_h-\vec{V}_0\right)=-\int_0^h\frac{\partial\rho}{\partial t}dy-\int_0^h\frac{\partial\left(\rho\vec{V}_X\right)}{\partial x}dy-\int_0^h\frac{\partial\left(\rho\vec{V}_Z\right)}{\partial z}dy \qquad \text{… (4.50)}$$

Where $\left(V_y\right)_{y=h}=V_h \quad and \quad \left(V_y\right)_{y=0}=V_0$

As the upper limit *h* is the function of the coordinates *x*, *z* the integration before differentiation can be performed by using Leibnitz's rule and using the boundary conditions that

(i). At y=0 $V_x=0$ and $V_z=0$

(ii) At y=h $V_x=U$ and $V_z=0$ } … (4.51)

And noting that $V_h=U\frac{\partial h}{\partial x}+\frac{\partial h}{\partial t}$ and $V_0=0$, the following equation will result:

$$\frac{\partial}{\partial x}\left[\frac{\rho h}{12\mu}\left\{h^2+12\Lambda^2-6N\Lambda h\coth\frac{Nh}{2\Lambda}\right\}\frac{\partial p}{\partial x}\right]+\frac{\partial}{\partial z}\left[\frac{\rho h}{12\mu}\left\{h^2+12\Lambda^2-6N\Lambda h\coth\frac{Nh}{2\Lambda}\right\}\frac{\partial p}{\partial z}\right]=\frac{\partial}{\partial x}\left(\frac{\rho Uh}{2}\right)+\frac{\partial(\rho h)}{\partial t} \qquad \text{… (4.52)}$$

For incompressible fluid flow equation (4.50) reduces to give the Reynolds equation for incompressible fluid flow in micropolar lubrication:

$$\frac{\partial}{\partial x}\left[\frac{h^3}{\mu}\Phi(\Lambda,N,h)\frac{\partial p}{\partial x}\right]+\frac{\partial}{\partial z}\left[\frac{h^3}{\mu}\Phi(\Lambda,N,h)\frac{\partial p}{\partial z}\right]=6\frac{\partial(Uh)}{\partial x}+12\frac{\partial h}{\partial t} \qquad \text{… (4.53)}$$

Where, $\Phi(\Lambda,N,h)=\left\{1+12\frac{\Lambda^2}{h^2}-6\frac{N\Lambda}{h}\coth\frac{Nh}{2\Lambda}\right\}$ … (4.54)

Introducing the rotating coordinate system and considering that the journal centre is rotating an angular velocity $\boldsymbol{\omega}_p$, equation (4.53) becomes:

$$\frac{\partial}{\partial x}\left[\frac{h^3}{\mu}\Phi(\Lambda,N,h)\frac{\partial p}{\partial x}\right]+\frac{\partial}{\partial z}\left[\frac{h^3}{\mu}\Phi(\Lambda,N,h)\frac{\partial p}{\partial z}\right]=6\frac{\partial(Uh)}{\partial x}+12\frac{\partial h}{\partial t}-12\omega_p\frac{\partial h}{\partial \theta} \quad \textbf{… (4.55)}$$

Equation (4.55) represents the modified Reynolds equation in rotating coordinate system in micropolar lubrication.

CHAPTER 5 STEADY STATE CHARACTERISTICS OF FINITE HYDRODYNAMIC JOURNAL BEARING

5.1 Introduction

This chapter deals with the theoretical analysis of the steady state characteristics of finite journal bearings lubricated with micropolar fluids. The steady state analysis is important for the subsequent linear analysis for determining the threshold of instability of the journal bearings.

Prakash and Sinha [52] studied the steady state characteristics of an infinitely long journal bearing considering a two dimensional flow field. Huang *et al* .[60], Khonsari and Brewe [61] made same study on the steady state characteristics of journal bearing system lubricated with incompressible micropolar lubricant. In the present chapter a comprehensive parametric study has been made of the steady state characteristics *viz.* load parameter, and attitude angle, of the journal/bearing systems lubricated with micropolar fluids.

In the analysis the governing modified Reynolds equation in the non-dimensional form satisfying the boundary conditions has been solved by finite difference technique with successive over-relaxation scheme. The steady state non-dimensional pressure profiles thus obtained is used to determine the steady state characteristics mentioned above. The results of the analysis are compared with the similar available results of earlier authors.

5.2 Steady State Theoretical Analysis

5.2.1 Governing Equation for Steady State

A schematic diagram of a journal bearing in micropolar lubrication with the appropriate coordinate system used for the purpose of analysis is shown in *figure.5.1*. The journal is considered to rotate 45^0 with a steady angular velocity about its axis.

The governing modified Reynolds equation (4.52) is:

$$\frac{\partial}{\partial x}\left[\frac{\rho h}{12\mu}\left\{h^2+12\Lambda^2-6N\Lambda h\coth\frac{Nh}{2\Lambda}\right\}\frac{\partial p}{\partial x}\right]+\frac{\partial}{\partial z}\left[\frac{\rho h}{12\mu}\left\{h^2+12\Lambda^2-6N\Lambda h\coth\frac{Nh}{2\Lambda}\right\}\frac{\partial p}{\partial z}\right]$$
$$=\frac{\partial}{\partial x}\left(\frac{\rho U h}{2}\right)+\frac{\partial(\rho h)}{\partial t}$$

And the governing modified Reynolds equation (4.52) for two-dimensional flow of micropolar lubricant under steady state condition is written as:

$$\frac{\partial}{\partial x}\left[\frac{{h_0}^3}{\mu}\Phi(\Lambda,N,h_0)\frac{\partial p_0}{\partial x}\right]+\frac{\partial}{\partial z}\left[\frac{{h_0}^3}{\mu}\Phi(\Lambda,N,h_0)\frac{\partial p_0}{\partial z}\right]=6U\frac{\partial h_0}{\partial x} \qquad \textbf{… (5.1)}$$

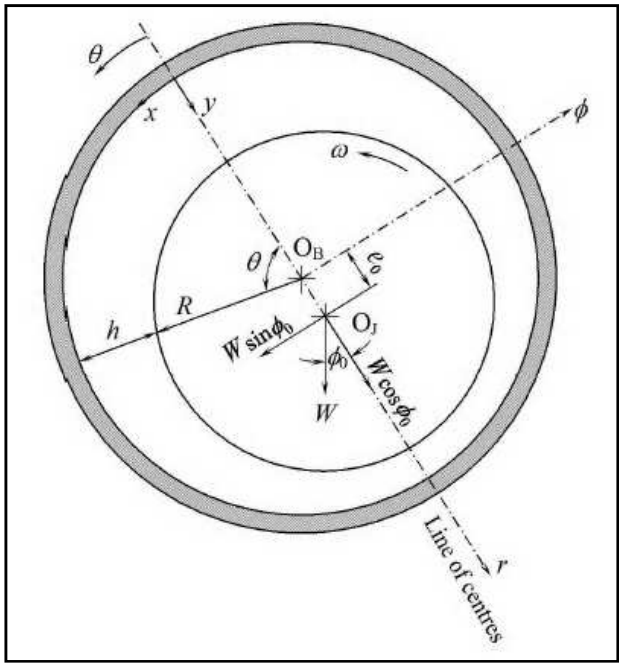

Figure 5.1: Hydrodynamic Journal Bearing Under Steady State Condition

With the following substitutions

$$\theta=\frac{x}{R},\qquad \bar{z}=\frac{2z}{L},\qquad \bar{h}_0=\frac{h_0}{C},\qquad \bar{p}_0=\frac{p_0C^2}{\mu\omega R^2},\qquad l_m=\frac{C}{\Lambda}$$

Equation (5.1) will reduce to its non-dimensional form as:

$$\frac{\partial}{\partial\theta}\left[\bar{g}(l_m,N,\bar{h}_0)\frac{\partial\bar{p}_0}{\partial\theta}\right]+\left(\frac{D}{L}\right)^2\frac{\partial}{\partial\bar{z}}\left[\bar{g}(l_m,N,\bar{h}_0)\frac{\partial\bar{p}_0}{\partial\bar{z}}\right]=\frac{1}{2}\frac{\partial\bar{h}_0}{\partial\theta} \qquad \textbf{… (5.2)}$$

Where; $\bar{\Phi}(l_m,N,\bar{h}_0)=\left\{1+\frac{12}{\bar{h}_0^2l_m^2}-6\frac{N}{\bar{h}_0l_m}\coth\left(\frac{Nl_m\bar{h}_0}{2}\right)\right\}$

and $\bar{g}\left(l_m, N, \bar{h}_0\right) = \frac{\bar{h}_0^3}{12}\bar{\Phi}\left(l_m, N, \bar{h}_0\right) = \frac{\bar{h}_0^3}{12} + \frac{\bar{h}_0}{l_m^2} - \frac{N\bar{h}_0^2}{2l_m}\coth\left(\frac{Nl_m\bar{h}_0}{2}\right)$

As $\bar{h}_0 = 1 + \varepsilon_0 \cos\theta = \bar{h}_0(\theta)$ is a function of θ only,

$\bar{g}\left(l_m, N, \bar{h}_0\right) = \bar{g}(\theta)$ is also a function of θ only.

Equation (5.2) is further simplified to the following non-dimensional form under steady state condition for finite journal bearings

$$C_A \frac{\partial \bar{h}_0}{\partial \theta} \cdot \frac{\partial \bar{P}_0}{\partial \theta} + C_B \left\{ \frac{\partial^2 \bar{p}_0}{\partial \theta^2} + \left(\frac{D}{L}\right)^2 \frac{\partial^2 \bar{p}_0}{\partial \bar{z}^2} \right\} = \frac{1}{2}\frac{\partial \bar{h}_0}{\partial \theta} \qquad \text{… (5.3)}$$

Where,

$$C_A = \frac{\bar{h}_0^2}{4} + \frac{1}{l_m^2} - \frac{N\bar{h}_0}{l_m}\coth\left(\frac{Nl_m\bar{h}_0}{2}\right) + \frac{N^2\bar{h}_0^2}{4}\cos ech^2\left(\frac{Nl_m\bar{h}_0}{2}\right) \qquad \text{… (5.4)}$$

$$and \quad C_B = \frac{\bar{h}_0^3}{12} + \frac{\bar{h}_0}{l_m^2} - \frac{N\bar{h}_0^2}{2l_m}\coth\left(\frac{Nl_m\bar{h}_0}{2}\right) \qquad \text{… (5.5)}$$

Boundary conditions for equation (5.3) are as follows:

1. The pressures at the ends of the bearing are zero

$$\bar{p}_0(\theta, \pm 1) = 0$$

2. The pressures distribution is symmetrical about the midplane of the bearing

$$\frac{\partial \bar{p}_0(\theta, 0)}{\partial \bar{z}} = 0$$

3. Cavitation boundary condition

$$\frac{\partial \bar{p}_0(\theta_2, \bar{z})}{\partial \theta} = 0, \qquad \bar{p}_0(\theta, \bar{z}) = 0 \qquad \text{for } \theta \geq \theta_2$$

… (5.6)

where, θ_2 represents the angular coordinate at which the film cavitates.

5.2.2 Numerical Solution for Pressures

5.2.2.1 Finite Difference Method: Equation (5.3) is solved by using finite difference method with successive over-relaxation scheme as described explicitly by Castelli *et.al* [66**]** to obtain the steady state pressure distribution $\overline{P}_0$, satisfying the boundary conditions as given in equation (5.6). Following the geometrical and operational symmetry of the bearing over its midplane, the half of the bearing length is considered and the bearing surface area is divided into a number of rectangular meshes of size $\Delta\theta \times \Delta\bar{z}$ each. Representing a grid point as (i,j), where i and j represent the coordinates along $x(\theta)$ and $z(\bar{z})$ directions respectively, the first and second order derivatives of pressures are approximated by central difference method as follows:

$$\left.\begin{aligned} \frac{\partial \overline{p_0}}{\partial \theta} &= \frac{(\overline{p_0})_{i+1,j} - (\overline{p_0})_{i-1,j}}{2(\Delta\theta)} \\ \frac{\partial^2 \overline{p_0}}{\partial \theta^2} &= \frac{(\overline{p_0})_{i+1,j} - 2(\overline{p_0})_{i,j} + (\overline{p_0})_{i-1,j}}{(\Delta\theta)^2} \\ \frac{\partial^2 \overline{p}_0}{\partial \bar{z}^2} &= \frac{(\overline{p}_0)_{i,j+1} - 2(\overline{p}_0)_{i,j} + (\overline{p}_0)_{i,j-1}}{(\Delta \bar{z}^2)} \end{aligned}\right\} \quad \text{… (5.7)}$$

5.2.2.2 Pressure Profiles

With the above representations equation (5.3) can be expressed in the finite difference form as

$$(\overline{p}_0)_i = C_1(\overline{p}_0)_{i+1,j} + C_2(\overline{p}_0)_{i-1,j} + C_3(\overline{p}_0)_{i,j+1} + C_3(\overline{p}_0)_{i,j-1} + C_4 \quad \text{… (5.8)}$$

Where,

$$\left.\begin{aligned} C_0 &= 2\left[1 + \left(\frac{D}{L}\right)^2 \left(\frac{\Delta\theta}{\Delta\bar{z}}\right)^2\right] & C_1 &= \frac{1}{2}\left[1 - \frac{(C_A)_i \varepsilon_0 (\Delta\theta) Sin\theta_i}{2(C_B)_i}\right] \\ C_2 &= \frac{1}{2}\left[1 + \frac{(C_A)_i \varepsilon_0 (\Delta\theta) Sin\theta_i}{2(C_B)} \right] & C_3 &= \frac{1}{C_0}\left(\frac{D}{L}\right)^2 \left(\frac{\Delta\theta}{\Delta\bar{z}}\right)^2 \\ C_4 &= \frac{\varepsilon_0 (\Delta\theta)^2 \sin\theta_i}{2(C_B)_i} \;; \quad \theta_i = i(\Delta\theta) \end{aligned}\right\} \quad \text{… (5.9)}$$

Where, $(C_A)_i$ and $(C_B)_i$ are to be evaluated using equation (5.4)and (5.5) resp. in which $\overline{h_0} = (\bar{h}_0)_i$ and $\frac{\partial \overline{h_0}}{\partial \theta} = \left(\frac{\partial \overline{h_0}}{\partial \theta}\right)$ are to be calculated corresponding to each θ_i.

To compute the non-dimensional pressures numerically the number of divisions along θ-and z -axes *i.e.* along bearing circumference and bearing length, considering half of the bearing length, are taken as 44 and 12 respectively. Since the pressure distribution is symmetrical about z =0, it is sufficient to solve the pressure distribution for one-half of the bearing length. Iteration is started considering initial pressures at all mesh points to be zero and the computed grid pressures are modified through successive over-relaxation scheme. The convergence criterion for iteration is $\left|\frac{\sum \bar{p}_o^{n+1} - \sum \bar{p}_0^{n}}{\sum \bar{p}_0^{n+1}}\right| \leq 0.001$ where n represents the number of iterations, as specified by Castelli *et.al* [66].It is found that the rate of convergence is greatly influenced by the proper selection of the over-relaxation factor. The choice of the over-relaxation factor is done on a trial basis. However for quick convergence in some cases the over-relaxation factor may be chosen as high as 1.30. In this particular analysis it is taken as 1.03.

5.2(a) Solution Scheme

A computer program based on the analysis described in previous sections is developed to obtain static and dynamic characteristics of finite hydrodynamic journal bearing using micropolar fluid. The flow chart of an iterative scheme used to obtain the different micropolar parameters has been shown in *figure 5.2*.

1. The solution for steady state and dynamic state pressure has been obtained by taking boundary condition for pressure $\bar{p}_0, \bar{p}_1$ & $\bar{p}_2$ is equal to zero.
2. The input parameters have been taken in three separate sets based on Load carrying capacity and Altitude cycle (N^2, ε_0 & L/D) for steady state and Dynamic state characteristics.
3. the dynamic characteristics is obtained by perturbered pressure $\bar{p}_1, \bar{p}_2$ for stability analysis of the bearing in terms of critical mass parameter $\overline{M}_c$ and whirl ratio(λ_R), which not only included the steady state parameter but also the stiffness, and damping coefficient for external support is used for this. $\bar{K}$=0.0001 & $\bar{D}$= 0.001 & $\bar{Z}$ = 0.01

4. FDM method has been used to solve the convergence criterion for iteration, i.e. $\left|\frac{\sum_{p_0}^{-n+1}-\sum_{p_0}^{-n}}{\sum_{p_0}^{-n+1}}\right| \le 0.001$ for $\overline{p}_0$ and $\left|\frac{\sum_{p_i}^{n+1}-\sum_{p_i}^{n}}{\sum_{p_i}^{n+1}}\right| \le 0.001$ for $\overline{p}_1$ and $\overline{p}_2$.
5. Rate of convergence has been found by the over relaxation method.
6. The results of Newtonian fluids and present work has been compared and plotted in the form of graph in the respected section.

Table.1: Bearing geometric and micropolar fluid parameters

Bearing Geometric Parameters	
Slenderness Ratio (*L/D*)	0.5,1,1.5,2
Eccentricity Ratio (ε_o)	0.5
Micropolar Fluid Parameters	
Coupling number (N^2)	0.1,0.3,0.5,0.7,0.9
Non dimensional Characteristic length (l_m)	0.1 to 0.9

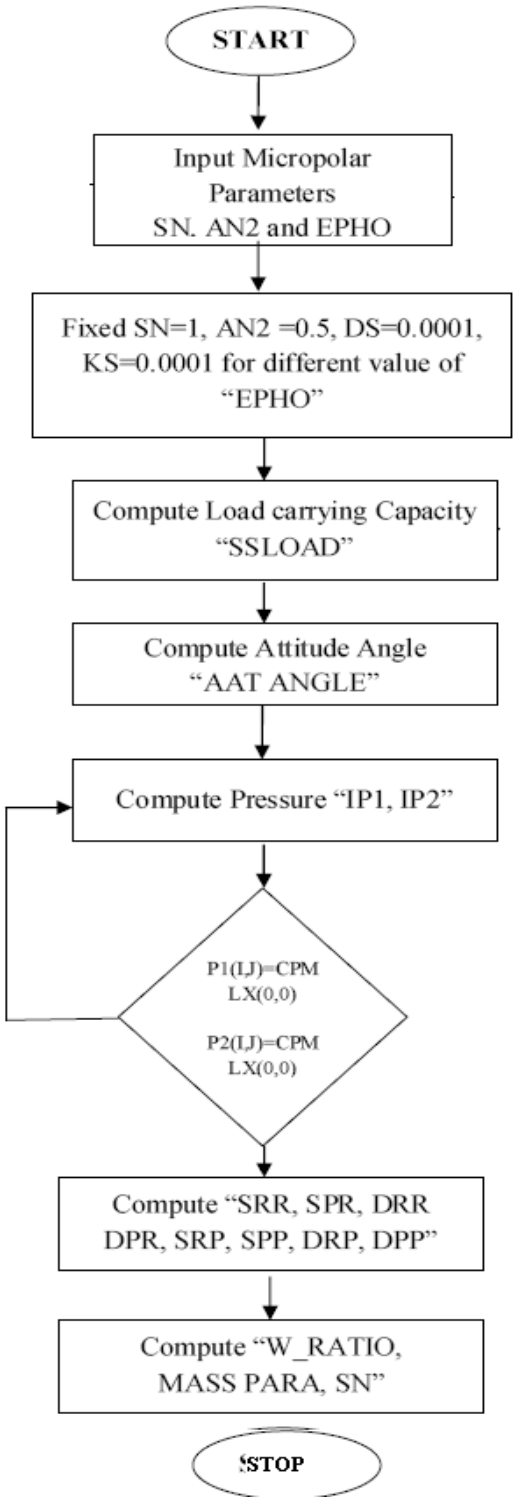

Figure 5.2 Solution Schemes for Micropolar Lubrication for Flexibly Finite Bearing

5.3 Results and Discussion

The schematic diagram of the journal is shown in *Figure .5.1.* Since the steady state characteristics *viz.,* Load carrying capacity & Attitude angle**,** dependent on the steady state film pressure $\overline{p}_0$, which, in turn, depends upon the micropolar parameters l_m, *N*, eccentricity ratio ε_o and the slenderness ratio *L/D,* detailed parametric studies are done to show their effects in the respective non-dimensional form of steady state pressure profiles, steady state load, attitude angle and the results have been compared with the respective values for Newtonian fluid, thereby validating the methods and computer codes.

5.3(a) Validation

In order to check the validity of the analysis and the solution procedure, the results for finite flexibly supported hydrodynamic bearing with micropolar fluid are obtained from the developed program and compare with the results of Das et al [68]. The validation of the dimensionless load capacity of the journal bearings as a function of l_m for *L/D* = 1.0, ε_o = 0.5, $\overline{D}_S = 0.0001$, $\overline{K}_S = 0.0001$ and $\overline{Z} = 0.01$when coupling number *N* is taken as a variable parameters with following values .

Table 1

l_m	SSLoad Newtonian	SSLoad $N^2 = 0.1$	SSLoad $N^2 = 0.3$	SSLoad $N^2 = 0.5$	SSLoad $N^2 = 0.7$	SSLoad $N^2 = 0.9$
1	3.44192	3.82378	4.90890	6.83469	11.23220	31.20350
5	3.44192	3.81146	4.74766	6.12168	8.40222	13.23850
10	3.44192	3.77762	4.46926	5.25087	6.20161	7.45124
20	3.44192	3.70758	4.09394	4.42754	4.74801	5.07048
30	3.44192	3.65257	3.90188	4.10024	4.27510	4.44345
40	3.44192	3.61347	3.79644	3.93155	4.05218	4.15983
50	3.44192	3.58547	3.72808	3.83053	3.92114	4.00332
60	3.44192	3.56481	3.68140	3.76656	3.83589	3.90095

From these value coupling number *N*, the load capacity reduces with l_m and approaches asymptotically to the Newtonian value as $l_m \to \infty$At a finite value of l_m the load parameter increases as coupling number is increased, also shown in *figure 5.2,*

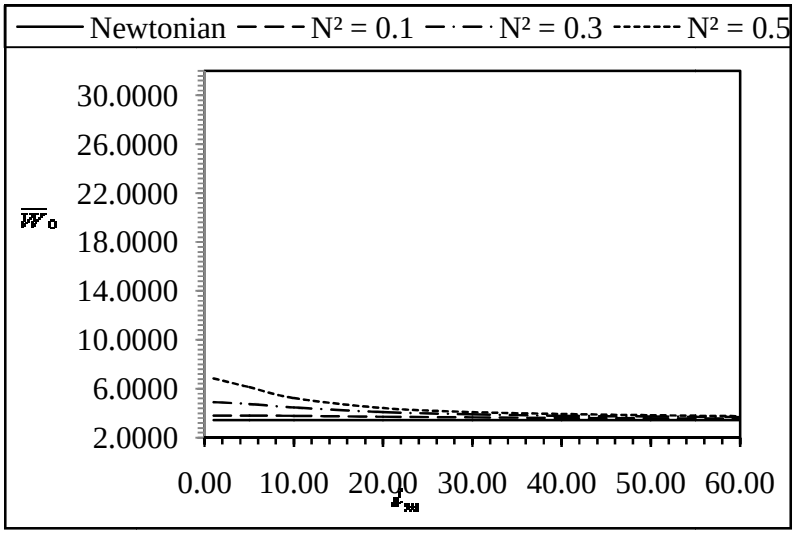

Figure 5.2.1 Validation of Results

5.3.1 Load Carrying Capacity

5.3.1(a) Steady State Effect of Coupling Number (*N*)

Figure.5.2 (a) shows the variation of the dimensionless load capacity of the journal bearings as a function of l_m for *L/D* = 1.0, ε_o = 0.5, $\overline{D}_S = 0.0001$, $\overline{K}_S = 0.0001$ and $\overline{Z} = 0.01$when coupling number *N* is taken as a parameter. It is found from the figure that for any coupling number *N*, the load capacity reduces with l_m and approaches asymptotically to the Newtonian value as $l_m \to \infty$At a finite value of l_m the load parameter increases as coupling number is increased, The reason is that an increase in N means an enhanced coupling between the angular and linear momentum of the micro-particles, which results on increased effective viscosity, which, in turn, increase the non dimensional pressure and thereby the load carrying capacity. Moreover, as $l_m \to 0$ the load parameter increases rapidly as *N* increases. This is expected since the micropolar effect will be significant either when the characteristic material length is large or the clearance is small. The second case is very important here as *C* is usually very small in hydrodynamic journal bearing. As $l_m \to 0$ the velocity and the other flow characteristics will reduce to their equivalents in the Newtonian theory with μ everywhere replaced by $\left(\mu + \frac{1}{2}\chi\right)$, as gradient of microrotational velocity across film thickness is very small. Hence effectively the viscosity has been enhanced. So, when the non-dimensional load has been referred to the Newtonian viscosity, it is increased by a factor

$\left(\mu+\frac{1}{2}\chi\right)/\mu$ at $l_m \to 0$. The decrease in the load capacity to the asymptotic value at $l_m \to \infty$ can be explained by the fact that an increase in l_m indicates a decrease in the characteristics length of the substructure, which will be vanished as $l_m \to \infty$ and thus the micropolar fluid will then reduce to a Newtonian fluid in its behavior.. $\left(\mu+\frac{1}{2}\chi\right)/\mu$ is equal to $\{1/(1-N^2)\}$ by virtue of definition of *N*. So at $l_m \to 0$ at higher value of *N*, $\{1/(1-N^2)\}$ is more and so $\overline{W_o}$ is more. In between $l_m \to 0$ and $l_m \to \infty$, at $N \neq 0$, the effect of angular momentum equation will modify Reynolds' equation through coupling number. Hence following are the same explanation as that given for the steady state pressure; the enhanced pressure will increase the non-dimensional load carrying capacity.

5.3.1 (b) Steady State Effect of Eccentricity Ratio (ε_o)

Figure .5.2 (b) shows the variation of load parameter with l_m for N^2 = 0.5, *L/D* = 1.0, $\overline{D_S} = 0.0001$, $\overline{K_S} = 0.0001$ and $\overline{Z} = 0.01$, when ε_o is considered as a parameter. It can be discerned that for a particular value of l_m, the non-dimensional load carrying capacity though increases in both types of lubrication as ε_o is increased, the rate of increase in $\overline{W_o}$ in micropolar lubrication is found to be more rapid than that in the Newtonian lubrication. It is also found that the load parameter at any eccentricity ratio is considerably higher than that for Newtonian value at lower values of l_m and converges to that for Newtonian fluid as $l_m \to \infty$.

5.3.1 (c) Effect of Slenderness Ratio (*L/D*)

Variation of load parameter with *l*m for N^2 = 0.5, $\varepsilon_o = 0.5$, $\overline{D_S} = 0.0001$, $\overline{K_S} = 0.0001$ and $\overline{Z} = 0.01$, when *L/D* ratio is considered as a parameter is shown in *figure 5.2 (c).* A scrutiny of the figure reveals that as *L/D* increases the value of load parameter also increases. For any *L/D* ratio the load parameter in micropolar fluid asymptotically converges to that for the Newtonian fluid as l_m approaches infinity. The load parameter in micropolar fluid increases at the higher rate than that in the Newtonian fluid at higher values of *L/D.*

5.3.2 Steady State Attitude Angle

5.3.2 (a)Effect of Coupling Number (*N*)

Figure .5.3 (a) shows the variation of the attitude angle with micropolar parameter l_m for

L/D = 1.0, ε_o = 0.5, $\overline{D}_S = 0.0001$, $\overline{K}_S = 0.0001$ and $\overline{Z} = 0.01$ when coupling number *N* as treated a parameter. It can be seen from the figure that for a particular value of l_m attitude angle decreases as *N* is increased. Furthermore, as l_m increases the values of the attitude angle converge asymptotically to that for the Newtonian fluid. For any coupling number, attitude angle initially decreases with increase in l_m reaching a minimum and then reversing the trend as l_m is further increased. It is found that the optimum value of l_m at which ϕ_0 becomes a minimum increases with a decrease in *N*. It can be demonstrated that to the left of the optimum l_m, micropolar effect becomes significant and to the right of this micropolar effect diminishes. Further at l_m = 0, the attitude angle remains the same as that for the Newtonian fluid. The reason is that components of non-dimensional forces along the line of centers and perpendicular to it will be increased by the same factor $\left(\mu + \frac{1}{2}\chi\right)/\mu$ and the attitude angle being the function of the ratio of the two will remain unaffected.

5.3.2 (b) Effect of Eccentricity Ratio (ε_o)

Effect of the eccentricity ratio on attitude angle has been shown in *Fig.5.3 (b)*, for N^2 = 0.5, *L/D* = 1.0, $\overline{D}_S = 0.0001$, $\overline{K}_S = 0.0001$ and $\overline{Z} = 0.01$. It is found from the figure that at any l_m, attitude angle decreases with increase in ε_o. Furthermore, the effect of micropolar parameter l_m becomes more pronounced at higher ε_o.The optimum micropolarity is found to be almost independent of ε_o and occurs at l_m around 10.0.

5.3.2 (c) Effect of Slenderness Ratio (*L/D*)

Figure.5.3 (c) shows the variation of attitude angle with l_m for N^2 = 0.5, ε_o = 0.5, $\overline{D}_S = 0.0001$, $\overline{K}_S = 0.0001$, $\overline{Z} = 0.01$ and *L/D* ratio as a parameter. The scrutiny of the figure reveals that as *L/D* ratio increases ϕ_0 increases for any value of l_m. There is an optimum l_m for pronounced micropolar effect. This optimum value is again found to be marginally affected by *L/D* ratio and occurs at around l_m = 10.0 for present case of study. At higher values of l_m attitude angle converges to that for Newtonian fluid at any *L/D* ratio. It is further found that below the optimum value of l_m the attitude angle rapidly increases to that for Newtonian fluid at l_m = 0. The difference in the values of ϕ_0 in the micropolar fluid and that in the Newtonian fluid is found almost unaffected by the change in *L/D* value.

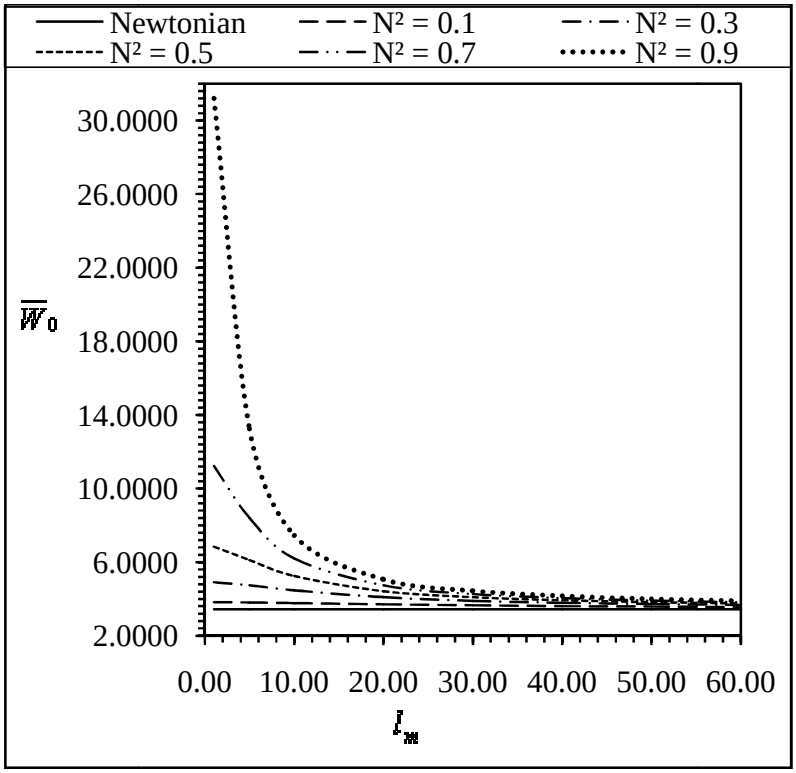

Figure 5.2 (a): Variation of $\overline{W}_0$ with l_m for various values of N^2.

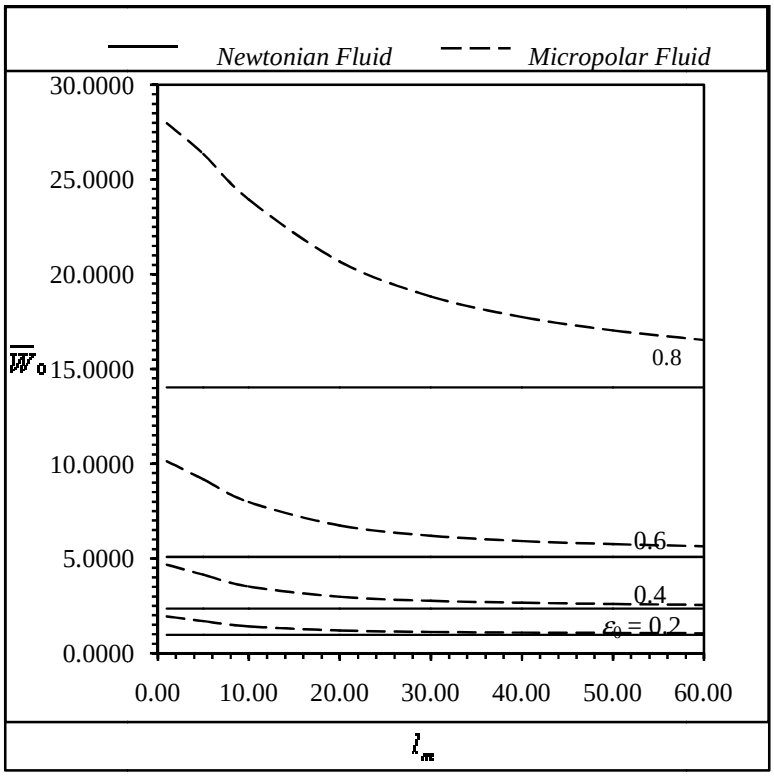

Figure 5.2 (b): Variation of $\overline{W}_0$ with l_m for various values of ε_0.

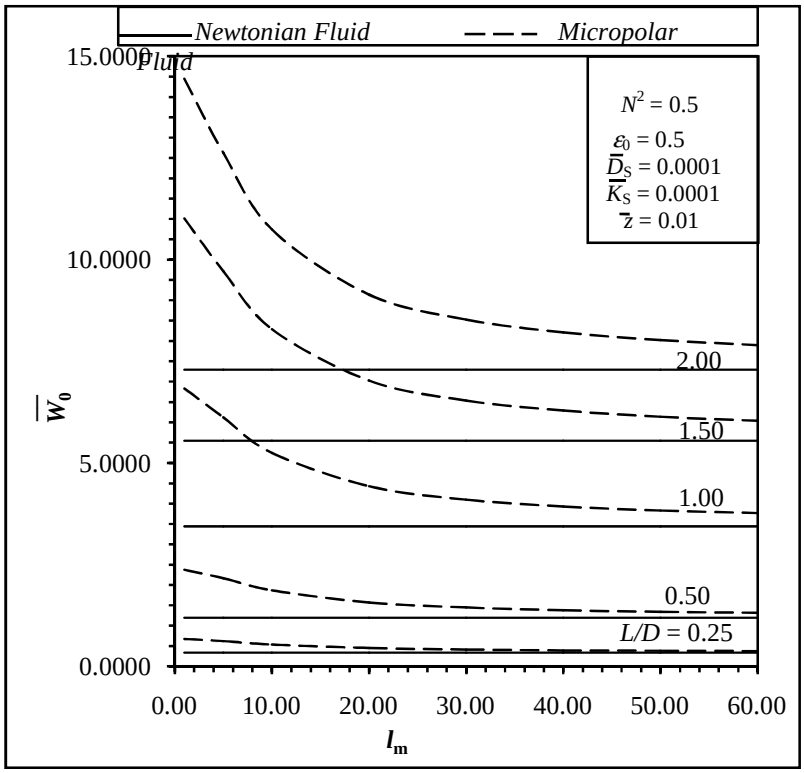

Figure 5.2 (c): Variation of $\bar{W}_0$ with l_m for various values of *L/D*-ratio.

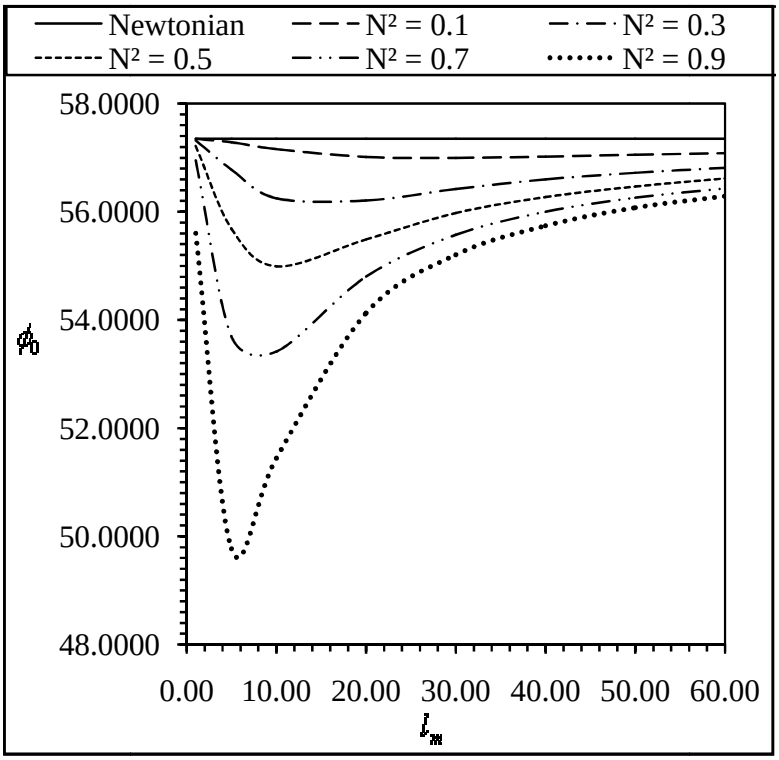

Figure 5.3 (a): Variation of ϕ_0 with l_m for various values of N^2

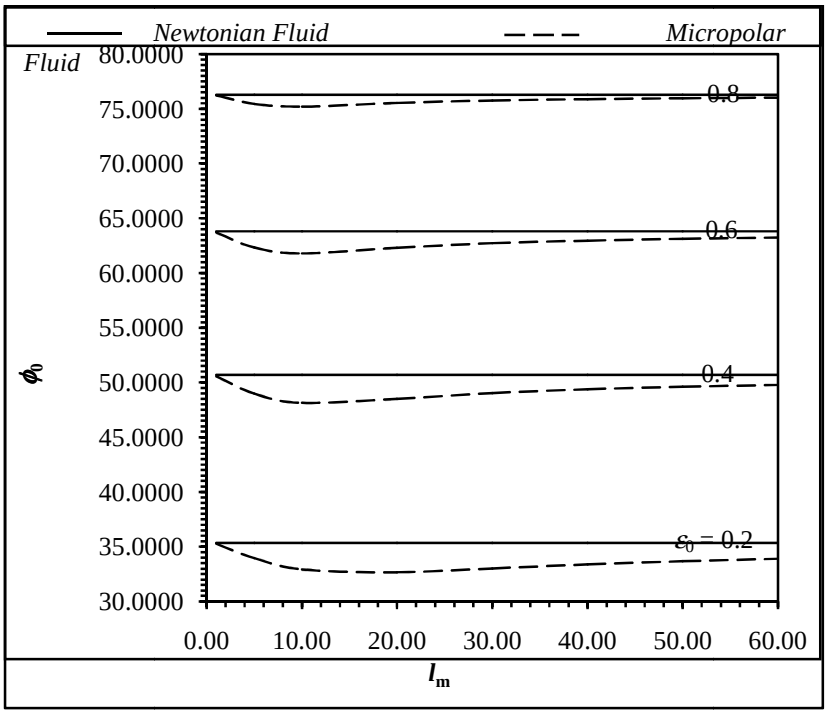

Figure 5.3 (b): Variation of ϕ_0 with l_m for various values of ε_0

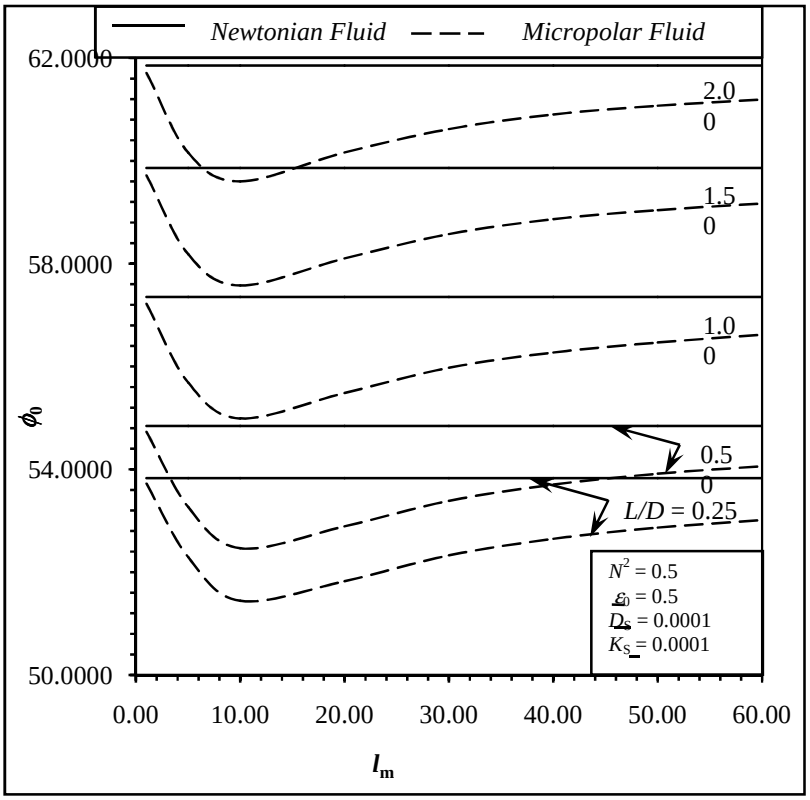

Figure 5.3 (c): Variation of ϕ_0 with l_m for various values of L/D ratio.

CHAPTER 6 DYNAMIC STATE CHARACTERISTICS OF FINITE HYDRODYNAMIC JOURNAL BEARING

6.1 Introduction

Dynamic analysis of finite hydrodynamic journal bearings lubricated with micropolar lubrication regime. A linearised technique in the form of small order perturbations of eccentricity ratio (ε_0) and attitude angle (ϕ_0) has been adopted to simplify Reynolds Equation and Equations of Motion. This method eliminates the time dependent terms and the dynamic pressure can be computed conveniently by using the finite difference method with successive over-relaxation scheme.

Perturbed pressures enables one to compute the four components of stiffness and damping coefficients of the bearings by the numerical integration of the perturbed pressure fields along the line of centers and perpendicular to the line of centers.

6.1.1 Stiffness and Damping

It will be shown subsequently that the real parts of these integrals will give to some scale the components of stiffness and the imaginary parts the components of damping coefficients.

6.1.2 Oil Whirl

Apart from the stiffness and damping coefficients another dynamic quantity is the threshold of oil whirl stability, an important phenomenon exhibited by rotor/bearing system. Because of the oil whirl, the shaft center shifts away from the static equilibrium position, whirls in an orbit and may ultimately come in contact with the bearing surface, and the bearing may fail due to seizure. Therefore, a study of oil whirl instability is important in bearing design. Oil whirl can be induced by several conditions including:

1. Light dynamic and preload forces
2. Excessive bearing wear or clearance
3. A change in oil properties
4. An increase or decrease in oil pressure or oil temperature; improper bearing design (sometimes an over design for the actual shaft loading)
5. Fluid leakage in the shroud of blades and shaft labyrinth seals
6. Change in internal damping (hysteretic, or material damping, or dry (coulomb) friction)

7. Gyroscopic effects, especially on overhung rotors with excessive overhang.

Keeping this in view, the threshold for oil whirl for a rigid rotor in self acting cylindrical journal bearings of finite length lubricated with micropolar fluid has been analyzed theoretically. In this analysis, the journal is also assumed to execute small harmonic oscillation about its static equilibrium position, such that first order perturbation can be applied without serious error. The equations of motion of the journal have been written using the oil stiffness and damping coefficients, and the resulting equations have been investigated for oil whirl stability.

The results of the analysis are shown in the form of graphs and the effects of various parameters like micropolar parameters, eccentricity ratio, and slenderness ratio are studied and discussed.

6.2 Dynamic State Theoretical Analysis for Finite Bearing

6.2.1 Governing equation for dynamic: A schematic diagram of a journal bearing in micropolar lubrication with the appropriate coordinate system used for the purpose of analysis is shown in Fig 6.1. The journal is considered to rotate with a steady angular velocity ω about its axis and it is further assumed that the journal undergoes a steady whirl in an elliptic orbit with a frequency ω_p about its mean steady state position. The governing modified Reynolds equation (4.52) for two-dimensional flow of micropolar lubricant with the following substitutions:

$$\left.\begin{aligned} &\theta = \frac{x}{R}, \quad \bar{z} = \frac{2z}{L}, \qquad \bar{h} = \frac{h}{C}, \\ &\bar{p} = \frac{pC^2}{\mu\omega R^2}, \quad l_m = \frac{C}{\Lambda}, \qquad \tau = \omega t \end{aligned}\right\} \qquad \text{…(6.1)}$$

will reduce to its non-dimensional form as

$$\frac{\partial}{\partial\theta}\left[\bar{g}\left(l_m, N, \bar{h}\right)\frac{\partial\bar{p}}{\partial\theta}\right] + \left(\frac{D}{L}\right)^2 \frac{\partial}{\partial\bar{z}}\left[\bar{g}\left(l_m, N, \bar{h}\right)\frac{\partial\bar{p}}{\partial\bar{z}}\right] = \frac{1}{2}\left(1 - 2\phi'\right)\frac{\partial\bar{h}}{\partial\theta} + \frac{\partial\bar{h}}{\partial\tau} \qquad \text{…(6.2)}$$

Where, $\bar{\Phi}\left(l_m, N, \bar{h}\right) = \left\{1 + \frac{12}{\bar{h}^2 l_m^2} - \frac{6N}{\bar{h} l_m}\coth\left(\frac{N l_m \bar{h}}{2}\right)\right\}$

$$\phi' = \frac{\partial \phi}{\partial \tau} \quad and \quad \bar{g}\left(l_m, N, \bar{h}\right) = \frac{\bar{h}^3}{12}\bar{\Phi}\left(l_m, N, \bar{h}\right) = \frac{\bar{h}^3}{12} + \frac{\bar{h}}{l_m^2} - \frac{N\bar{h}^2}{2l_m}\coth\left(\frac{Nl_m\bar{h}}{2}\right)$$

As $\bar{h} = \bar{h}(\theta)$ is a function of only. $\bar{g}$ (l_m,N,$\bar{h}$) = $\bar{g}$ ( ) is also function of only.

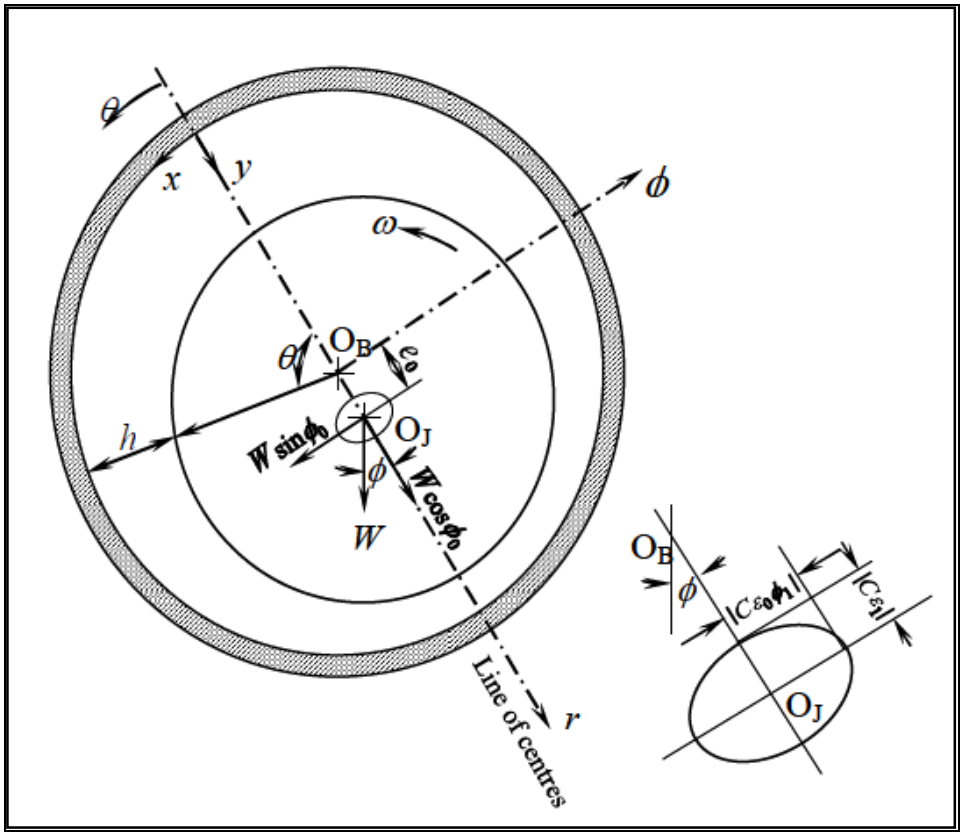

Figure 6.1: Hydrodynamic Journal Bearings under Dynamic Operating Condition

6.2.2 Perturbation Technique

The concept of the perturbation technique is to provide small order perturbation to the eccentricity ratio and attitude angle assuming the journal to execute small harmonic oscillation about its static equilibrium position, to eliminate the time dependent terms without serious error.

First order perturbation method is utilized for non-dimensional pressure and local film thickness with assumption that the journal whirls about its mean steady state position given by the eccentricity ratio ($_0$) with amplitudes **Re** ($\varepsilon_1 e^{i\lambda_R t}$) and **Re** ($\varepsilon_0 e^{i\lambda_R t}$) *along* the line of

centers and perpendicular to the line of centers respectively for which the non-dimensional pressure and local film thickness will be as follows

$$\bar{p} = \bar{p}_0 + \bar{p}_1 \varepsilon_1 e^{i\lambda R\tau} + \bar{p}_2 \varepsilon_0 \phi_1 e^{i\lambda R\tau} \quad \textbf{… (6.3)}$$

$$\bar{h} = \bar{h}_0 + \varepsilon_1 e^{i\lambda_R \tau} \cos\theta + \varepsilon_0 \phi_1 e^{i\lambda_R \tau} \sin\theta \quad \textbf{… (6.4)}$$

Where,

$\bar{h}_0 = 1 + \varepsilon_0 \cos\theta$; $\quad \varepsilon = \varepsilon_0 + \varepsilon_1 e^{i\lambda_R \tau}$;

$\phi = \phi_0 + \phi_1 e^{i\lambda_R \tau}$ and $\lambda_R = \dfrac{\omega_p}{\omega}$

The parameters with suffix '0' correspond to steady-state condition.

Substituting equation (6.3) and (6.4) into equation (6.2) and collecting the first order terms of $\varepsilon_1$and $\varepsilon_0 \phi_1$ the following two equations are obtained:

$$C_A \frac{\partial \bar{h}_0}{\partial\theta}\frac{\partial \bar{p}_1}{\partial\theta} + \left\{-C_A \sin\theta + (C_C \cos\theta)\frac{\partial \bar{h}_0}{\partial\theta}\right\}\frac{\partial \bar{p}_0}{\partial\theta} + C_B\left\{\frac{\partial^2 \bar{p}_1}{\partial\theta^2} + \left(\frac{D}{L}\right)^2 \frac{\partial^2 \bar{p}_1}{\partial \bar{z}^2}\right\}$$

$$+ (C_A \cos\theta)\left\{\frac{\partial^2 \bar{p}_0}{\partial\theta^2} + \left(\frac{D}{L}\right)^2 \frac{\partial^2 \bar{p}_0}{\partial \bar{z}^2}\right\} = -\frac{1}{2}\sin\theta + i\lambda_R \cos\theta \quad \textbf{… (6.5)}$$

$$C_A \frac{\partial \bar{h}_0}{\partial\theta}\frac{\partial \bar{p}_2}{\partial\theta} + \left\{C_A \cos\theta + (C_C \sin\theta)\frac{\partial \bar{h}_0}{\partial\theta}\right\}\frac{\partial \bar{p}_0}{\partial\theta} + C_B\left\{\frac{\partial^2 \bar{p}_2}{\partial\theta^2} + \left(\frac{D}{L}\right)^2 \frac{\partial^2 \bar{p}_2}{\partial \bar{z}^2}\right\}$$

$$+ (C_A \sin\theta)\left\{\frac{\partial^2 \bar{p}_0}{\partial\theta^2} + \left(\frac{D}{L}\right)^2 \frac{\partial^2 \bar{p}_0}{\partial \bar{z}^2}\right\} = \frac{1}{2}\cos\theta + i\lambda_R\left(\sin\theta - \frac{1}{\varepsilon_0}\frac{\partial \bar{h}_0}{\partial\theta}\right) \quad \textbf{… (6.6)}$$

Where, C_A and C_B are obtained from equation (5.4) and (5.5) resp.

and

$$C_C = \frac{\bar{h}_0^2}{2} + N^2 \bar{h}_0 \cos ech^2\left(\frac{Nl_m \bar{h}_0}{2}\right) - \frac{N}{l_m}\coth\left(\frac{Nl_m \bar{h}_0}{2}\right)$$

$$- \frac{N^3 l_m \bar{h}_0^2}{4}\cos ech^2\left(\frac{Nl_m \bar{h}_0}{2}\right)\coth\left(\frac{Nl_m \bar{h}_0}{2}\right) \quad \textbf{… (6.7)}$$

Equations (6.5) and (6.6) represent the governing differential equations for perturbed pressures.

The boundary conditions for the perturbed pressures are as follows:

1. The perturbed pressures at the ends of the bearing are zero

$$\bar{p}_1(\theta,\pm 1) = \bar{p}_2(\theta,\pm 1) = 0 \qquad \text{… (6.8)}$$

2. The perturbed pressure distributions are symmetrical about the midplane of the bearing

$$\frac{\partial \bar{p}_1(\theta,0)}{\partial \bar{z}} = \frac{\partial \bar{p}_2(\theta,0)}{\partial \bar{z}} = 0 \qquad \text{… (6.9)}$$

3. All perturbed pressure in the cavitated zone are zero

$$\bar{p}_1(\theta_1, \bar{z}) = \bar{p}_2(\theta_2, \bar{z}) = 0,$$

$$\bar{p}_1(\theta, \bar{z}) = \bar{p}_2(\theta, \bar{z}) = 0, \qquad \text{for } \theta \geq \theta_2 \qquad \text{… (6.10)}$$

Where, θ_2 represents the angular coordinate where the film cavitates.

6.2.3. Numerical Solution for Pressures

6.2.3.1. Finite Difference Method

Equations (6.5) and (6.6) are solved by using finite difference method with successive over relaxation scheme discussed by **Castelli *et al* [66]** to obtain the perturbed pressure distributions $\bar{p}_1$ and $\bar{p}_2$, satisfying the boundary conditions as given in equations (6.8), (6.9), (6.10). Following the geometrical and operational symmetry of the bearing over its mid-plane, the half of the bearing length is considered and the bearing surface area is divided into a number of rectangular meshes of size $\left(\Delta\theta \times \Delta\bar{z}\right)$ each. The first and second order derivatives of pressures are approximated by central difference method as follows:

$$\left.\begin{aligned} \frac{\partial \bar{p}_n}{\partial \theta} &= \frac{(\bar{p}_n)_{i+1,j} - (\bar{p}_n)_{i-1,j}}{2(\Delta\theta)} \\ \frac{\partial^2 \bar{p}_n}{\partial \theta^2} &= \frac{(\bar{p}_n)_{i+1,j} - 2(\bar{p}_n)_{i,j} + (\bar{p}_n)_{i-1,j}}{(\Delta\theta)^2} \\ \frac{\partial^2 \bar{p}_n}{\partial \bar{z}^2} &= \frac{(\bar{p}_n)_{i,j+1} - 2(\bar{p}_n)_{i,j} + (\bar{p}_n)_{i,j-1}}{(\Delta\bar{z})^2} \end{aligned}\right\} \quad \text{Where, n=1, 2} \qquad \text{… (6.11)}$$

6.2.3.2 Perturbed Pressure Equations for Dynamic Analysis

With the help of finite difference technique as stated in equation (6.11) and the boundary conditions in equation (6.8) to (6.10), the two equations (6.5) and (6.6) are reduced to give the following pressure equations

$$(\bar{p}_1)_{i,j} = C_1(\bar{p}_1)_{i+1,j} + C_2(\bar{p}_1)_{i-1,j} + C_3(\bar{p}_1)_{i,j+1} + C_3(\bar{p}_1)_{i,j-1} + C_5(\bar{p}_0)_{i,j-1} + C_6(\bar{p}_0)_{i+1,j} + C_7(\bar{p}_0)_{i-1,j} + C_8(\bar{p}_0)_{i,j+1} + C_8(\bar{p}_0)_{i,j-1} + C_9 \quad \text{… (6.12)}$$

$$(\bar{p}_2)_{i,j} = C_1(\bar{p}_2)_{i+1,j} + C_2(\bar{p}_2)_{i-1,j} + C_3(\bar{p}_2)_{i,j+1} + C_3(\bar{p}_2)_{i,j-1} + C_{10}(\bar{p}_0)_{i,j-1} + C_{11}(\bar{p}_0)_{i+1,j} + C_{12}(\bar{p}_0)_{i-1,j} + C_{13}(\bar{p}_0)_{i,j+1} + C_{13}(\bar{p}_0)_{i,j-1} + C_{14} \quad \text{… (6.13)}$$

where C_0, C_1 , C_2, and C_3 are as stated in equation (5.9) and

$$C_5 = \left(\frac{(C_A)_i}{(C_B)_i} Cos\theta_i\right);$$

$$C_6 = \frac{1}{C_0}\left[\frac{(C_A)_i}{(C_B)_i}\left\{\cos\theta_i - \frac{\Delta\theta}{2}\sin\theta_i\right\} - \frac{(C_C)_i}{2(C_B)_i}\varepsilon_0(\Delta\theta)\sin\theta_i\cos\theta_i\right];$$

$$C_7 = \frac{1}{C_0}\left[\frac{(C_A)_i}{(C_B)_i}\left\{\cos\theta_i - \frac{\Delta\theta}{2}\sin\theta_i\right\} + \frac{(C_C)_i}{2(C_B)_i}\varepsilon_0(\Delta\theta)\sin\theta_i\cos\theta_i\right];$$

$$C_8 = \left(\frac{1}{C_0}\right)\left(\frac{(C_A)_i}{(C_B)_i}\right)\left(\frac{D}{L}\right)^2\left(\frac{\Delta\theta}{\Delta\bar{z}}\right)^2\cos\theta_i;$$

$$C_9 = \frac{(\Delta\theta)^2}{2C_0(C_B)_i}(\sin\theta_i - i2\lambda_R\cos\theta_i); \qquad C_{10} = -\frac{(C_A)_i}{(C_B)_i}\sin\theta_i \quad \text{… (6.14)}$$

$$C_{11} = \frac{1}{C_0}\left[\frac{(C_A)_i}{(C_B)_i}\left\{\sin\theta_i - \frac{\Delta\theta}{2}\cos\theta_i\right\} - \frac{(C_C)_i}{2(C_B)_i}\varepsilon_0(\Delta\theta)\sin^2\theta_i\right];$$

$$C_{12} = \frac{1}{C_0}\left[\frac{(C_A)_i}{(C_B)_i}\left\{\sin\theta_i - \frac{\Delta\theta}{2}\cos\theta_i\right\} + \frac{(C_C)_i}{2(C_B)_i}\varepsilon_0(\Delta\theta)\sin^2\theta_i\right];$$

$$C_{13} = \left(\frac{1}{C_0}\right)\left(\frac{(C_A)_i}{(C_B)_i}\right)\left(\frac{D}{L}\right)^2\left(\frac{\Delta\theta}{\Delta\bar{z}}\right)^2\sin\theta_i; \; C_{14} = -\frac{(\Delta\theta)^2}{2C_0(C_B)_i}(\cos\theta_i - i4\lambda_R\sin\theta_i);$$

$$\theta_i = i(\Delta\theta)$$

where, $(C_A)_i$, $(C_B)_i$ and $(C_C)_i$ are to be evaluated by using equations (5.4),(5.6) and (6.7), in which $\bar{h}_0 = (\bar{h}_0)_i$ and $\frac{\partial \overline{h_0}}{\partial \theta} = \left(\frac{\partial \overline{h_0}}{\partial \theta}\right)_i$ are to be calculated corresponding to each θ_i.

6.2.4 Finite Bearing Stiffness and Damping Coefficients

The components of the dynamic load along the line of centers and perpendicular to the line of centers corresponding to perturbed pressure ($p_1 \varepsilon_1 e^{i\lambda_R t}$) in *R*-direction can be written as under

$$(W_d)_R e^{i\lambda_R \tau} = -2\int_0^{L/2} \int_{\theta_1}^{\theta_2} p_1 \cos\theta \varepsilon_1 e^{i\lambda_R \tau} R d\theta dz \quad \textbf{… (6.15)}$$

and $$(W_d)_\phi e^{i\lambda_R \tau} = -2\int_0^{L/2} \int_{\theta_1}^{\theta_2} p_1 \sin\theta \varepsilon_1 e^{i\lambda_R \tau} R d\theta dz \quad \textbf{… (6.16)}$$

As the journal executes small harmonic oscillation about its steady state position in an elliptic orbit, the components of dynamic load can be expressed as a spring load and viscous damping load as

$$(W_d)_R e^{i\lambda_R \tau} = S_{RR} C\varepsilon_R + D_{RR} \frac{d}{dt}(C\varepsilon_R) \quad \textbf{…(6.17)}$$

and $$(W_d)_\phi e^{i\lambda_R \tau} = S_{\phi R} C\varepsilon_R + D_{\phi R} \frac{d}{dt}(C\varepsilon_R) \quad \textbf{…(6.18)}$$

Combining equations (6.15) through (6.16), non-dimensionalising and noting that $\varepsilon_R = \varepsilon_1 e^{i\lambda R t}$ the following non-dimensional components of stiffness and damping coefficient results:

Stiffness in r-direction due to disturbance in r-direction

$$\bar{S}_{RR} = -\,\mathrm{Re}\left[2\int_0^1 \int_{\theta_1}^{\theta_2} \bar{p}_1 \cos\theta \, d\theta d\bar{z}\right] \quad \textbf{...(6.19)}$$

Stiffness in φ direction due to disturbance in r-direction

$$\bar{S}_{\phi R} = -\,\mathrm{Re}\left[2\int_0^1 \int_{\theta_1}^{\theta_2} \bar{p}_1 \sin\theta \, d\theta d\bar{z}\right] \quad \textbf{...(6.20)}$$

Damping co-efficient in r-direction due to disturbance in r-direction

$$\bar{D}_{RR} = -\,\mathrm{Im}\left[2\int_0^1 \int_{\theta_1}^{\theta_2} \bar{p}_1 \cos\theta \, d\theta d\bar{z}\right] \Big/ \lambda_R \quad \textbf{...(6.21)}$$

Damping co-efficient in φ-direction due to disturbance in r-direction

$$\overline{D}_{\phi R} = -\,\mathrm{Im}\left[2\int_0^1 \int_{\theta_1}^{\theta_2} \overline{p}_1 \sin\theta\, d\theta\, d\overline{z}\right] \Big/ \lambda_R \qquad \textbf{...(6.22)}$$

Similarly, considering dynamic displacement of the journal along Φ direction, it can be shown that:

Stiffness in r-direction due to disturbance in φ-direction

$$\overline{S}_{R\phi} = -\,\mathrm{Re}\left[2\int_0^1 \int_{\theta_1}^{\theta_2} \overline{p}_2 \cos\theta\, d\theta\, d\overline{z}\right] \qquad \textbf{...(6.23)}$$

Stiffness in φ-direction due to disturbance in φ-direction

$$\overline{S}_{\phi\phi} = -\,\mathrm{Re}\left[2\int_0^1 \int_{\theta_1}^{\theta_2} \overline{p}_2 \sin\theta\, d\theta\, d\overline{z}\right] \qquad \textbf{...(6.24)}$$

Damping co-efficient in r-direction due to disturbance in φ -direction

$$\overline{D}_{R\phi} = -\,\mathrm{Im}\left[2\int_0^1 \int_{\theta_1}^{\theta_2} \overline{p}_2 \cos\theta\, d\theta\, d\overline{z}\right] \Big/ \lambda_R \qquad \textbf{...(6.25)}$$

Damping co-efficient in φ-direction due to disturbance in φ-direction

$$\overline{D}_{\phi\phi} = -\,\mathrm{Im}\left[2\int_0^1 \int_{\theta_1}^{\theta_2} \overline{p}_2 \sin\theta\, d\theta\, d\overline{z}\right] \Big/ \lambda_R \qquad \textbf{...(6.26)}$$

where,

$$\overline{S}_{ij} = \frac{2C^3 S_{ij}}{\mu\omega R^3 L} \text{ and } \overline{D}_{ij} = \frac{2C^3 D_{ij}}{\mu R^3 L},\ i = R,\phi \text{ and } j = R,\phi$$

As the dynamic pressure distributions $\overline{p}_1$ and $\overline{p}_2$ have been obtained by finite difference method, the above components of stiffness and damping coefficients can be easily obtained by numerical integration using Simpson's 1/3-rd rule.

6.2.5. Equation of Motion for Finite Hydrodynamic Bearing

The dynamic pressure distribution $\overline{p}_1$ & $\overline{p}_2$ have been obtained by finite difference method and stiffness and damping co-efficient also have been calculated by numerical integration using Simpson's 1/3 rule. Stiffness and damping co-efficient thus obtained can now be employed to study the stability of the flexibility supported hydrodynamic oil journal bearing can be written as:

Equation of motion of rotor in ‘r’ direction is:

$$m_R\left[A_r+\frac{d^2e_r}{dt^2}-e_r\left(\frac{d\phi}{dt}\right)^2\right]+S_{rr}e_r+D_{rr}\frac{de_r}{dt}+S_{r\phi}e_\phi+D_{r\phi}\frac{de_\phi}{dt}=w_0\cos\phi \quad \textbf{… (6.27)}$$

Equation of motion of rotor in ‘Φ’ direction is:

$$m_R\left[A_\phi+\frac{d^2e_\phi}{dt^2}+2e_re_\phi\right]+S_{\phi\phi}e_\phi+D_{\phi\phi}\frac{de_\phi}{dt}+S_{\phi r}e_r+D_{\phi r}\frac{de_r}{dt}=w_0\sin\phi \quad \textbf{… (6.28)}$$

Equation of motion of the bearing (neglecting the weight of bearing) in ‘r’ direction:

$$m_b[A_r]-S_{rr}e_r-D_{rr}\frac{de_r}{dt}-S_{r\phi}e_\phi-D_{r\phi}\frac{de_\phi}{dt}=-\left(Kx_b+d\frac{dx_b}{dt}\right)\sin\phi-\left(Ky_b+d\frac{dy_b}{dt}\right)\cos\phi$$

… (6.29)

And equation of motion of bearing in ‘Φ’ direction is:

$$m_b[A_\phi]-S_{\phi\phi}e_\phi-D_{\phi\phi}\frac{de_\phi}{dt}-S_{\phi r}e_r-D_{\phi r}\frac{de_r}{dt}=-\left(Kx_b+d\frac{dy_b}{dt}\right)\cos\phi+\left(Ky_b+d\frac{dy_b}{dt}\right)\sin\phi$$

… (6.30)

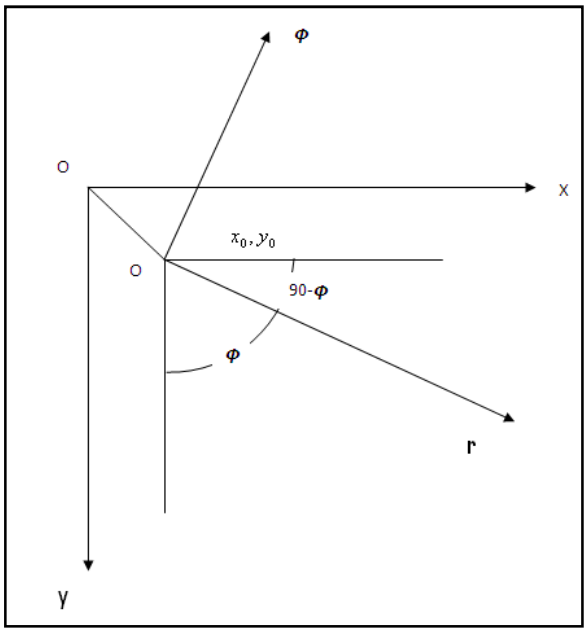

Figure 6.2: Schematic diagram of co-ordinate system

where K and d are external Stiffness and Damping co-efficient. Here for the system

$$A_r = \ddot{x}_b \sin\phi + \ddot{y}_b \cos\phi \quad \text{And} \quad A_\phi = \ddot{x}_b \cos\phi - \ddot{y}_b \sin\phi$$

Now the following substitution are made

$$x_b = c.\bar{x}_b = c\left(\bar{x}_0 + \bar{x}_1 e^{i\lambda_R t}\right); \qquad y_b = c.\bar{y}_b = c\left(\bar{y}_0 + \bar{y}_1 e^{i\lambda_R t}\right)$$

here; $\bar{x}_0$, $\bar{y}_0$ are steady state non-dimensional co-ordinates of center of bearing.

and $\bar{x}_1, \bar{y}_1, \varepsilon_1, \varepsilon_0$ & ϕ_1 are 1st order perturbation

$$\phi = \phi_0 + \phi_1 e^{i\lambda_R t}$$

$$e_r = \bar{e}_r.c = c\left(\varepsilon_0 + \varepsilon_1 e^{i\lambda_R t}\right); \qquad e_\phi = \bar{e}_\phi.c = c\left(\varepsilon_0\phi_0 + \varepsilon_0\phi_1 e^{i\lambda_R t}\right)$$

here; ε_0 =Steady state eccentricity ratio

$$\cos\phi = \cos\phi_0 - \phi_1 e^{i\lambda_R t}\sin\phi_0; \qquad \sin\phi = \sin\phi_0 - \phi_1 e^{i\lambda_R t}\cos\phi_0$$

here; ϕ_0 =steady state altitude angle

$$S_{ij} = \frac{\eta U R^2 L}{2C^3}.\bar{S}_{ij}; \qquad D_{ij} = \frac{\eta R^3 L}{2C^3}.\bar{D}_{ij} \qquad w_0 = \frac{\eta U R^2 L}{2C^3}.\bar{w}_0$$

$$T = \omega_p.t \quad : \quad \omega_p/\omega = \lambda \quad : \quad m_b/m_R = Z$$

$\bar{m} = \dfrac{m_R C w^2}{w_0}$ (Bearing stability parameter)

Now using the above substitution and equation co-efficient on both sides, we have the equation of motion in the following non-dimensional form:

$$-\lambda^2\bar{m}\bar{w}_0\left[\bar{x}_1\sin\phi_0 + \bar{y}_1\cos\phi_0\right] + \left(-\lambda^2\bar{m}\bar{w}_0 + \bar{S}_{rr} + i\lambda\bar{D}_{rr}\right)\varepsilon_1 + \left(\bar{S}_{r\phi}\varepsilon_0 + i\lambda\bar{D}_{r\phi}\varepsilon_0 + \bar{w}_0\sin\phi_0\right)\phi_1 = 0 \qquad \textbf{… (6.31)}$$

$$-\lambda^2\overline{mw}_0[\bar{x}_1\cos\phi_0-\bar{y}_1\sin\phi_0]+\left(\bar{S}_{\phi r}+i\lambda\bar{D}_{\phi r}\right)\varepsilon_1 +\left(\bar{S}_{\phi\phi}\varepsilon_0-\lambda^2\overline{mw}_0+\bar{S}_{rr}+i\lambda\bar{D}_{\phi\phi}\varepsilon_0+\overline{w}_0\cos\phi_0\right)\phi_1=0 \quad \text{... (6.32)}$$

$$\left(-\lambda^2 z\overline{mw}_0+\bar{k}+i\lambda\bar{d}\right)\sin\phi_0\bar{x}_1+\left(-\lambda^2 z\overline{mw}_0+\bar{k}+i\lambda\bar{d}\right)\cos\phi_0\bar{y}_1 +\left(\bar{S}_{rr}+i\lambda\bar{D}_{rr}\right)\varepsilon_1+\left(-\bar{S}_{r\phi}\varepsilon_0-i\lambda\bar{D}_{r\phi}\varepsilon_0+\bar{k}\bar{x}_0\cos\phi_0-\bar{k}\bar{y}_0\sin\phi_0\right)\phi_1=0 \quad \text{... (6.33)}$$

$$\left(-\lambda^2 z\overline{mw}_0+\bar{k}+i\lambda\bar{d}\right)\cos\phi_0\bar{x}_1+\left(-\lambda^2 z\overline{mw}_0-\bar{k}-i\lambda\bar{d}\right)\sin\phi_0\bar{y}_1+\left(-\bar{S}_{\phi r}-i\lambda\bar{D}_{\phi r}\right)\varepsilon_1 +\left(-\bar{S}_{\phi\phi}\varepsilon_0-i\lambda\bar{D}_{\phi\phi}\varepsilon_0-\bar{k}\bar{x}_0\sin\phi_0-\bar{k}\bar{y}_0\cos\phi_0\right)\phi_1=0 \quad \text{... (6.34)}$$

For steady state condition:

$$\bar{k}\bar{x}_0\sin\phi_0+\bar{k}\bar{y}_0\cos\phi_0=\bar{S}_{rr}\varepsilon_0+\bar{S}_{r\phi}\varepsilon_0\phi_0$$

and $$\bar{k}\bar{x}_0\cos\phi_0-\bar{k}\bar{y}_0\sin\phi_0=\bar{S}_{\phi r}\varepsilon_0+\bar{S}_{\phi\phi}\varepsilon_0\phi_0$$

From which $\bar{x}_0$ & $\bar{y}_0$ are calculated as

$$\bar{x}_0=(1/\bar{k})\left[\left(\bar{S}_{rr}\varepsilon_0+\bar{S}_{r\phi}\varepsilon_0\phi_0\right)\sin\phi_0+\left(\bar{S}_{\phi r}\varepsilon_0+\bar{S}_{\phi\phi}\varepsilon_0\phi_0\right)\cos\phi_0\right]$$

$$\bar{y}_0=(1/\bar{k})\left[\left(\bar{S}_{rr}\varepsilon_0+\bar{S}_{r\phi}\varepsilon_0\phi_0\right)\cos\phi_0-\left(\bar{S}_{\phi r}\varepsilon_0+\bar{S}_{\phi\phi}\varepsilon_0\phi_0\right)\sin\phi_0\right]$$

Now the following substitution are imposed

$$\bar{P}_1=(\bar{x}_1\sin\phi_0+\bar{y}_1\cos\phi_0)$$

$$\bar{q}_1=(\bar{y}_1\sin\phi_0-\bar{x}_1\cos\phi_0)$$

$$\bar{b}_1=(\bar{x}_0\sin\phi_0+\bar{y}_0\cos\phi_0)$$

$$\bar{b}_2=(\bar{y}_0\sin\phi_0-\bar{x}_0\cos\phi_0)$$

Therefore the equation of motion takes the configuration as

$$-\lambda^2\overline{mw}_0\bar{P}_1+\left(-\lambda^2\overline{mw}_0+\bar{S}_{rr}+i\lambda\bar{D}_{rr}\right)\varepsilon_1+\left(\bar{S}_{r\phi}\varepsilon_0-i\lambda\bar{D}_{r\phi}\varepsilon_0+\overline{w}_0\sin\phi_0\right)\phi_1=0 \quad \text{... (6.35)}$$

$$\lambda^2\overline{mw}_0\bar{q}_1+\left(\bar{S}_{\phi r}+i\lambda\bar{D}_{\phi r}\right)\varepsilon_1+\left(-\lambda^2\overline{mw}_0\varepsilon_0+\bar{S}_{\phi\phi}\varepsilon_0+i\lambda\bar{D}_{\phi\phi}\varepsilon_0+\overline{w}_0\cos\phi_0\right)\phi_1=0 \quad \text{... (6.36)}$$

$$\left(-z\lambda^2\overline{mw}_0-\bar{k}-i\lambda\bar{d}\right)\bar{P}_1+\left(-\bar{S}_{rr}-i\lambda\bar{D}_{rr}\right)\varepsilon_1+\left(-\bar{S}_{r\phi}\varepsilon_0-i\lambda\bar{D}_{r\phi}\varepsilon_0-\bar{k}\bar{b}_2\right)\phi_1=0 \quad \text{... (6.37)}$$

And

$$\left(z\lambda^2\overline{m}\overline{w}_0-\overline{k}-i\lambda\overline{d}\right)\overline{q}_1+\left(-\overline{S}_{\phi r}-i\lambda\overline{D}_{\phi r}\right)\varepsilon_1+\left(-\overline{S}_{\phi\phi}\varepsilon_0-i\lambda\overline{D}_{\phi\phi}\varepsilon_0-\overline{k}\overline{b}_1\right)\phi_1=0 \quad \textbf{... (6.38)}$$

Now for non-trivial solution, the determinant of the above equations (6.35), (6.36), (6.37), and (6.38) must vanish. Equating real and imaginary parts of equation (obtained by expanding the determinant of the equations for non-trivial solution) separately to zero, the following two equations result:

$$A_{11}\overline{m}^4+A_{12}\overline{m}^3+A_{13}\overline{m}^2+A_{14}\overline{m}+A_{15}=0 \quad \textbf{... (6.39)}$$

$$A_{12}\overline{m}^3+A_{22}\overline{m}^2+A_{23}\overline{m}+A_{24}=0 \quad \textbf{... (6.40)}$$

Where;

$$A_{11}=C_{21}.\lambda^8\overline{w}_0{}^4 \quad \textbf{... (6.41)}$$

$$A_{12}=C_{22}.\lambda^6\overline{w}_0{}^3 \quad \textbf{... (6.42)}$$

$$A_{13}=C_{23}.\lambda^6\overline{w}_0{}^2+C_{24}.\lambda^4\overline{w}_0{}^2 \quad \textbf{... (6.43)}$$

$$A_{14}=C_{25}.\lambda^4\overline{w}_0+C_{27}.\lambda^2\overline{w}_0 \quad \textbf{... (6.44)}$$

$$A_{15}=C_{26}.\lambda^4+C_{28}.\lambda^2+C_{29} \quad \textbf{... (6.45)}$$

$$A_{21}=C_{31}.\lambda^6\overline{w}_0{}^3 \quad \textbf{... (6.46)}$$

$$A_{22}=C_{32}.\lambda^4\overline{w}_0{}^2 \quad \textbf{... (6.47)}$$

$$A_{23}=C_{33}.\lambda^4\overline{w}_0+C_{34}.\lambda^2\overline{w}_0 \quad \textbf{... (6.48)}$$

$$A_{24}=C_{35}.\lambda^2+C_{36} \quad \textbf{... (6.49)}$$

$$C_{21}=-Z^2\varepsilon_0 \quad \textbf{... (6.50)}$$

$$C_{22}=Z\overline{S}_{rr}\varepsilon_0+Z\overline{S}_{\phi\phi}\varepsilon_0+2Z\overline{k}\varepsilon_0+Z^2\overline{S}_{\phi\phi}\varepsilon_0+Z^2\overline{w}_0\cos\phi_0+Z\overline{k}\overline{b}_1 \quad \textbf{... (6.51)}$$

$$\begin{aligned}C_{23}=\;&\overline{D}_{rr}\overline{D}_{\phi\phi}\varepsilon_0-\overline{D}_{r\phi}\overline{D}_{\phi r}\varepsilon_0-2Z\overline{D}_{\phi r}\overline{D}_{r\phi}\varepsilon_0+\overline{d}\overline{D}_{rr}\varepsilon_0+2Z\overline{D}_{rr}\overline{D}_{\phi\phi}\varepsilon_0+\overline{d}\overline{D}_{\phi\phi}\varepsilon_0\\&+D^2\overline{D}_{rr}\overline{D}_{\phi\phi}\varepsilon_0+2Z\overline{d}\overline{D}_{rr}\varepsilon_0+2Z\overline{d}\overline{D}_{\phi\phi}\varepsilon_0-Z^2\overline{D}_{\phi r}\overline{D}_{r\phi}\varepsilon_0+\overline{d}^2\varepsilon_0\end{aligned} \quad \textbf{... (6.52)}$$

$$\begin{aligned}C_{24}=\;&-\overline{S}_{rr}\overline{S}_{\phi\phi}\varepsilon_0-\overline{S}_{rr}\overline{k}\overline{b}_1+\overline{S}_{r\phi}\overline{S}_{\phi r}\varepsilon_0+\overline{S}_{\phi r}\overline{k}\overline{b}_1+2Z\overline{S}_{r\phi}\overline{S}_{\phi r}\varepsilon_0+Z\overline{S}_{\phi r}\overline{k}\overline{b}_2-Z\overline{S}_{rr}\overline{w}_0\cos\phi_0\\&-\overline{k}\overline{S}_{rr}\varepsilon_0-2Z\overline{S}_{rr}\overline{S}_{\phi\phi}\varepsilon_0-Z\overline{k}\overline{S}_{rr}\overline{b}_1-\overline{k}\overline{S}_{\phi\phi}\varepsilon_0-\overline{k}^2\overline{b}_1+Z\overline{S}_{\phi r}\overline{w}_0\sin\phi_0-\overline{k}^2\varepsilon_0\\&-2Z\overline{k}\overline{S}_{rr}\varepsilon_0-2Z\overline{k}\overline{S}_{\phi\phi}\varepsilon_0-Z^2\overline{S}_{rr}\overline{S}_{\phi\phi}\varepsilon_0-2Z\overline{k}\overline{w}_0\cos\phi_0-Z^2\overline{S}_{rr}\overline{w}_0\cos\phi_0\\&+Z^2\overline{S}_{r\phi}\overline{S}_{\phi r}\varepsilon_0+Z^2\overline{S}_{\phi r}\overline{w}_0\sin\phi_0\end{aligned} \quad \textbf{... (6.53)}$$

$$C_{25} = 2\overline{kD}_{\phi r}\varepsilon_0 + 2\overline{dD}_{\phi r}\overline{S}_{r\phi}\varepsilon_0 + \overline{dkb}_2\overline{D}_{\phi r} + 2\overline{d}\,\overline{S}_{\phi r}\overline{D}_{r\phi}\varepsilon_0 - 2\overline{kD}_{\phi\phi}\overline{D}_{rr}\varepsilon_0 - 2\overline{d}\,\overline{S}_{rr}\overline{D}_{\phi\phi}\varepsilon_0$$
$$- 2\overline{d}\,\overline{S}_{\phi\phi}\overline{D}_{rr}\varepsilon_0 - \overline{dD}_{rr}\overline{w}_0\cos\phi_0 - \overline{dD}_{rr}\overline{kb}_1 + \overline{dD}_{\phi r}\overline{w}_0\sin\phi_0 - \overline{d}^{\,2}\overline{S}_{rr}\varepsilon_0 - \overline{d}^{\,2}\overline{S}_{\phi\phi}\varepsilon_0$$
$$- \overline{d}^{\,2}\overline{w}_0\cos\phi_0 - 2Z\overline{kD}_{\phi\phi}\overline{D}_{rr}\varepsilon_0 - 2\overline{dkD}_{rr}\varepsilon_0 - 2\overline{dkD}_{\phi\phi}\varepsilon_0 - Z\overline{dD}_{rr}\overline{S}_{\phi\phi}\varepsilon_0 - 2Z\overline{dD}_{rr}\overline{w}_0\cos\phi_0$$
$$- 2Z\overline{d}\,\overline{S}_{rr}\overline{D}_{\phi\phi}\varepsilon_0 + 2Z\overline{kD}_{\phi r}\overline{D}_{r\phi}\varepsilon_0 + 2Z\overline{d}\,\overline{S}_{r\phi}\overline{D}_{\phi r}\varepsilon_0 + 2Z\overline{dD}_{\phi r}\overline{w}_0\sin\varepsilon_0 + 2Z\overline{d}\,\overline{S}_{\phi r}\overline{D}_{r\phi}\varepsilon_0$$

... (6.54)

$$C_{26} = -\overline{d}^{\,2}\overline{D}_{rr}\overline{D}_{\phi\phi}\varepsilon_0 + \overline{d}^{\,2}\overline{D}_{r\phi}\overline{D}_{\phi r}\varepsilon_0 \qquad \textbf{... (6.55)}$$

$$C_{27} = -2\overline{k}\,\overline{S}_{r\phi}\overline{S}_{\phi r}\varepsilon_0 - \overline{k}^{\,2}\overline{S}_{\phi r}\overline{b}_2 + 2\overline{k}\,\overline{S}_{rr}\overline{S}_{\phi\phi}\varepsilon_0 + \overline{k}\,\overline{S}_{rr}\overline{w}_0\cos\phi_0 + \overline{k}^{\,2}\overline{S}_{rr}\overline{b}_1 - \overline{k}\,\overline{S}_{\phi r}\overline{w}_0\sin\phi_0$$
$$+ \overline{k}^{\,2}\overline{S}_{rr}\varepsilon_0 + \overline{k}^{\,2}\overline{S}_{\phi\phi}\varepsilon_0 + 2Z\overline{k}\,\overline{S}_{rr}\overline{S}_{\phi\phi}\varepsilon_0 + \overline{k}^{\,2}\overline{w}_0\cos\phi_0$$
$$+ 2Z\overline{k}\,\overline{S}_{rr}\overline{w}_0\cos\varepsilon_0 - 2Z\overline{k}\,\overline{S}_{r\phi}\overline{S}_{\phi r}\varepsilon_0 - 2Z\overline{k}\,\overline{S}_{\phi r}\overline{w}_0\sin\phi_0$$

... (6.56)

$$C_{28} = -\overline{d}^{\,2}\overline{S}_{rr}\overline{S}_{\phi\phi}\varepsilon_0 + \overline{d}^{\,2}\overline{S}_{rr}\overline{w}_0\cos\phi_0 + \overline{k}^{\,2}\overline{D}_{rr}\overline{D}_{\phi\phi}\varepsilon_0 + 2\overline{dkD}_{rr}\overline{S}_{\phi\phi}\varepsilon_0$$
$$+ 2\overline{dkD}_{rr}\overline{w}_0\cos\phi_0 + 2\overline{dkD}_{\phi\phi}\overline{S}_{rr}\varepsilon_0 - \overline{k}^{\,2}\overline{D}_{\phi r}\overline{D}_{r\phi}\varepsilon_0 - \overline{d}^{\,2}\overline{S}_{r\phi}\overline{S}_{\phi r}\varepsilon_0 \qquad \textbf{... (6.57)}$$
$$- \overline{d}^{\,2}\overline{S}_{\phi r}\overline{w}_0\sin\phi_0 - 2\overline{dk}\,\overline{S}_{r\phi}\overline{D}_{\phi r}\varepsilon_0 - 2\overline{dkD}_{\phi r}\overline{w}_0\sin\phi_0 - 2\overline{dk}\,\overline{S}_{\phi r}\overline{D}_{r\phi}\varepsilon_0$$

$$C_{29} = -\overline{k}^{\,2}\overline{S}_{rr}\overline{S}_{\phi\phi}\varepsilon_0 - \overline{k}^{\,2}\overline{S}_{rr}\overline{w}_0\cos\phi_0 + \overline{k}^{\,2}\overline{S}_{r\phi}\overline{S}_{\phi r}\varepsilon_0 + \overline{k}^{\,2}\overline{S}_{\phi r}\overline{w}_0\sin\phi_0 \qquad \textbf{... (6.58)}$$

$$C_{31} = Z\overline{D}_{rr}\varepsilon_0 + Z\overline{D}_{\phi\phi}\varepsilon_0 + 2Z\overline{d}\varepsilon_0 + Z^2\overline{D}_{rr}\varepsilon_0 + Z^2\overline{D}_{\phi\phi}\varepsilon_0 = 0 \qquad \textbf{... (6.59)}$$

$$C_{32} = -\overline{S}_{rr}\overline{D}_{\phi\phi}\varepsilon_0 - \overline{D}_{rr}\overline{S}_{\phi\phi}\varepsilon_0 - \overline{D}_{rr}\overline{kb}_1 + \overline{S}_{r\phi}\overline{D}_{\phi r}\varepsilon_0 + \overline{D}_{\phi r}\overline{kb}_2 + \overline{S}_{\phi r}\overline{D}_{r\phi}\varepsilon_0 + 2Z\overline{D}_{\phi r}\overline{S}_{r\phi}\varepsilon_0 + Z\overline{D}_{r\phi}\overline{kb}_2$$
$$+ 2Z\overline{S}_{\phi r}\overline{D}_{r\phi}\varepsilon_0 - Z\overline{D}_{rr}w_0\cos\phi_0 - \overline{kD}_{rr}\varepsilon_0 + Z\overline{D}_{\phi r}w_0\sin\phi_0 - Z\overline{dk}\varepsilon_0 - 2Z\overline{d}\,\overline{S}_{\phi\phi}\varepsilon_0$$
$$- 2Z\overline{d}w_0\cos\phi_0 - Z^2\overline{S}_{\phi\phi}\overline{D}_{rr}\varepsilon_0 - Z^2\overline{D}_{rr}w_0\cos\phi_0 - Z^2\overline{S}_{rr}\overline{D}_{\phi\phi}\varepsilon_0 + Z^2\overline{D}_{\phi r}\overline{S}_{r\phi}\varepsilon_0$$
$$+ Z^2\overline{D}_{\phi r}w_0\sin\phi_0 + Z^2\overline{S}_{\phi r}\overline{D}_{r\phi}\varepsilon_0 - 2Z\overline{kD}_{rr}\varepsilon_0 - 2Z\overline{kD}_{\phi\phi}\varepsilon_0$$

... (6.60)

$$C_{33} = 2\overline{dD}_{\phi r}\overline{D}_{r\phi}\varepsilon_0 - 2\overline{dD}_{rr}\overline{D}_{\phi\phi}\varepsilon_0 - 2Z\overline{dD}_{rr}\overline{D}_{\phi\phi}\varepsilon_0 - \overline{d}^{\,2}\overline{D}_{rr}\varepsilon_0 - \overline{d}^{\,2}\overline{D}_{\phi\phi}\varepsilon_0 \qquad \textbf{... (6.61)}$$

$$
\begin{aligned}
C_{34} = & -2\overline{D}_{\phi r}\overline{S}_{r\phi}\varepsilon_0 - k\overline{D}_{r\phi}\overline{b}_2 - 2\overline{k}\overline{S}_{\phi r}\overline{D}_{r\phi}\varepsilon_0 - 2\overline{d}\overline{S}_{\phi r}k\overline{b}_2 + 2\overline{k}\overline{S}_{rr}\overline{D}_{\phi\phi}\varepsilon_0 + 2\overline{k}\overline{S}_{\phi\phi}\overline{D}_{rr}w_0\cos\phi_0 \\
& + 2\overline{d}\overline{S}_{\phi\phi}\overline{S}_{rr}\varepsilon_0 + \overline{d}\overline{S}_{rr}w_0\cos\phi_0 + \overline{dk}\overline{b}_1\overline{S}_{rr} + \overline{k}^2\overline{b}_1\overline{D}_{rr} - \overline{d}\overline{S}_{\phi r}w_0\sin\phi_0 - \overline{k}\overline{D}_{\phi r}w_0\sin\phi_0 \\
& + 2\overline{dk}\overline{S}_{rr}\varepsilon_0 + 2\overline{dk}\overline{S}_{\phi\phi}\varepsilon_0 + 2\overline{dk}w_0\cos\phi_0 + 2Z\overline{d}\overline{S}_{rr}\overline{S}_{\phi\phi}\varepsilon_0 + 2Z\overline{d}\overline{S}_{rr}w_0\cos\phi_0 + \overline{k}^2\overline{D}_{\phi\phi}\varepsilon_0 \\
& + 2Z\overline{k}\overline{S}_{\phi\phi}\overline{D}_{rr}\varepsilon_0 + 2Z\overline{k}\overline{D}_{rr}w_0\cos\phi_0 + 2Z\overline{k}\overline{S}_{rr}\overline{D}_{\phi\phi}\varepsilon_0 - 2Z\overline{k}\overline{D}_{\phi r}w_0\sin\phi_0 - 2Z\overline{k}\overline{S}_{\phi r}\overline{D}_{r\phi}\varepsilon_0 \\
& - 2Z\overline{d}\overline{S}_{r\phi}\overline{S}_{\phi r}\varepsilon_0 - 2Z\overline{d}\overline{S}_{\phi r}w_0\sin\phi_0
\end{aligned}
\qquad \text{… (6.62)}
$$

$$
\begin{aligned}
C_{35} = & 2\overline{dk}\overline{D}_{rr}\overline{D}_{\phi\phi}\varepsilon_0 + \overline{d}^2\overline{S}_{\phi\phi}\overline{D}_{rr}\varepsilon_0 + \overline{d}^2\overline{D}_{rr}\overline{w}_0\cos\phi_0 + \overline{d}^2\overline{S}_{rr}\overline{D}_{\phi\phi}\varepsilon_0 \\
& - \overline{d}^2\overline{S}_{r\phi}\overline{D}_{\phi r}\varepsilon_0 - \overline{d}^2\overline{D}_{\phi r}\overline{w}_0\sin\phi_0 - \overline{d}^2\overline{S}_{\phi r}\overline{D}_{r\phi}\varepsilon_0
\end{aligned}
\qquad \text{... (6.63)}
$$

$$
\begin{aligned}
C_{36} = & 2\overline{dk}\overline{S}_{rr}\overline{S}_{\phi\phi}\varepsilon_0 - 2\overline{dk}\overline{S}_{rr}\overline{w}_0\cos\phi_0 - \overline{k}^2\overline{S}_{\phi\phi}\overline{D}_{rr}\varepsilon_0 - \overline{k}^2\overline{D}_{rr}\overline{w}_0\cos\phi_0 \\
& - \overline{k}^2\overline{S}_{rr}\overline{D}_{\phi\phi}\varepsilon_0 + \overline{k}^2\overline{S}_{r\phi}\overline{D}_{\phi r}\varepsilon_0 + \overline{k}^2\overline{D}_{\phi r}\overline{w}_0\sin\phi_0 + \overline{k}^2\overline{S}_{\phi r}\overline{D}_{r\phi}\varepsilon_0 \\
& + 2\overline{dk}\overline{S}_{r\phi}\overline{S}_{\phi r}\varepsilon_0 + 2\overline{dk}\overline{S}_{\phi r}\overline{w}_0\sin\phi_0
\end{aligned}
\qquad \text{... (6.64)}
$$

The critical mass parameter & whirl ratio will be determined by satisfying the equations (6.39) & (6.40) employing Newton Raphson method.

6.2.6 Results and Discussion

The stability of the bearing is expressed in term of critical mass parameter $\left(\overline{M}_C\right)$ and whirl ratio $\left(\lambda_R\right)$, which not only depend upon the values of l_m, N, ε_0 and L/D-ratio, but also depend upon the values of non-dimensional forms of stiffness and damping coefficients of external support and the mass ratio. There variation are hence shown separately on critical mass parameter and whirl ratio as the functions of l_m, $\overline{D}_S$ and $\overline{K}_S$, $\overline{M}_C$ and λ_R are plotted in separate curves as the function of $\overline{D}_S$ and $\overline{K}_S$ for the parametric variation of l_m, N and L/D-ratio.

6.2.6.1 Finite Bearing Non-Dimensional Components of Stiffness and Damping Coefficients

6.2.6.1(a) Effect of Coupling Number (N)

Figures.6.3(a) to *6.3(h)* show the variation of the non-dimensional components of stiffness and damping coefficient as function of l_m, when coupling number (N) is considered as a

parameter, keeping ε_o, $L/D, \overline{D}_S$, $\overline{K}_S$ *and* $\overline{Z}$ fixed at 0.5, 1.0, 0.0001,0.0001,0.01 respectively.

It can be observed from the figures that at any value l_m, the direct components of stiffness $\overline{S}_{RR}$ and $\overline{S}_{\phi\phi}$ increase with an increase in coupling number. For any of value of *N*, $\overline{S}_{RR}$ and $\overline{S}_{\phi\phi}$ decrease with l_m and all the family of curves converge to the asymptotic value of these for Newtonian fluid as l_m becomes infinitely large. However, at $l_m \to 0$, $\overline{S}_{RR}$ and $\overline{S}_{\phi\phi}$ are much larger compared to those of Newtonian fluids. The reason for such enhanced components of stiffness at $l_m \to 0$ is the same as that for load parameter. Cross components of stiffness $\overline{S}_{R\phi}$ and $\overline{S}_{\phi R}$ follow the same trend as the direct components.

Direct and cross components of damping coefficient increase with coupling number for any value of l_m, but at large l_m $(l_m \to \infty)$, they approach the corresponding values for Newtonian fluid.

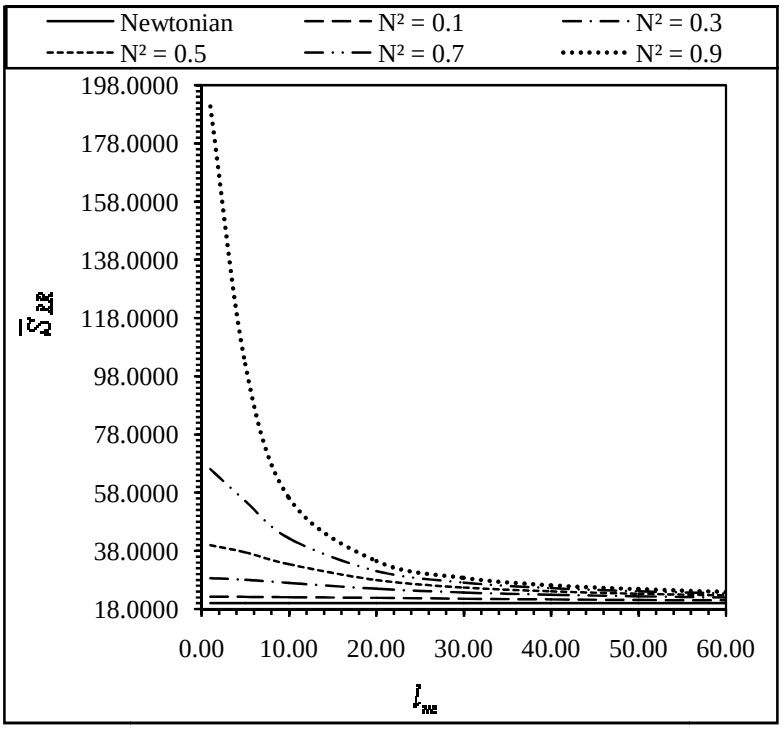

Figure.6.3 (a): Variation of $\overline{S}_{RR}$ with l_m for various values of N^2

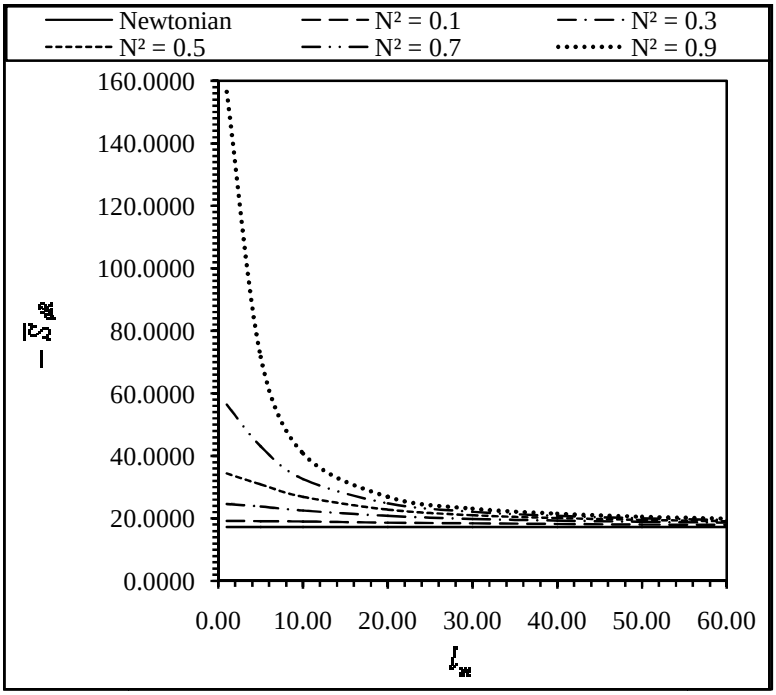

Figure.6.3 (b): Variation of $-\overline{S}_{\phi R}$ with l_m for various values of N^2

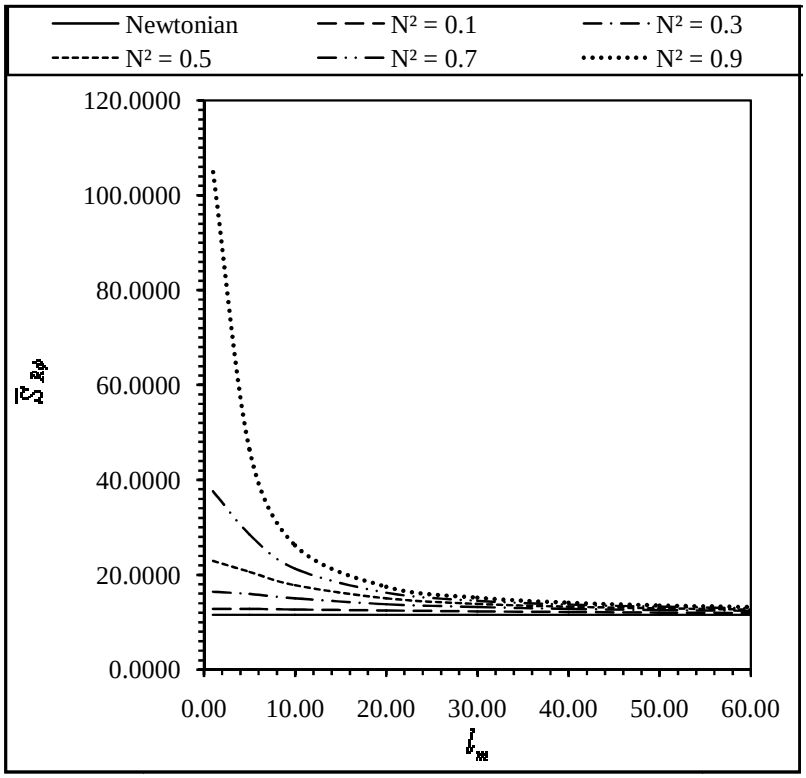

Figure.6.3 (c): Variation of $\overline{S}_{R\phi}$ with l_m for various values of N^2

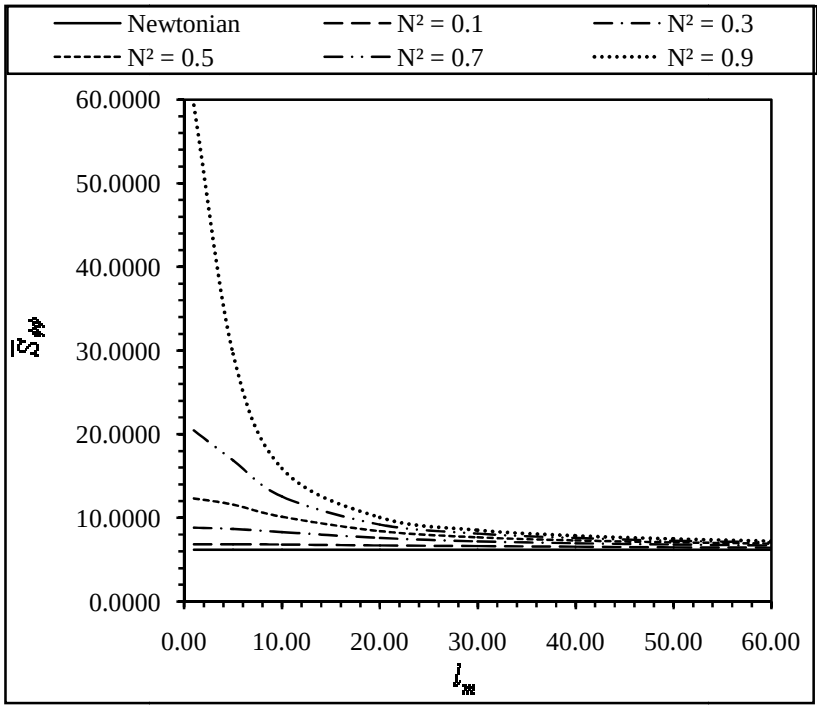

Figure.6.3 (d): Variation of $\overline{S}_{\phi\phi}$ with l_m for various values of N^2

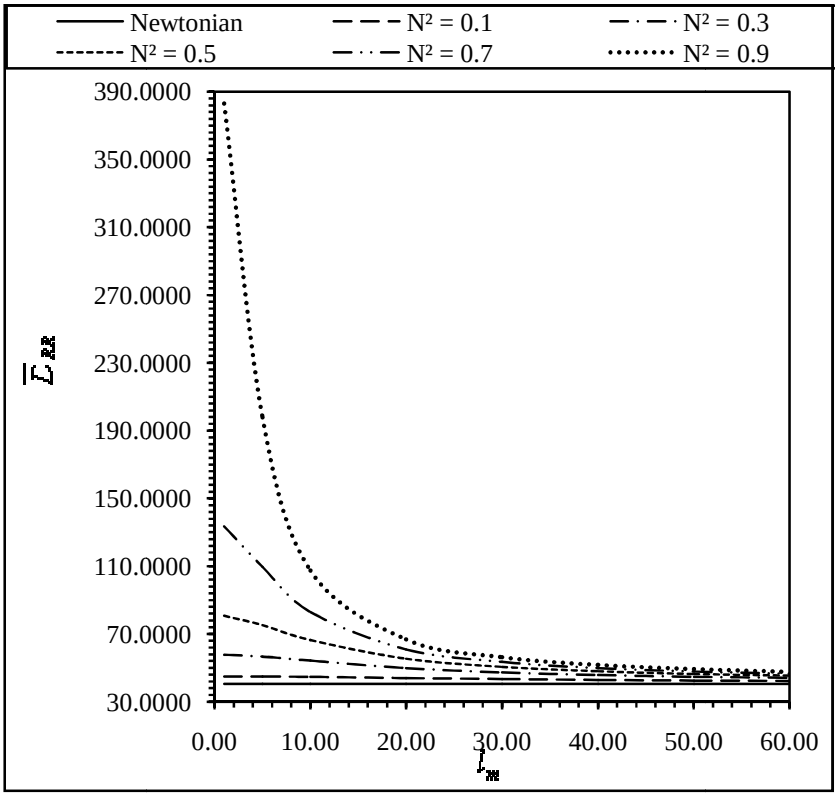

Figure.6.3 (e): Variation of $\overline{D}_{RR}$ with l_m for various values of N^2

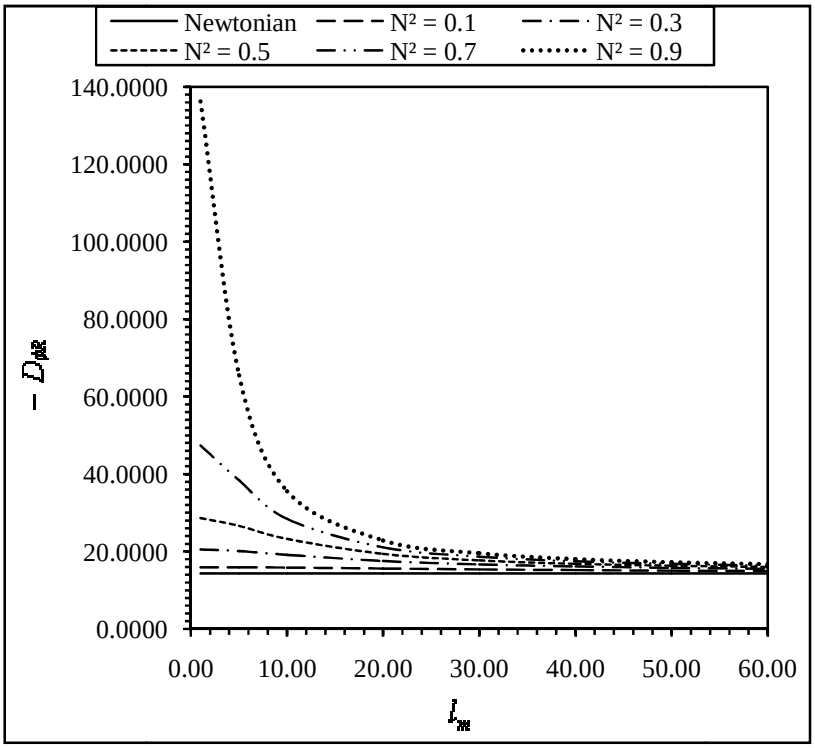

Figure.6.3 (f): Variation of $-\overline{D}_{\phi R}$ with l_m for various values of N^2

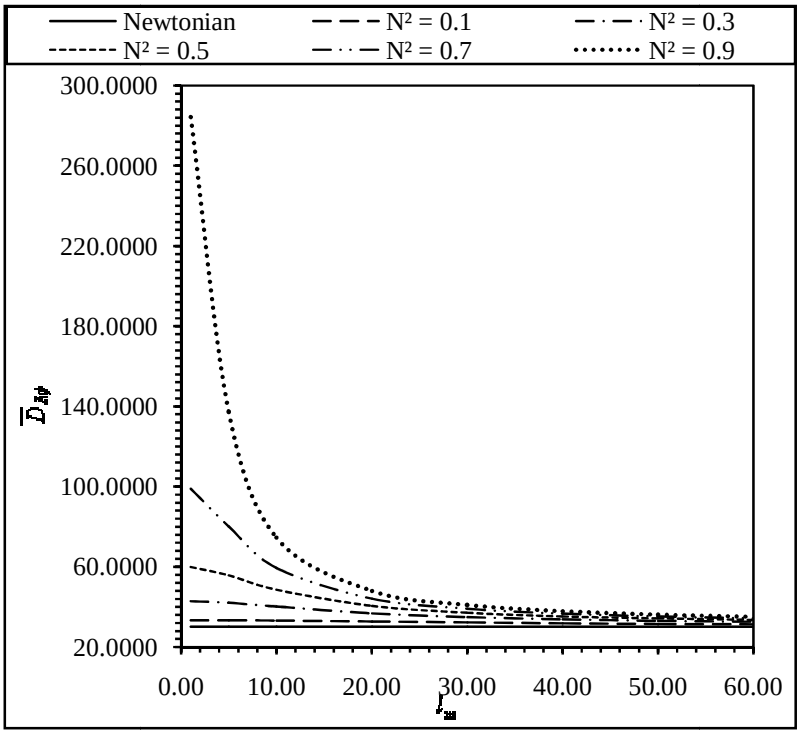

Figure.6.3 (g): Variation of $\overline{D}_{R\phi}$ with l_m for various values of N^2

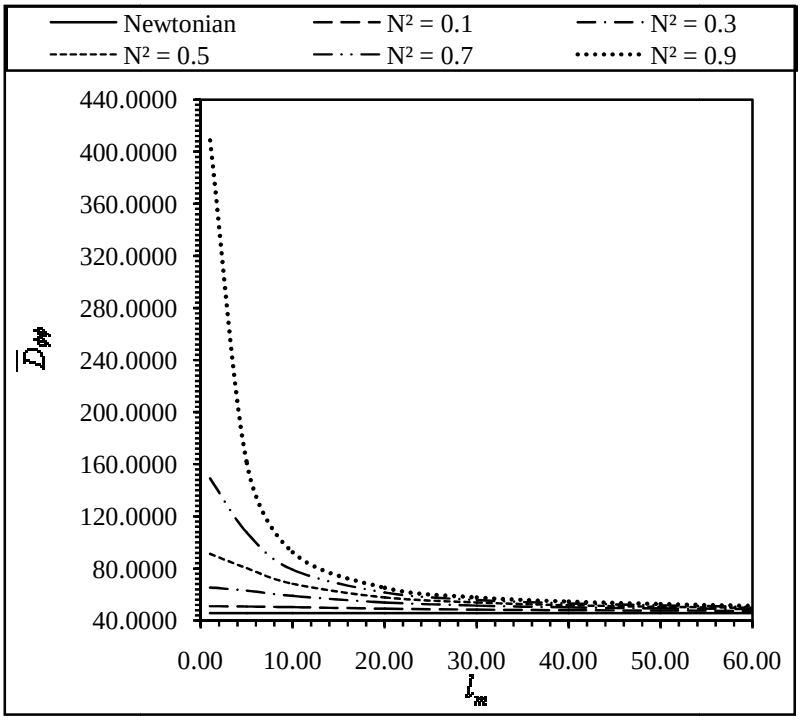

Figure.6.3 (h): Variation of $\overline{D}_{\phi\phi}$ with l_m for various values of N^2

6.2.6.1(b) Effect of Steady State Eccentricity Ratio (ε_o)

Figures.6.4 (a) to *6.4(h)* show the variations of non-dimensional components of stiffness and damping coefficients for different values of ε_o and l_m, when other factors *viz*, *L/D* = 1.0, ε_o = 0.5, $\overline{D}_S = 0.0001, \overline{K}_S = 0.0001, \overline{Z} = 0.01$ and $N^2=0.5$ are kept fixed. It can be observed from the referred figures that an increase in ε_o increases the magnitudes of the dynamic coefficients. It is further seen that all the curves in the micropolar fluid lubrication regime converge to those for Newtonian fluid lubrication regime at $l_m \to \infty$ at $l_m \to 0$ the values of all the coefficients are more than those for Newtonian fluid because of the reason discussed in chapter 5.

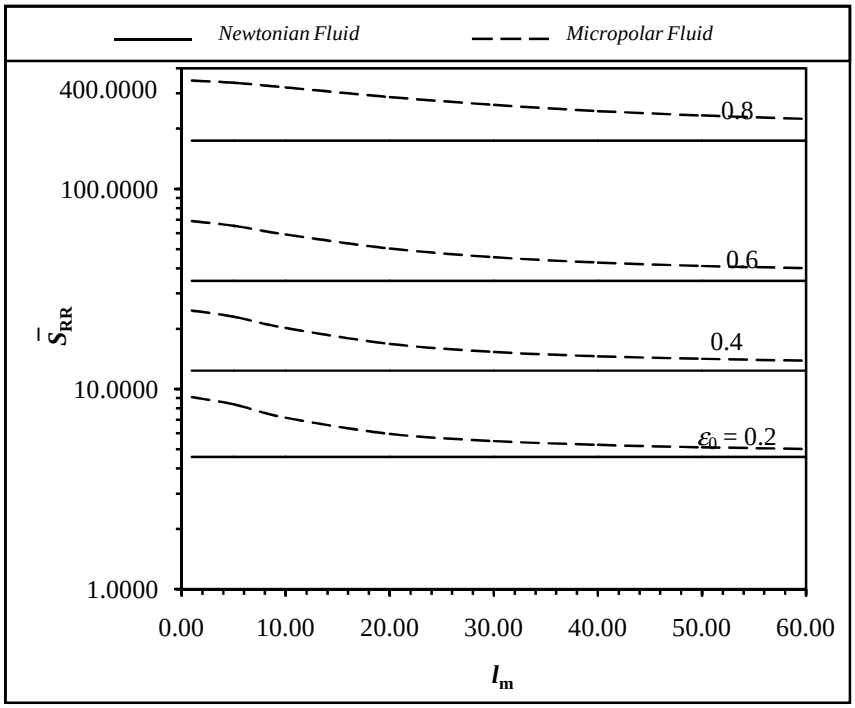

Figure.6.4 (a): Variation of $\bar{S}_{RR}$ with l_m for various values of ε_0.

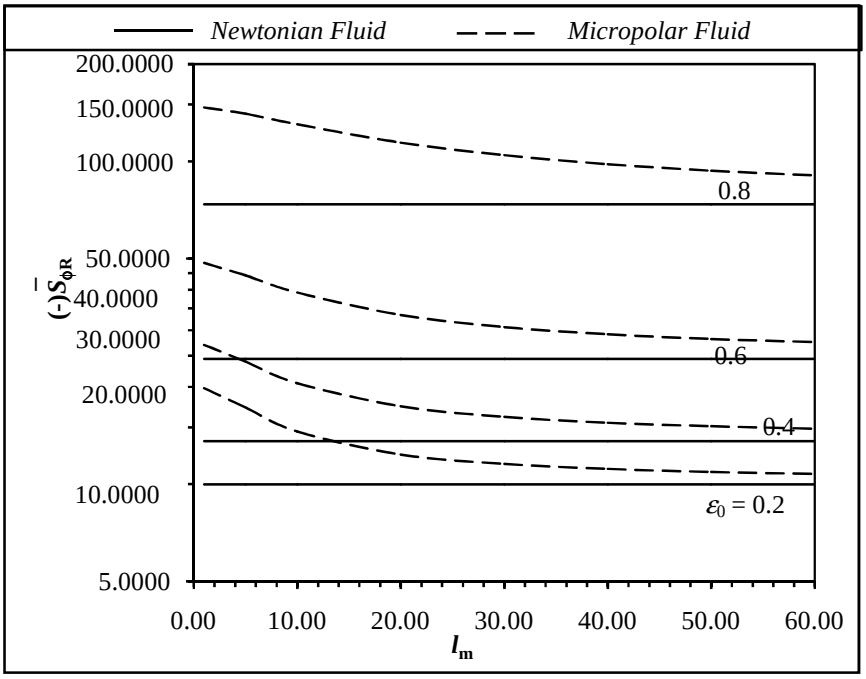

Figure.6.4 (b): Variation of $-\bar{S}_{\phi R}$ with l_m for various values of ε_0.

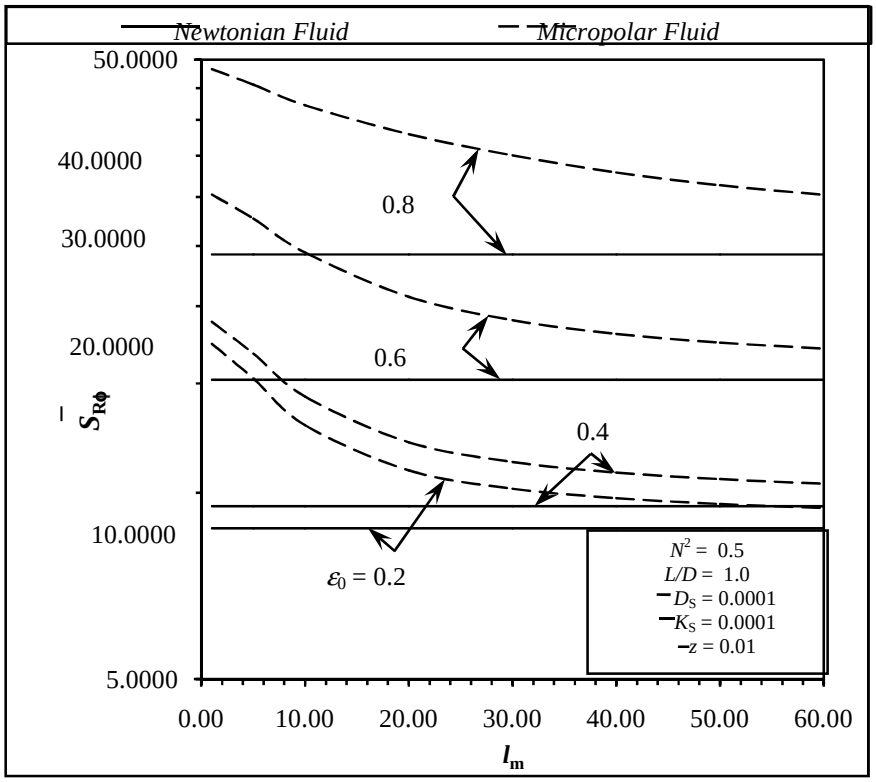

Figure.6.4 (c): Variation of $\overline{S}_{R\phi}$ with l_m for various values of ε_0

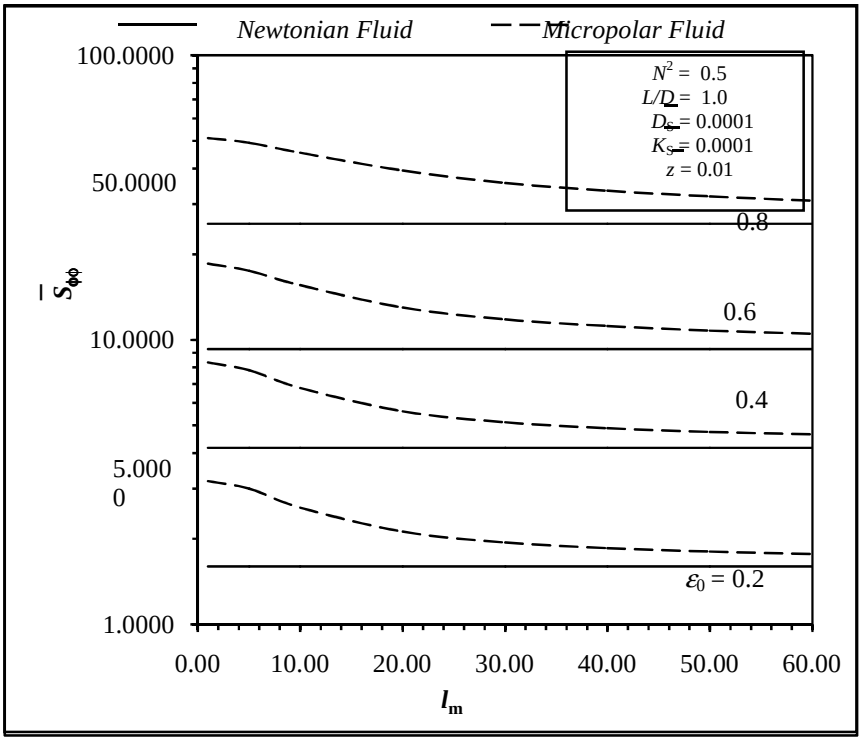

Figure.6.4 (d): Variation of $\overline{S}_{\phi\phi}$ with l_m for various values of ε_0.

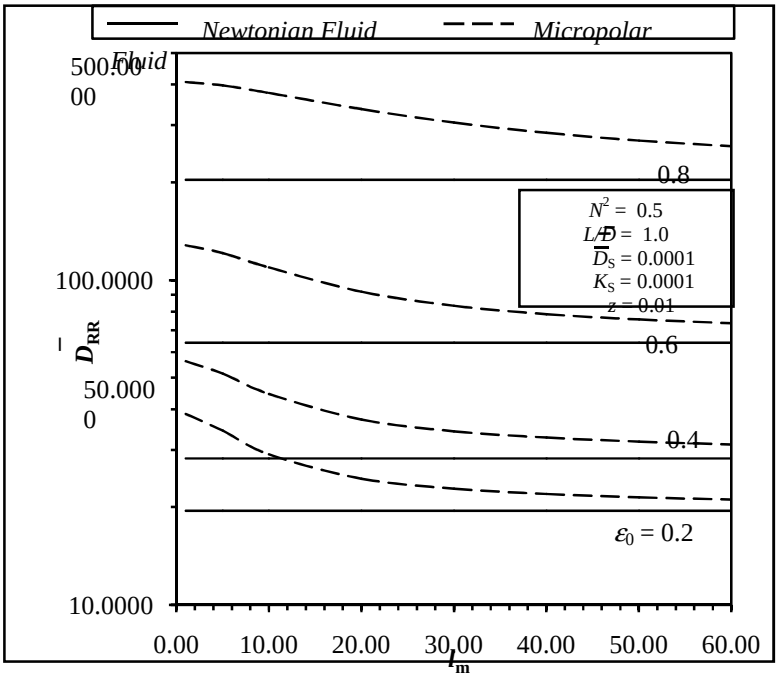

Figure.6.4 (e): Variation of $\bar{D}_{RR}$ with l_m for various values of ε_0 .

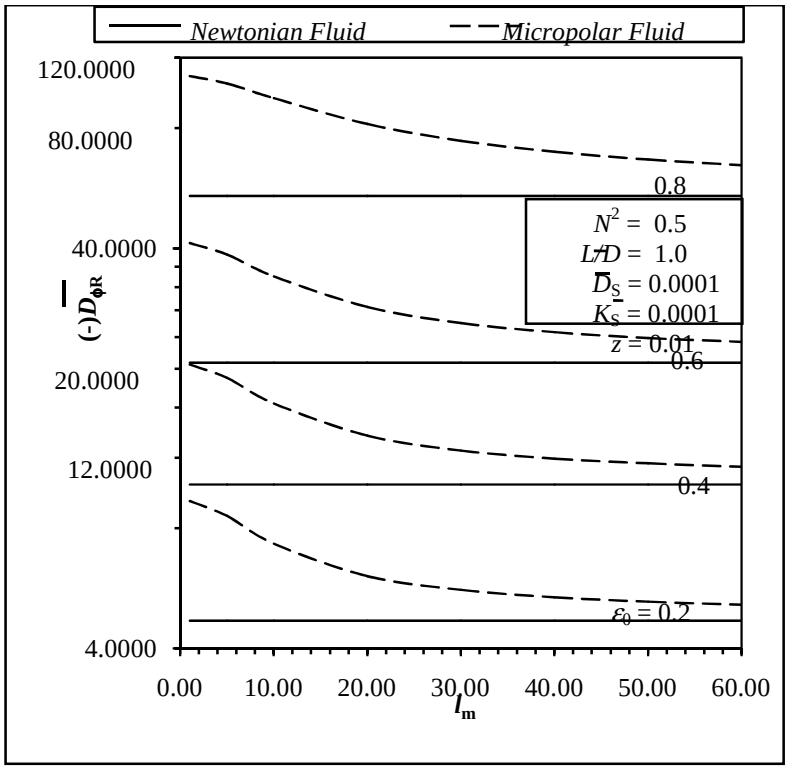

Figure.6.4 (f): Variation of $-\bar{D}_{\phi R}$ with l_m for various values of ε_0

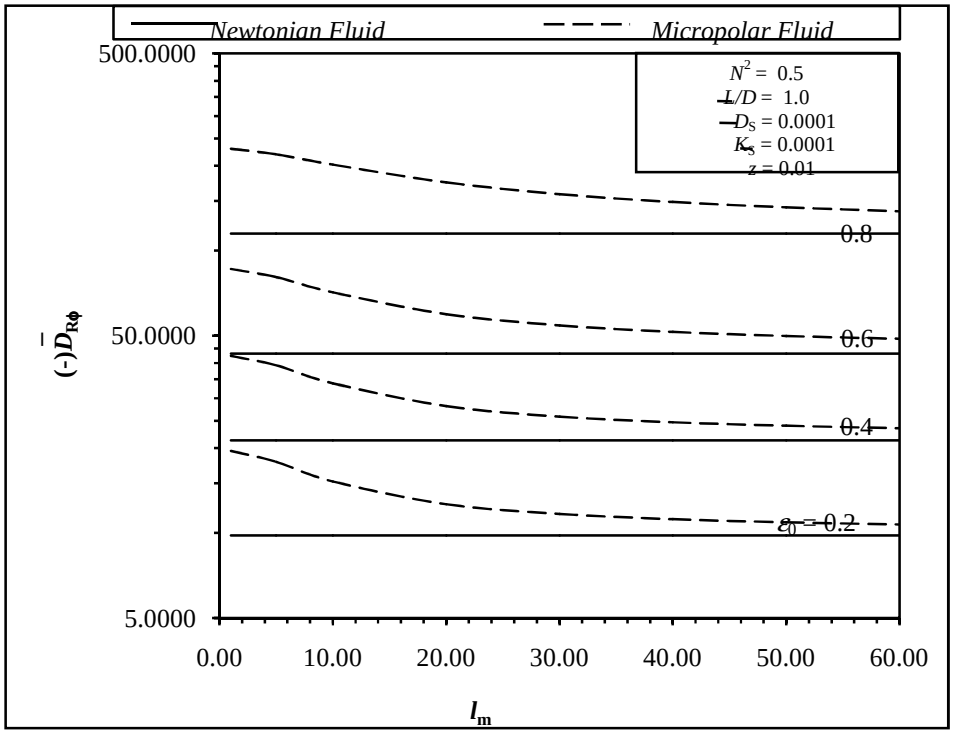

Figure.6.4 (g): Variation of $\overline{D}_{R\phi}$ with l_m for various values of ε_0 .

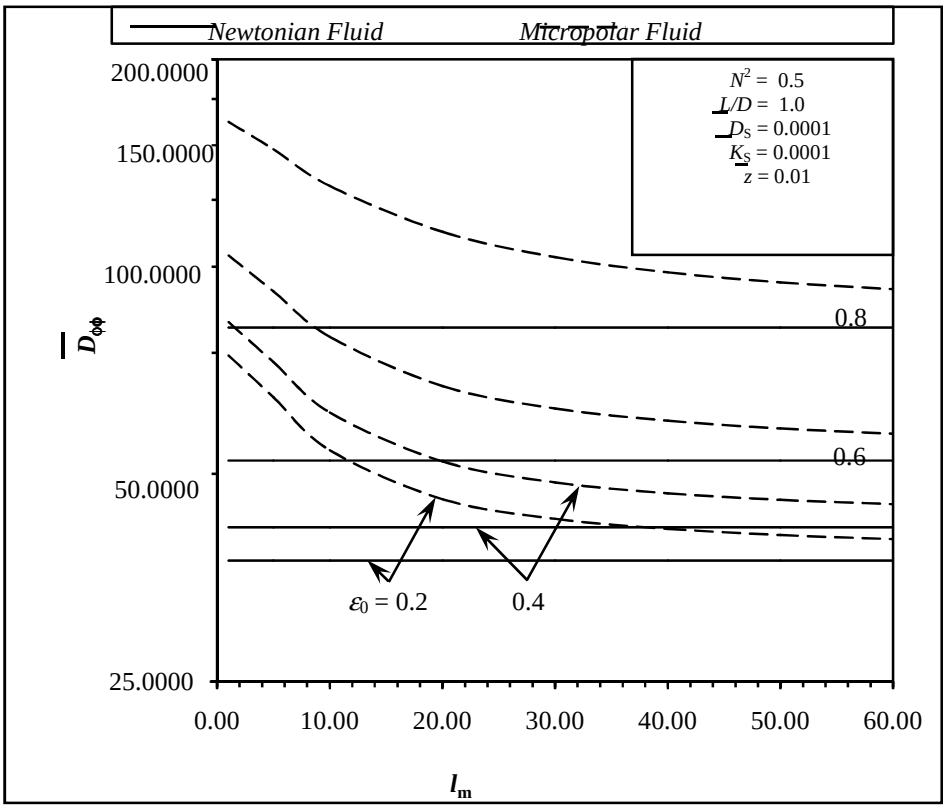

Figure.6.4 (h): Variation of $\overline{D}_{\phi\phi}$ with l_m for various values of ε_0.

6.2.6.1(c) Effect of Slenderness Ratio (*L/D*)

Figures.6.5 (a) to *6.5(h)* show the variations of non-dimensional components of stiffness and damping coefficients with respect to *l*m for parametric variation of *L/D* ratio, when other factors, *L/D* = 1.0, $\varepsilon_o = 0.5, \overline{D}_S = 0.0001$, $\overline{K}_S = 0.0001$, $\overline{Z} = 0.01$ and N^2=*0.5* are held fixed. It can be discerned from the figures that as *L/D* increases the dynamic coefficients also increase. At $l_m \to \infty$ there is tendency of all the curves to converge to the corresponding values for Newtonian fluid. At lower values of *l*m $(l_m \to \infty)$ micropolar lubrication gives enhanced values of dynamic coefficients compared to these for Newtonian fluid.

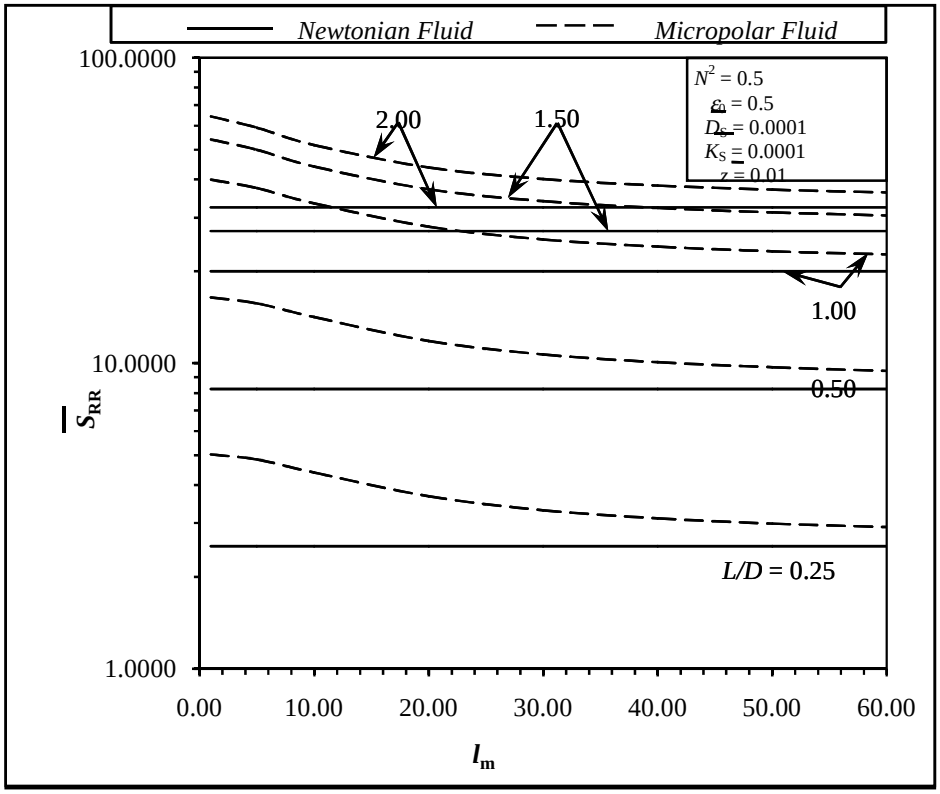

Figure.6.5 (a): Variation of $\overline{S}_{RR}$ with l_m for various values of L/D ratio.

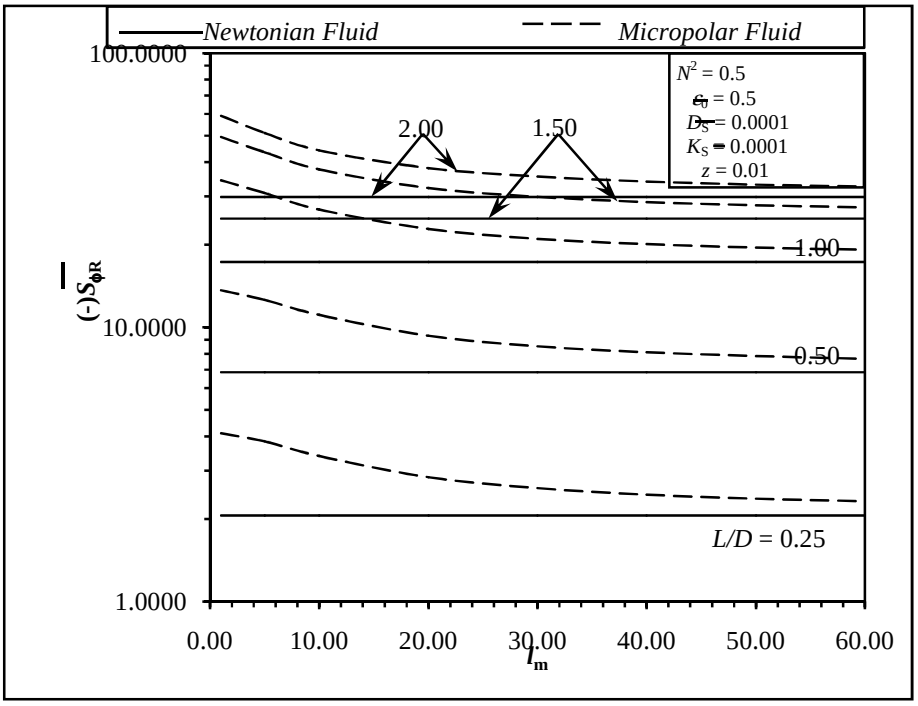

Figure.6.5 (b): Variation of $-\overline{S}_{\phi R}$ with l_m for various values of L/D ratio

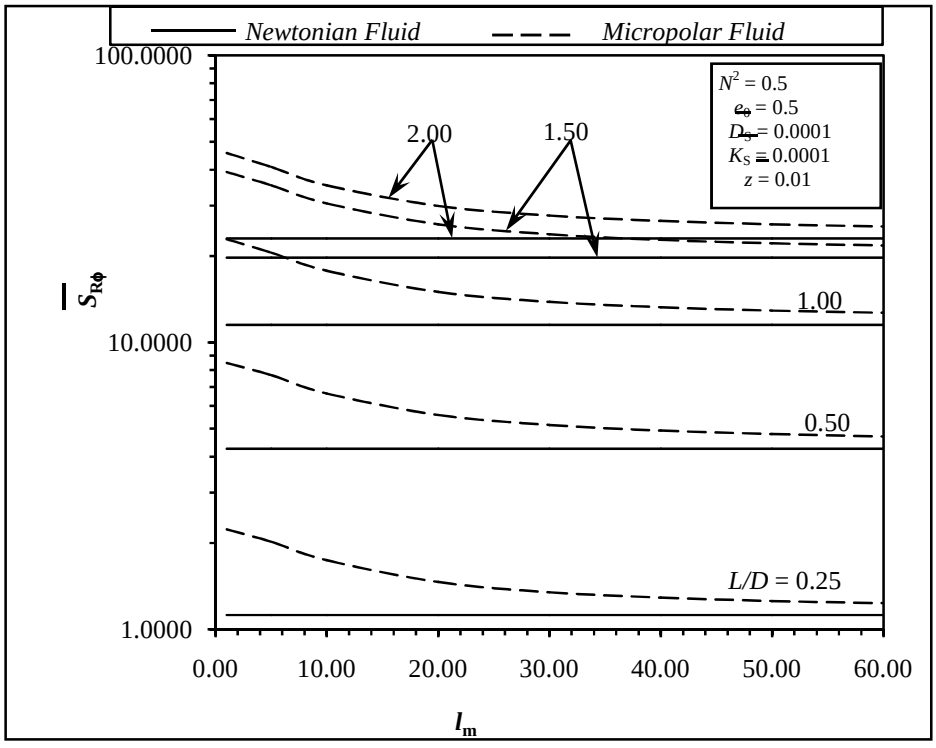

Figure.6.5 (c): Variation of with for various values of L/D ratio

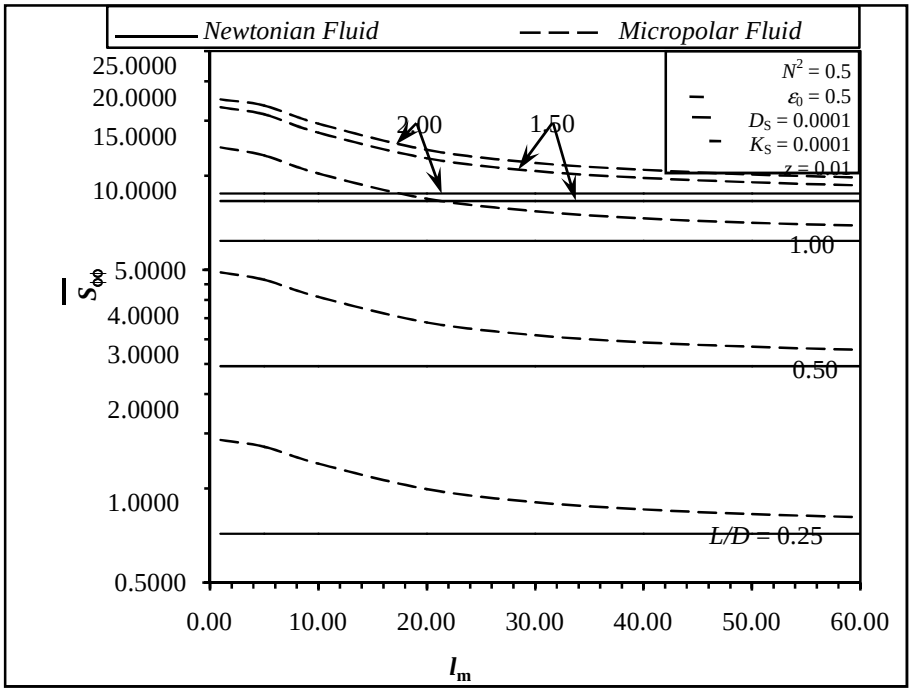

Figure.6.5 (d): Variation of $\bar{S}_{\phi\phi}$ with l_m for various values of L/D ratio.

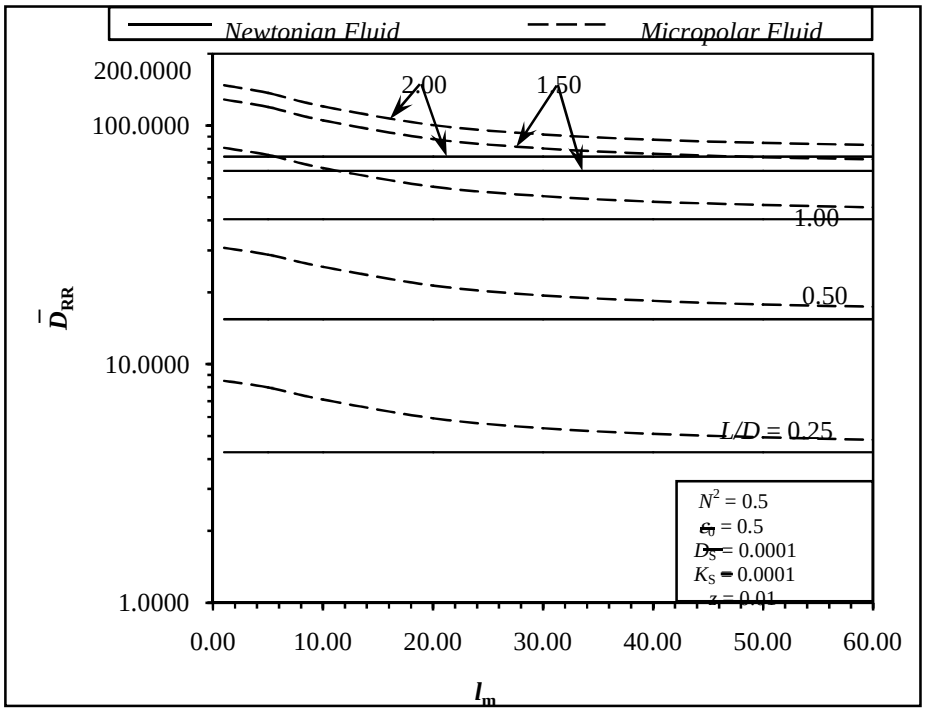

Figure.6.5 (e): Variation of $\bar{D}_{RR}$ with l_m for various values of L/D ratio.

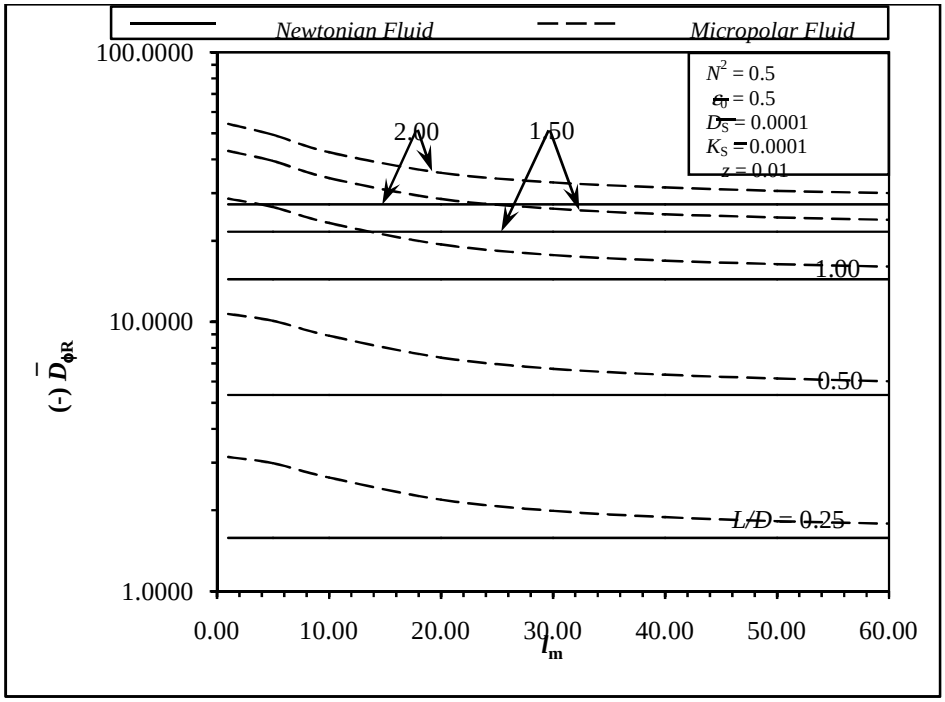

Figure.6.5 (f): Variation of $-\bar{D}_{\phi R}$ with l_m for various values of L/D ratio

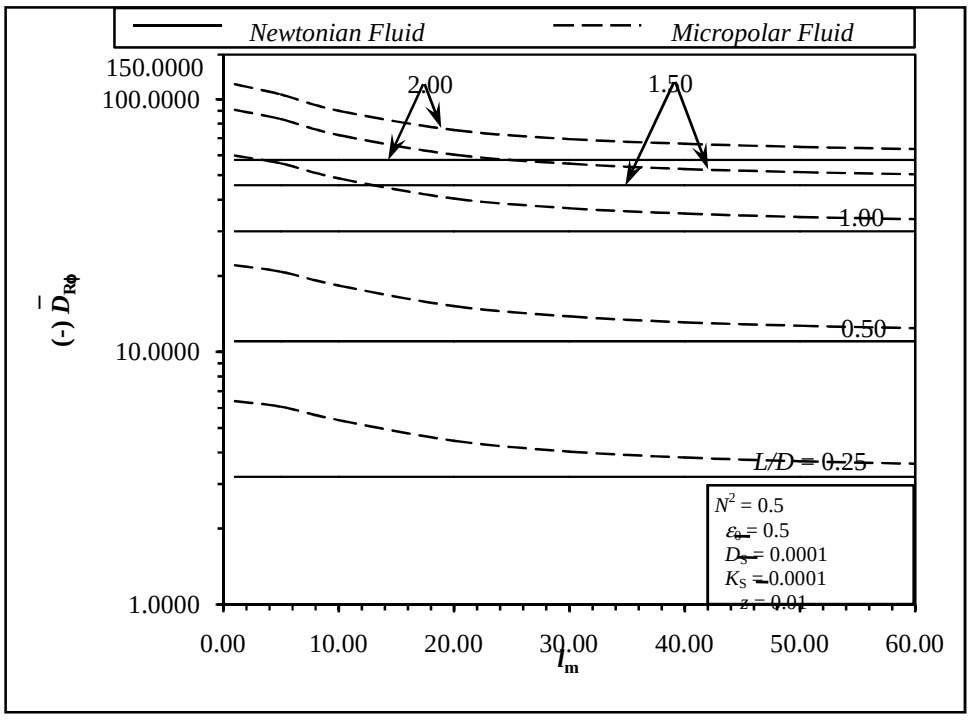

Figure.6.5 (g): Variation of - $\bar{D}_{R\phi}$ with l_m for various values of L/D ratio.

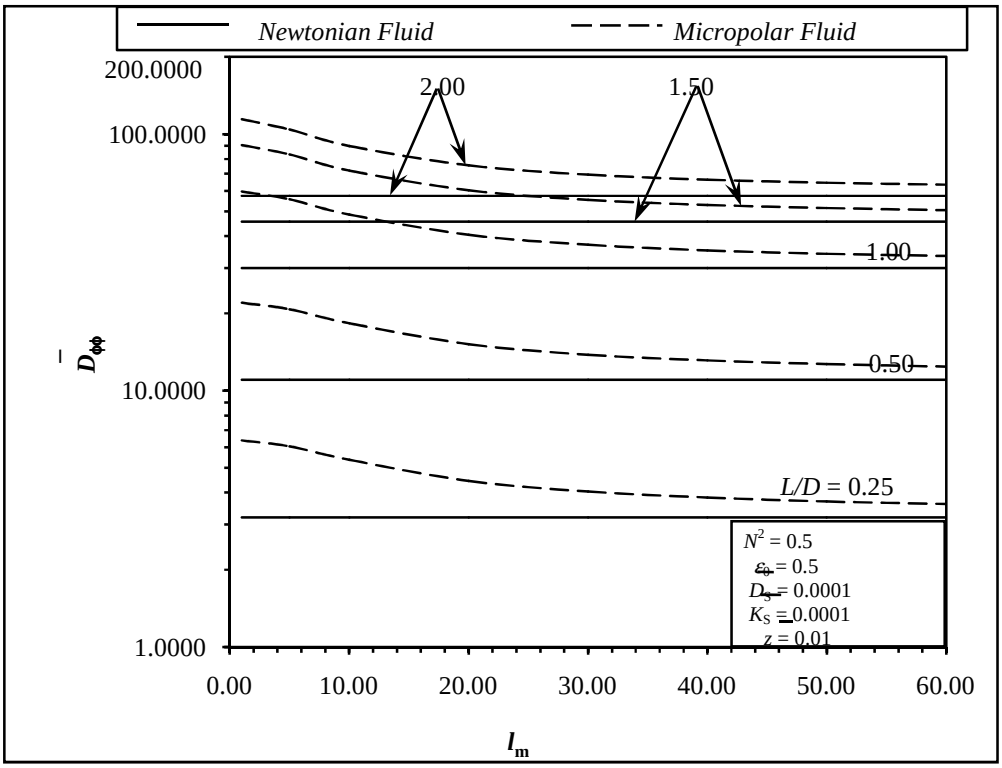

Figure.6.5 (h): Variation of $\overline{D}_{\phi\phi}$ with l_m for various values of L/D ratio.

2.6.2 Critical Mass Parameter ($\overline{M}_C$)

6.2.6.2(a) Effect of Coupling Number (*N*)

Figure.6.6 (a) shows the variation of critical mass parameter representing the threshold of stability as function of l_m, when, *L/D* = 1.0, $\varepsilon_o = 0.5, \overline{D}_S = 0.0001$, $\overline{K}_S = 0.0001$, $\overline{Z} = 0.01$ and *N* is considered as a parameter. It is found from the figure that the critical mass parameter increases as *N* is increased. Moreover, at any particular value of *N*, stability improves initially as l_m is increased, reaches a maximum to that for Newtonian fluid at large value of l_m.

The load carrying capacity increases in the micropolar fluid than in the Newtonian fluid. So with the same load in a Newtonian fluid the journal will run at higher eccentricity ratio than that in the micropolar fluid. As a result the stability in terms of critical mass parameter enhances in micropolar fluid than Newtonian fluid and exhibits the same trends as that of the load parameter.

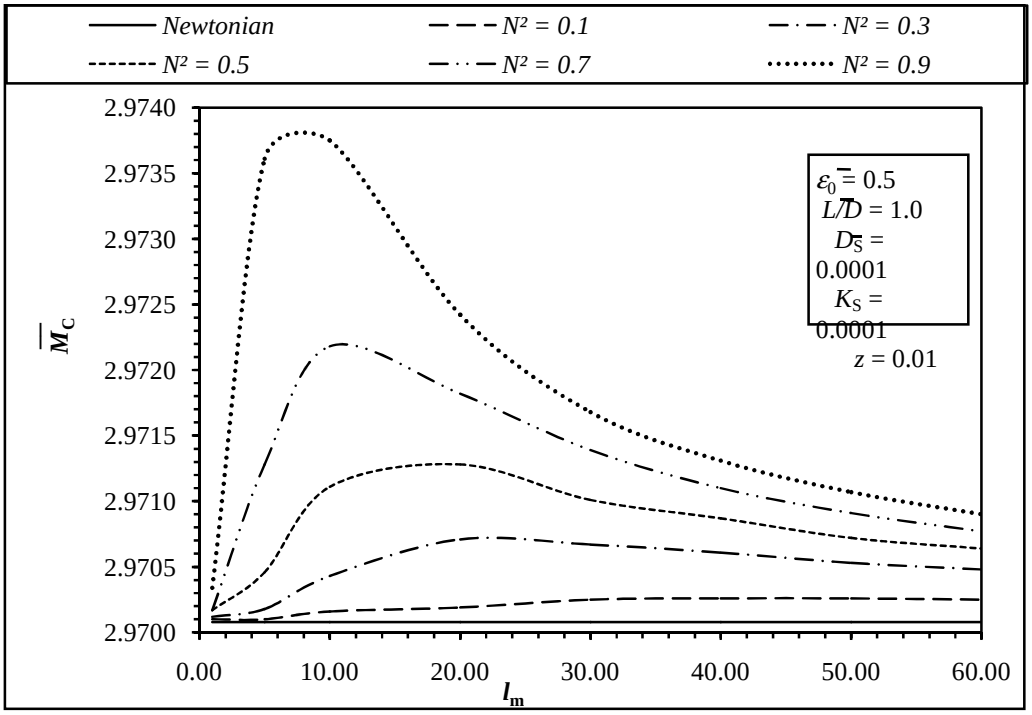

Figure.6.6 (a): Variation of $\overline{M}_C$ with l_m for various values of N^2

6.2.6.2(b) Effect of Steady State Eccentricity Ratio (ε_o)

The effect of variation of ε_o on $\overline{M}_C$ for, *L/D* = 1.0, ε_o = 0.5, $\overline{D}_S = 0.0001$, $\overline{K}_S = 0.0001$, $\overline{Z} = 0.01$ and *N* is shown in *Fig.6.6 (b)*. It is found from the figure that as ε_o increases and then increases critical mass parameter initially droops in the range ε_o = 0.2 and 0.6 and then increases irrespective of l_m.

All the curves, however, show the tendency of converging to the value corresponding to the Newtonian fluid at large value of l_m. For all the values ε_o of stability remain higher in micropolar fluids and attains the maximum value at around l_m=10

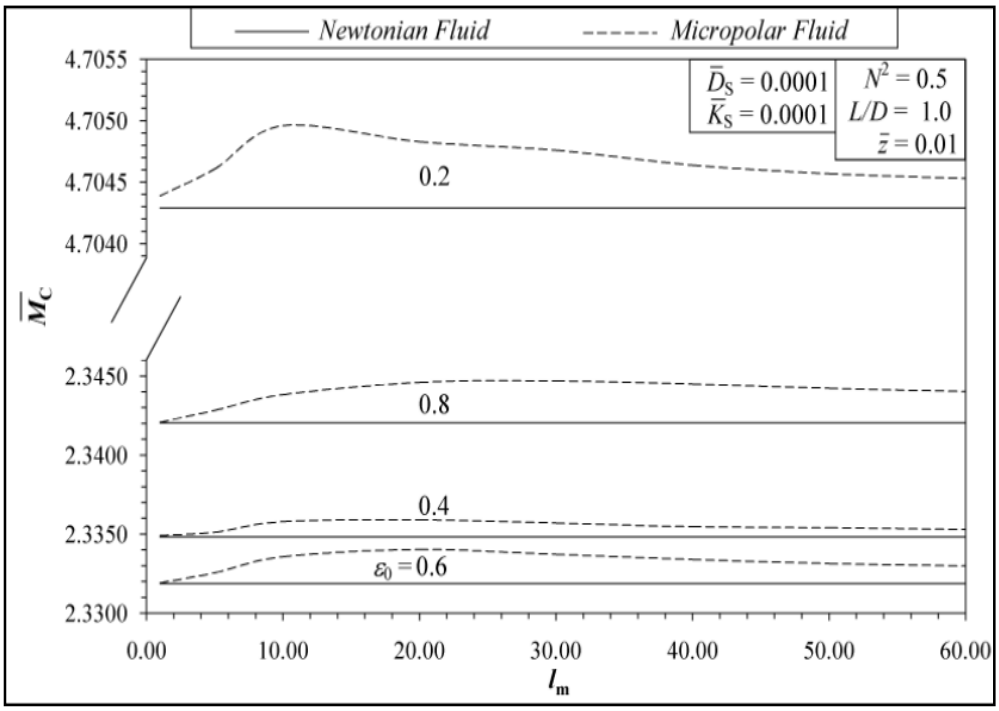

Figure.6.6 (b): Variation of $\overline{M}_C$ with l_m for various values of ε_0.

6.2.6.2(c) Effect of Slenderness Ratio (*L/D*)

The variation of $\overline{M}_C$ as a function of l_m for various values of L/D ratio is plotted in *figure* 6.6 *(c)* as the slenderness ratio increases the stability decreases in both type of lubrication.

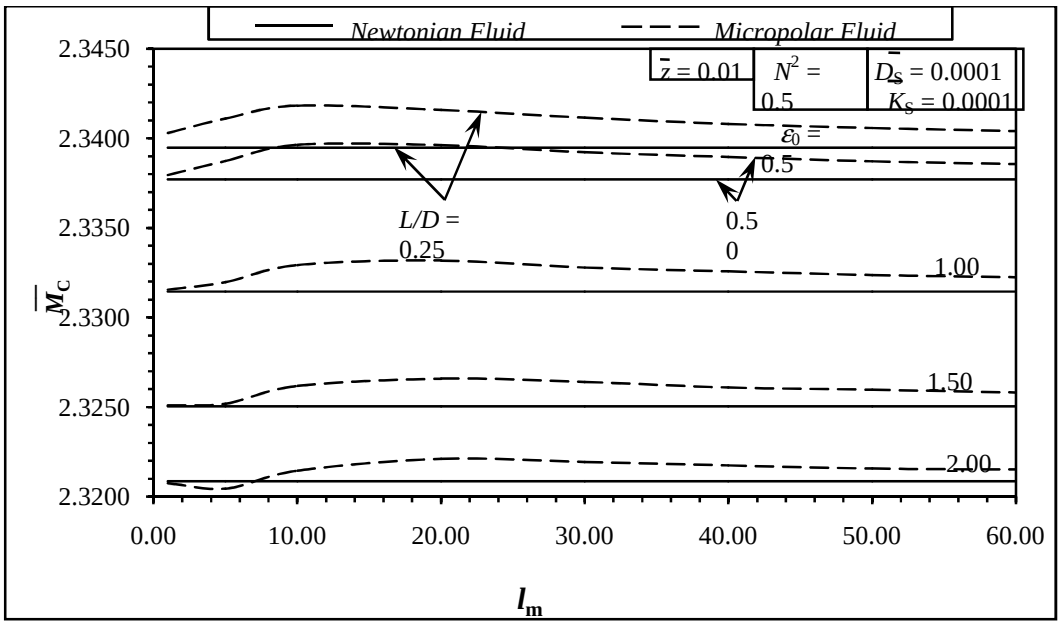

Figure.6.6 (c): Variation of $\overline{M}_C$ with l_m for various values of L/D ratio.

At higher value of L/D (L/D=2.0) the stability in micropolar lubricant initially droops below the Newtonian fluid as l_m increases and then becomes higher in micropolar fluid as l_m increases and then becomes higher in micropolar fluid then Newtonian fluid for l_m approximated greater then 7.0. For all other values of L/D ratio the stability always remains larger in micropolar regime. The maximum deviation from its Newtonian value shifts from l_m around 7.0 at L/D=0.25 to l_m around 21.0 at L/D=2.0. For all cases the values of critical mass parameter converge to the respective values in Newtonian fluid as $l_m \to 0, \text{and} \, l_m \to \infty$.

6.2.6.3 Whirl Ratio (λ_R)

6.2.6.3(a) Effect of Coupling Number (*N*)

Figure.6.7 (a) shows the variation of whirl ratio with l_m, when *N* is taken as a parameter for *L/D* = 1.0, $\varepsilon_o = 0.5, \overline{D}_S = 0.0001$, $\overline{K}_S = 0.0001$, $\overline{Z} = 0.01$ It can be seen from the figure that as coupling number increases, whirl ratio decreases. At a particular value of *N*, the whirl ratio initially decreases, reaches a minimum, then increases with further increase in l_m and ultimately converges to that for Newtonian fluid when l_m is indefinitely large. However, the variation of whirl ratio is very small.

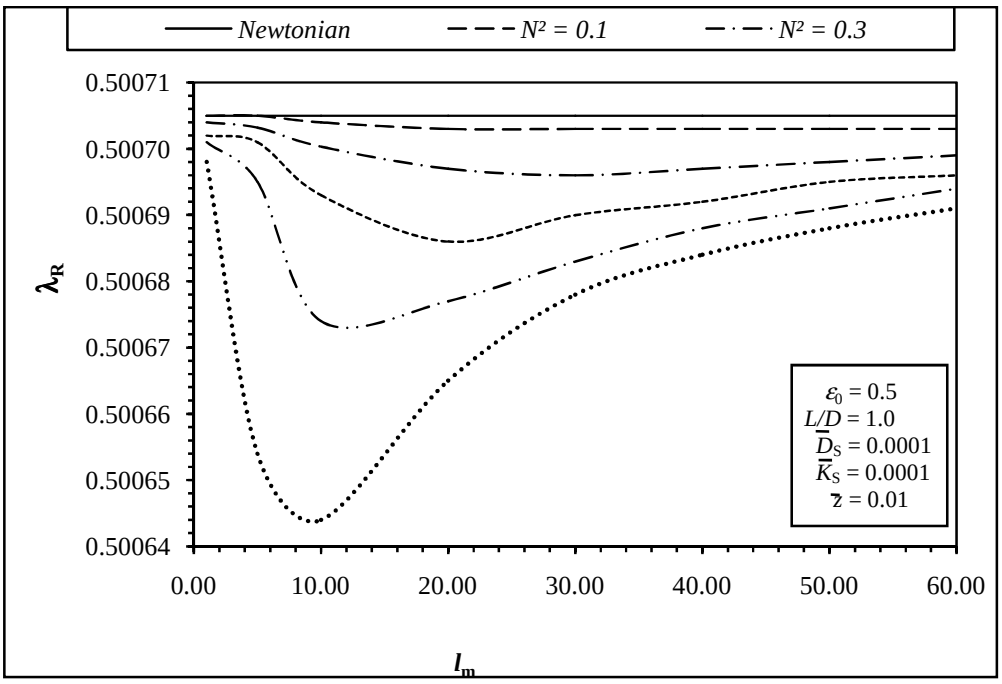

Figure.6.7 (a): Variation of λ_R with l_m for various values of N^2 ratio.

6.2.6.3(b) Effect of Steady State Eccentricity Ratio (ε_o)

The effect of (ε_o) on whirl ratio can be found from *figure.6.7 (b)* as a function of l_m for N^2=0.5, *L/D* = 1.0, ε_o = 0.5, $\overline{D}_S = 0.0001$, $\overline{K}_S = 0.0001$, $\overline{Z} = 0.01$. It can be seen from the figure that the variation of whirl ratio is small at $\varepsilon_o \le 0.6$ *i.e.* within 0.50057 and 0.50130. But at higher value of ε_o $(\varepsilon_o \le 0.6)$, λ_R decreases to about 0.50012.

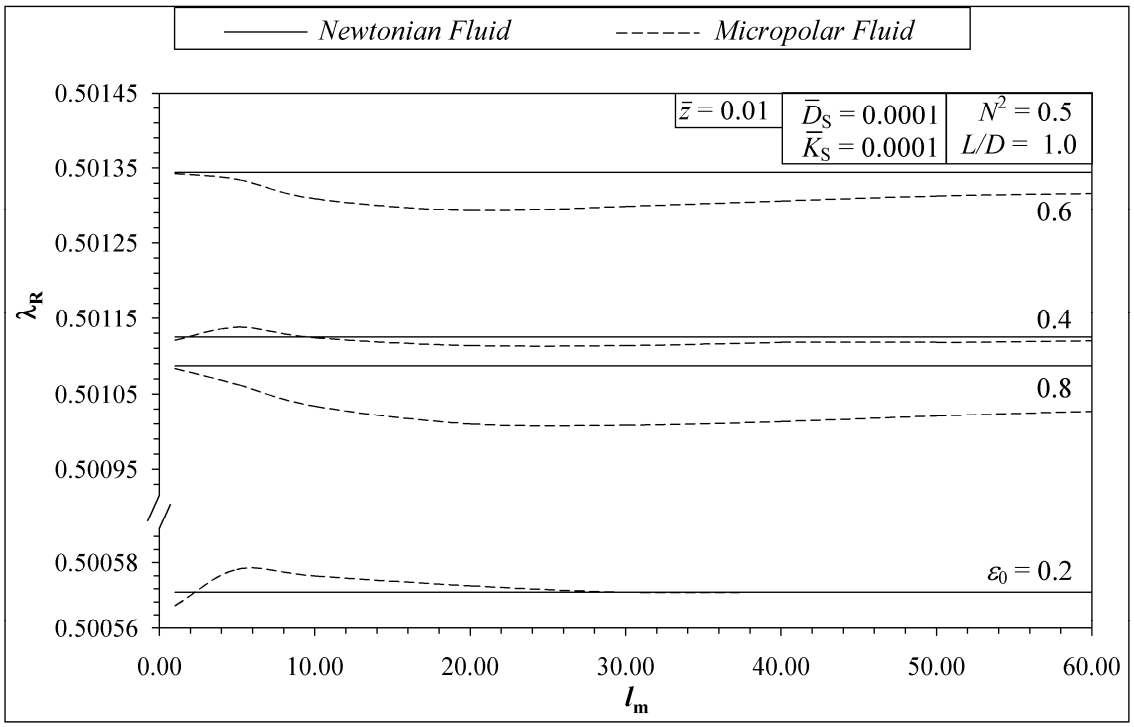

Figure.6.7 (b): Variation of λ_R with l_m for various values of ε_0

6.2.6.3(c) Effect of Slenderness Ratio (*L/D*)

The change in whirl ratio as shown in *figure.6.7(c)* for varying *L/D* at constant N^2=0.5, *L/D* = 1.0, ε_o = 0.5, $\overline{D}_S = 0.0001$, $\overline{K}_S = 0.0001$, $\overline{Z} = 0.01$ is, however, more distinct. The plot shows that the values of λ_R in the respective fluids increase for increase in *L/D* ratio from 0.25 to 1.5 and decreases for further increase inn L/D ratio upto 2.0.

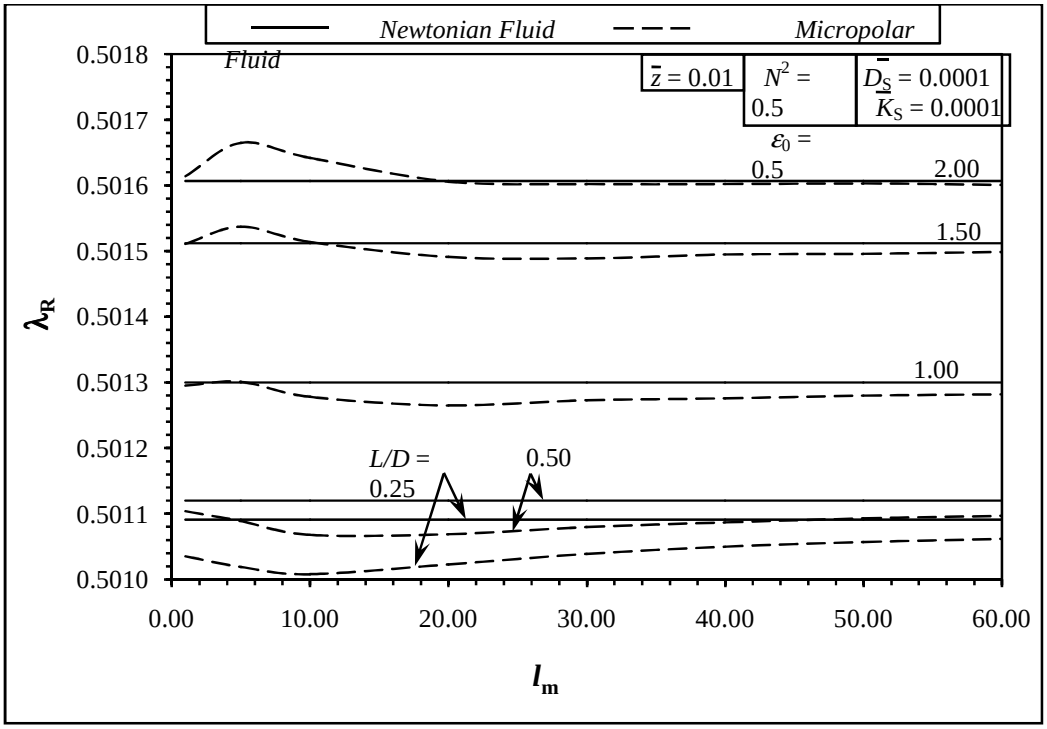

Figure.6.7 (c): Variation of λ_R with l_m for various values of L/D ratio.

6.2.6.4 Effect of Damping of External Support

Effect of damping of external support on critical mass parameter has been shown as plots of $\overline{M}_c$ vs. $\overline{D}_s$ for $l_m, N, \varepsilon_0, L/D$ separately in different plots.

6.2.6.4(a) Effect of Non-Dimensional Characteristic Length (l_m)

The combine effect of non dimensional characteristic length (l_m) and $\overline{D}_S$ is shown in *figure 6.8(a)* at N^2=0.5, ε_0=0.5, L/D=1.0, $\bar{z}$=0.01, and $\overline{K}_S$=0.0001. The range of study for $\overline{D}_S$ has been taken in between 10^{-6} and 10^{-3} as $\overline{D}_S$ is increased the value of $\overline{M}_c$ is decreased initially at a slower rate upto $\overline{D}_S$=0.0001 and then $\overline{M}_c$ droops at a higher rate with increase in $\overline{D}_S$. The highest stability is observed at l_m=20.0 for all value of $\overline{D}_S$, which reduces to the Newtonian value as l_m approaches to 0.0 and ∞. However for $l_m \geq 5.0$ at higher $\overline{D}_S$ the values of $\overline{M}_c$ falls at a higher rate.

6.2.6.4(b) Effect of Coupling Number(N)

The combined effect of coupling number N and $\overline{D}_S$ are plotted in *figure 6.8 (b)* at l_m=20.0, ε_0=0.5, L/D=1.0, $\bar{z}$=0.01, $\overline{K}_S$=0.0001 which exhibits the increase in $\overline{M}_c$ with increase in coupling number at any value of $\overline{D}_S$ with the Newtonian value being the lowest. The reason can be attributed to stronger coupling between linear and angular momentum resulting in more effective viscosity as N is increased. The stability decreases with the increase in $\overline{D}_S$.

The rate of decrease is predominant in the regime $\overline{D}_s \geq 0.0008$ than that in the region $\overline{D}_s = 10^{-6}$ and $\overline{D}_s = 8\times10^{-4}$.

6.2.6.4(c) Effect of Eccentricity Ratio (ε_0)

Figure.6.8 (c) shows the variation of $\overline{M}_c$ as a function of $\overline{D}_s$ at l_m=20.0, N^2=0.5, L/D=1.0 and $\overline{K}_S$=0.0001 for the parametric study of ε_0.The stability in micropolar fluid is always found higher than the Newtonian fluid at any value of ε_0

However the value of $\overline{M}_c$ initially falls from ε_0=0.1 to ε_0=0.5 and then increase with ε_0 upto ε_0=0.9 also the difference between the values of micropolar fluids and Newtonian fluid increase as ε_0 increases.1

6.2.6.4(d) Effect Of Slenderness Ratio

The stability in terms of $\overline{M}_c$ vs. $\overline{D}$ for parametric variation of L/D ratio at l_m=20.0, N^2=0.5, $\varepsilon_0 = 0.5$, $\overline{Z} = 0.1$ and $\overline{K}_S = 0.0001$ is observed in *figure 6.8 (d).* The stability in both types of lubricants is found to be decreased with increase in L/D ratio and micropolar fluid is always better choice in terms of stability than the Newtonian fluid. The stability is found to be marginally reduces $\overline{D}_S$ increases. The reason may be attributed to the higher load carrying capacity of the micropolar fluid over the Newtonian fluid.

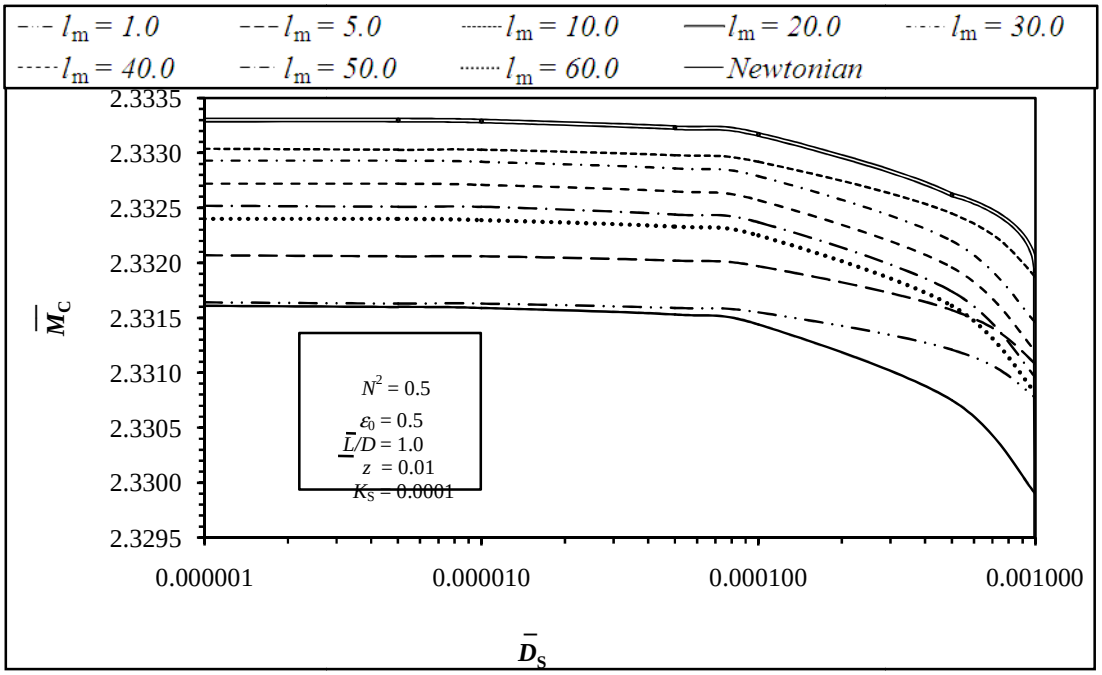

Figure.6.8 (a): Variation of $\overline{M}_C$ with $\overline{D}_S$ for various values of l_m.

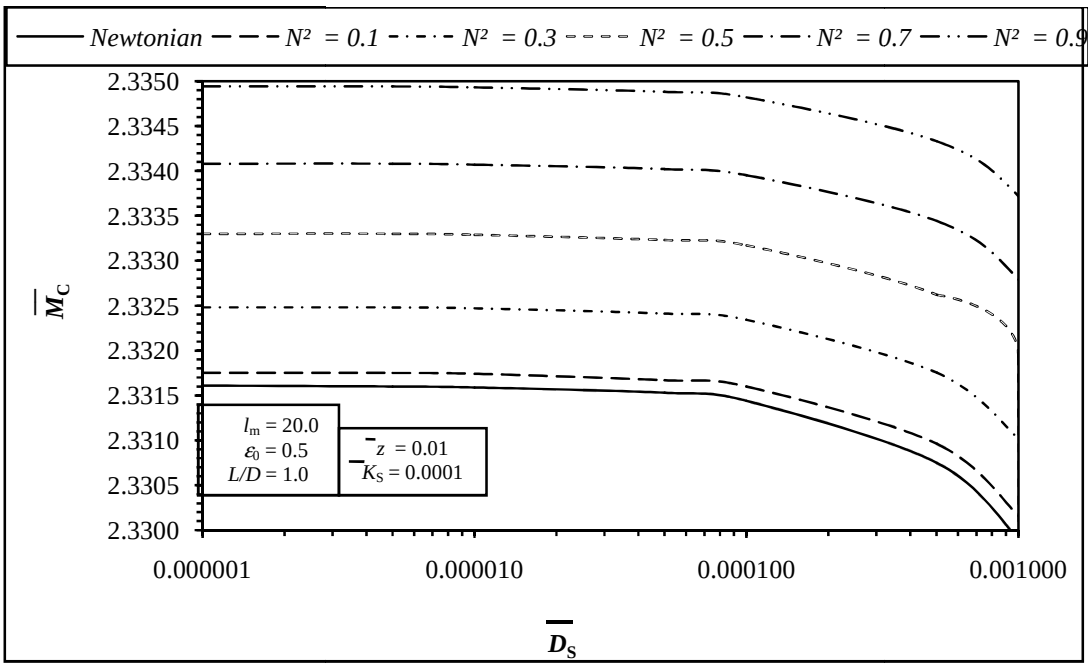

Figure.6.8 (b): Variation of $\overline{M}_C$ with $\overline{D}_S$ for various values of N^2.

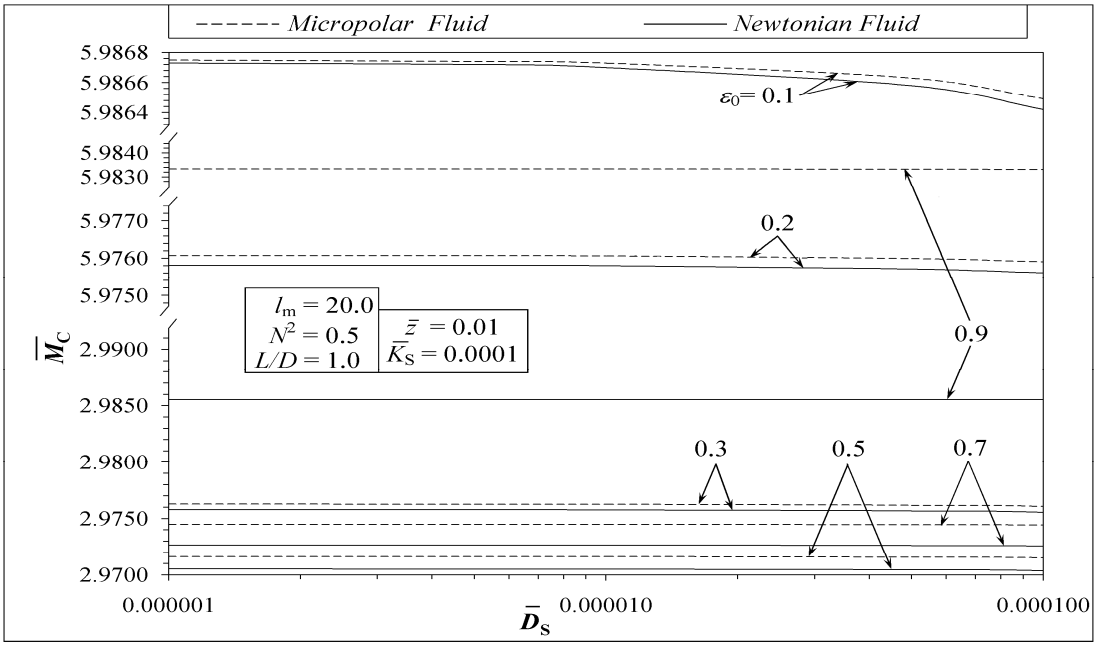

Figure.6.8 (c): Variation of $\overline{M}_C$ with $\overline{D}_S$ for various values of ε_0.

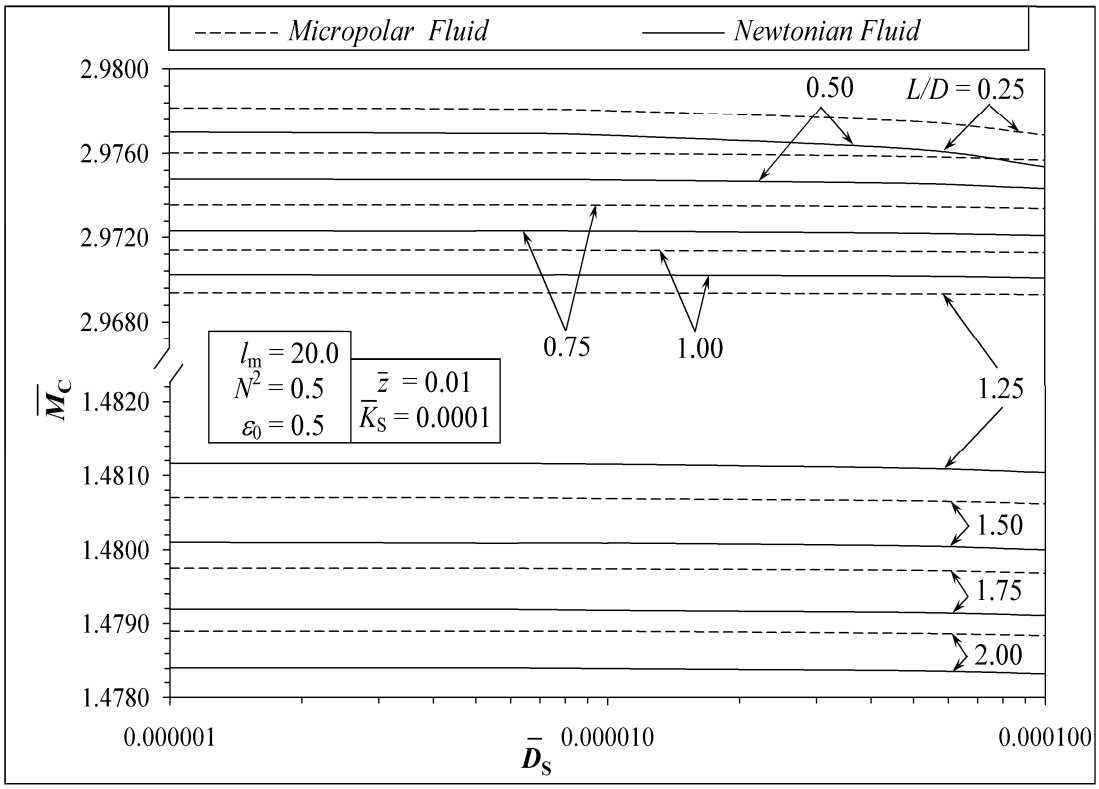

Figure.6.8 (d): Variation of $\overline{M}_C$ with $\overline{D}_S$ for various values of L/D ratio.

6.2.6.5 Critical Mass Parameter $(\overline{M}_C)$ Vs External Stiffness $(\overline{K}_S)$:

Figures 6.9 (a) to 6.9 (c) shows respectively the variation of $\overline{M}_C$ with $(\overline{K}_S)$ for various values of l_m, N^2 and ε_0. It is found from the figure that the maximum value of $\overline{M}_C$ is achieved at l_m =20, that means threshold stability is maximum at characteristics length (l_m =20).It can be found from the *figure 6.9 (a)* that critical mass parameter increases with increase in coupling number. It can be shown in the *figure 6.9 (b)* and *figure 6.9 (c)* that the value of $\overline{M}_C$ is constant at a particular value of external stiffness $(\overline{K}_S)$ after that critical mass parameter is gradually increase with increase in external stiffness. From *fig 6.2.6.5(c)* It can be found that critical mass parameter increases with increase in the value of external stiffness at various values of eccentricity ratio except 0.2 and 0.9. At eccentricity ratio 0.9 no change in the value of $\overline{M}_C$ with increase in $(\overline{K}_S)$ and at eccentricity ratio 0.2 critical mass parameter constant at particular value of $(\overline{K}_S)$ but after certain value of $(\overline{K}_S)$ critical mass parameter increase and then sudden decrease

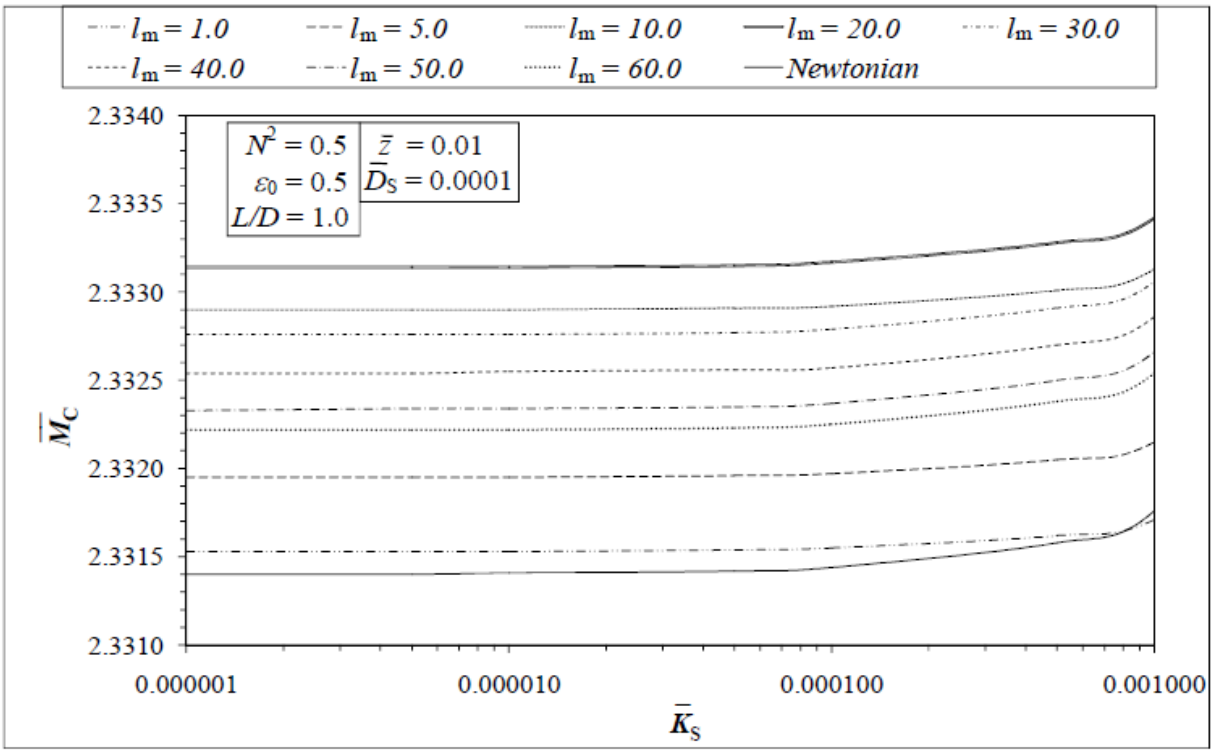

Figure.6.9 (a): Variation of $\overline{M}_C$ with $\overline{K}_S$ for various values of l_m.

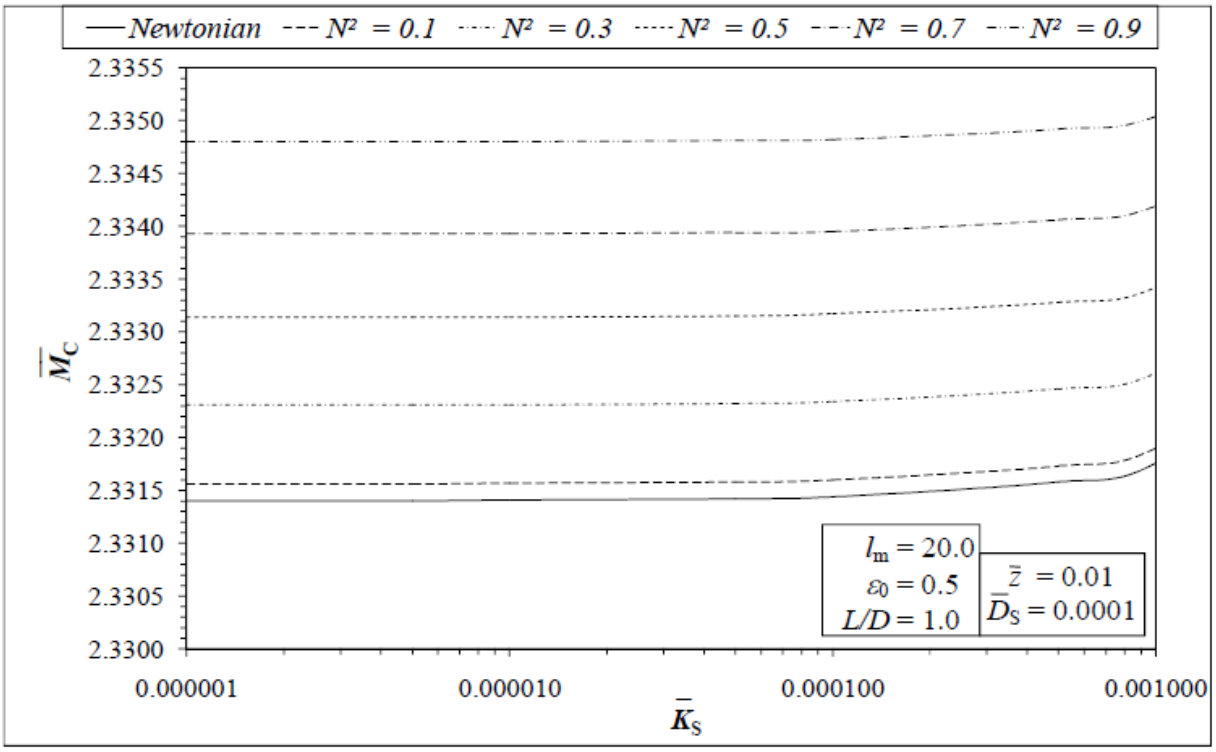

Figure.6.9 (b): Variation of $\overline{M}_C$ with $\overline{K}_S$ for various values of N^2.

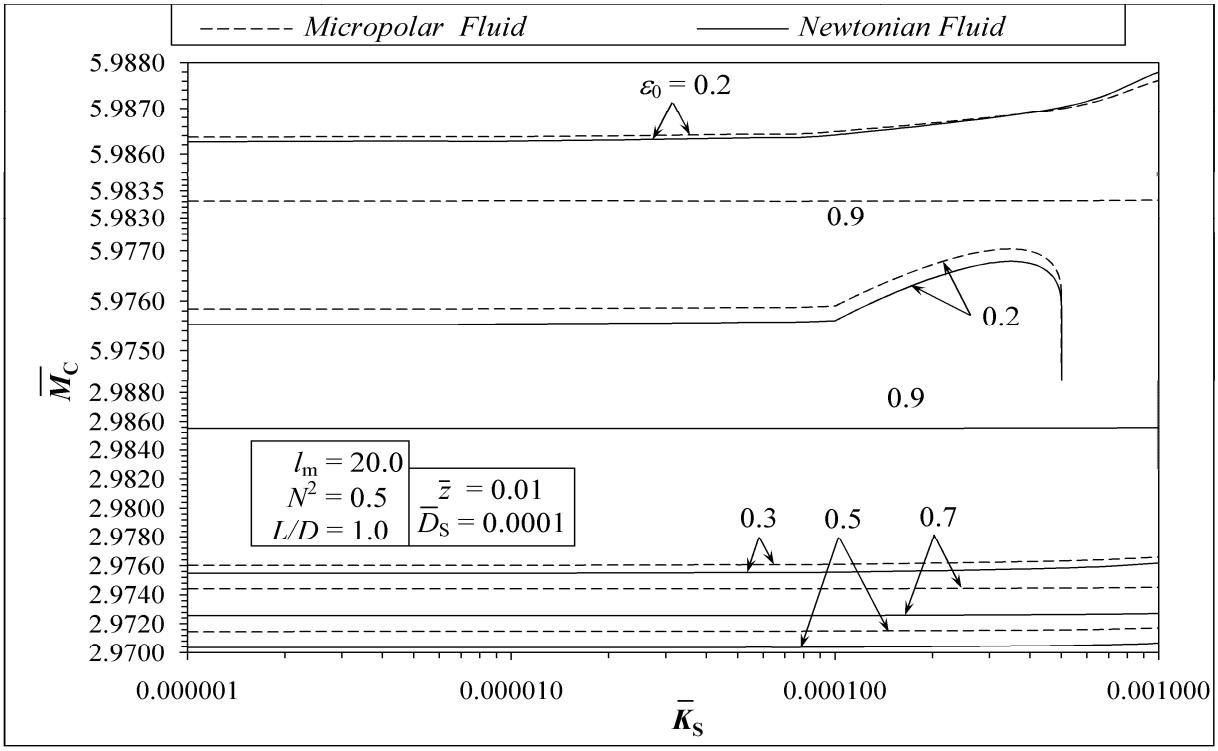

Figure.6.9 (c): Variation of $\overline{M}_C$ with $\overline{K}_S$ for various values of ε_0

CHAPTER 7 CONCLUSIONS AND SCOPE FOR FUTURE WORK

7.1 Conclusions:

In the present dissertation, the steady state and dynamic analysis of finite flexibly supported hydrodynamic journal bearings under micropolar lubrication are studied theoretically various static and dynamic characteristics.

Bearing characteristics have been studied and presented for a wide range of micropolar lubrication parameters as well as bearing parameters, so as to provide a guideline for the design of such bearings. From the studies and the results reported in the previous chapters, the following conclusions may be drawn.

Conclusion of study of steady state characteristics of finite flexibly supported hydrodynamic bearing

1. The steady state pressure increases, as the fluid becomes more and more micropolar.
2. The micropolar effect will be significant either when the characteristic material length is large or the clearance is small.
3. The non-dimensional load carrying capacity increases as the coupling number increases and non-dimensional characteristic length decreases. The load parameter converges to the Newtonian value as $N \rightarrow 0$ and $l_m \rightarrow 0$
4. Load parameter increases in both types of lubrication with the increase in eccentricity ratio and slenderness ratio.
5. The load parameter remains always higher in the micropolar fluid than that in the Newtonian fluid and is markedly pronounced in higher eccentricity ratio as well as in higher *L/D* ratio.
6. At $l_m = 0$, the attitude angle remains the same as that for the Newtonian fluid. The values of the attitude angle decrease as micropolar effect increases. The attitude angle also decreases as eccentricity ratio increases, but increases with *L/D* ratio.
7. Micropolar fluid always is a favourable choice over the Newtonian fluid as the friction parameter decreases with the increase in degree of micropolarity.

Conclusion of study of Dynamic state characteristics of finite flexibly supported hydrodynamic bearing

1. All non-dimensional components of direct and cross stiffness coefficients exhibit the similar relationship with the micropolar parameters as that of dimensionless steady state load.
2. At a certain value of l_m, all dimensionless response coefficients increase as the eccentricity ratio or the slenderness ratio increases when other parameters remain the same.
3. More micropolarity represents more stability in the bearing.
4. Higher eccentricity ratio favors the bearing towards higher stability.
5. The critical mass parameter increases as *N* is increased. Moreover, at any particular value of *N*, stability improves initially as l_m is increased, reaches a maximum to that for Newtonian fluid at large value of l_m.
6. The load carrying capacity increase in the micropolar fluid than in the Newtonian fluid
7. However a finite bearing with slenderness ratio around 1.0 is always preferable over the short or long bearing.
8. The values of the whirl ratio always remain around 0.5 and *L/D* = 1.0, ε_o = 0.5, $\overline{D}_S = 0.0001$, $\overline{K}_S = 0.0001$ and $\overline{Z} = 0.01$
9. Threshold stability is maximum at characteristics length (l_m =20).

7.2 Scope for Future Work:

Following are some suggested areas, which are related to the present work and deserve to be explored:

1. Theoretical and experimental study of journal bearing lubricated with micropolar fluid and considering the elastic deformation of the bearing liners.
2. The present work is purely a theoretical work on the static and dynamic characteristics of flexibly supported finite hydrodynamic journal bearings which is lubricated with micropolar fluids and these theoretical results could not be compared with the experimental data as there were no facilities of the kind required for conducting such an experimental to collect the data. So, there is a great scope for comparison of the present study of the bearings with the test results, if done carefully.
3. A non linear transient analysis of the same problem could be of more use and this will indicate that the actual growth of orbit and also the limit cycles for hydrodynamic bearing lubricated with micropolar fluid.
4. Thermodynamic analysis of the journal bearing system lubricated with micropolar fluids.

5. Analysis of different shaped bearings on flexibly support could be done and compared with the present results.

Only a selected set of variables have been considered in analyzing different parameters for time shortage. So, there is ample scope for similar analysis of the bearings considering wider range of variables.

REFERENCES

SR.N0. JOURNALS

1. **I. Newton,** "Mathematical Principles", London, 1668, Cajori's revision of Motle's translation,Univ. of California Press, 1946.

2. **N. Petroff,** "Friction in Machines and the Effect of Lubrication" (In Russian) Engng. J. St.Petersburg, Nos. 1,2,3,4, pp.71,228,377,530, 1883.

3. **B. Tower,** "First Report on Friction Experiments", Proc. Inst. Mech. Engrs., London, Vol.34,Nov., pp.632-666, 1883; "Second Report on Friction Experiments", Proc. Inst. Mech. Engrs. London, Vol.36, pp.58-70, 1885; "Third Report on Friction Experiments", Proc. Inst. Mech. Engrs., London, pp.173-205, 1888; "Fourth Report on Friction Experiments", Proc. Inst. Mech. Engrs., London, pp.111-140, 1891.

4. **O. Reynolds,** "On the Theory of Lubrication and Its Application to Mr. Beuchamp Tower'sExperiments, including An Experimental Determination of the Viscosity of Olive Oil", Phil.Trans. Roy. Soc., London, Vol.177, Pt.1, pp. 157-234, 1886.

5. **A. Kingsbury,** "Experiments with an Air Lubricated Journal", J. American Soc. Naval Engrs.,Vol.9, pp.267-292, 1897.

6. **A. Sommerfeld,** "Zur Hydrodynamischen Theorie der Schmiermittelneibung" Z. Maths. u.Physik, Vol.50, pp.97-155, 1904.

7. **W.J. Harrison,** "The Hydrodynamical Theory of Lubrication with Special Reference to Air as a Lubricant", Trans. Cambridge. Phil. Soc., Vol.22, No.III, pp.39-54, 1913.

8. **L. Rayleigh,** "Notes on the Theory of Lubrication", Phil. Mag., Vol.35, No.1, pp.1-12, 1918.

9. **D.G. Christopherson,** "A New Mathematical Method for the Solution of Film LubricationProblems", Proc. Inst. Mech. Engrs., London, Vol.146, pp.126-135, 1941.

10. **A. Cameron,** and **Mrs. L. Wood,** "The Full Journal Bearing", Proc. Inst. Mech. Engrs.,London, Vol.161, pp.59-64, 1949.

11. **G. Vogelpohl,** "Zur Integration der Reynoldschen Gleichung fur des Zapfenlager

EndlicherBreite", Ingenieur Archiv., Band.XIV, pp.192-212, 1943.

12. **F.W. Ocvirk,** "Short Bearing Approximation for Full Journal Bearings", NACA TN 2808.

13. **W.J. Harrison, "**The Hydrodynamic Theory of Lubrication of Cylindrical Bearings under variable Load",Trans.Cambridge. Phil.Soc., Vol.22, p.373, 1913.

14. **W. Kahlert,** "Der Einfluss der Tragheitskrafte bei der Hydrodynamischen Schmiermitteltheorie", Ingenieur Archiv., Band XVI, pp.321-342, 1948.

15. **F. Osterle,** and **E. Saibel,** "On the Effect of Lubricant Inertia in Hydrodynamic Lubrication",Z. Maths. u. Physik, Vol.6, pp.334-339, 1955.

16. **J.A. Coles,** and **C.J. Hughes,** "Oil Flow and Film extend in Complete Journal Bearings",Proc. Inst. Mech. Engrs., Vol.170, pp.499-510, 1956.

17. **B. Jacobson,** and **L. Floberg,** "The Finite Journal Bearing considering Vaporization", Trans.Chalmers Univ., Tech. Gothenburg. 189 & 190.

18 **O. Pinkus,** "Solution of Reynolds Equation for Finite Journal Bearings",Trans. ASME, Vol.80, pp.858-864, May 1958.

19 **A.A. Raimondi,** and **J. Boyd,** "A Solution for the Finite Journal Bearing and Its Application to Analysis and Design, I, II and III", Trans. ASLE, Vol.1, No.1, pp.159-209, 1958.

20 **B.C. Majumder,** "Torque of Misaligned Gas-lubricated Porous Journal earings", Wear, Vol.39, pp.55-61, 1976.

21 **O. Pinkus,** and **S.S. Bupara, "**Analysis of Misaligned Grooved Journal Bearings", J. Lub. Technol., Trans. ASME, Vol.101, pp.503-509, Oct. 1979.

22 **S.K. Guha,** "Analysis of Steady-state Characteristics of Misaligned Hydrodynamic Journal" Bearings with Isotropic Roughness Effect", J. Tribol. Int., Vol.33, pp.1-12, 2000.

23 **R. Holmes,** "The Role of Oil-film Bearings in Promoting Shaft Instability and the Remedial Effect of Damping", J. Tribol. Int., pp.243-248.

24 **H. Marsh,** "The Stability of Aerodynamics Gas Bearings". Part 2: Non-circular Bearings. Report for Ministry of Aviation , 1964.

25 **J. Kerr,** "The onset and cessation of Half-speed whirl in Air-lubricated Self Pressurized Journal Bearings". Proc. Inst, Mech. Engrs. Vol.180, Paper Number.221, 1966 (4^{th} Convention of Lubrication and Wear Group).

26 **R. Holmes,** "Instability Phenomenon due to Circular Bearing Oil Films", J.Mech. Engng. Sci.Vol.8, No.4, p.419, 1966.

27 **D.M. Smith,** "Dynamic Characteristics of Turbine Journal Bearings", Proc.Lub. Wear Conv. (Inst. Mech. Engrs., London), p.72, 1963.

28 **A. Akers; S. Michaelson,** and **A. Cameron,** "Stability Contours for a Whirling Finite Journal Bearing", J. Lub. Technol., Trans. ASME, pp.177-189, Jan. 1971.

29 **A. Kingsbury,** "A New Oil Testing Machine and Some of Its Results", Trans. ASME, Vol.24, p.144, 1903.

30 **E. Cosserat,** and **F. Cosserat,** "Théorie des Corps Deformables", Hermann et Fils, Paris, 1909.

31 **G.B. Jeffery,** "The Motion of Ellipsoidal Particles Immersed in A Viscous Fluid", Proc. Roy. Soc., London, Ser. A., Vol.102, pp.171-179, 1922.

32 **W. Hardy,** and **M. Nottage,** "Studies in Adhesion – I", Proc. Roy. Soc., London, Ser. A.,Vol.112, p.64, 1926.

33 **R. Buckley,** "Viscous Flow and Surface Films" U.S. Bureau of Standards Journal of Research, Research Paper No. 264, Vol.6, p.89, 1931.

34 **A. Anzelius,** The Annual of the Univ. of Uppsala, 1931.

35 **S.J. Needs,** "Boundary Film Investigations", Trans. ASME, Vol.62, pp.331-345, 1940.

36 **J.C. Henniker,** "The depth of the Surface Zone of a Liquid", Revs. Modern Physics, Vol.21, pp.322-341, 1949.

37 **G.I. Fuks,** "The Properties of Solutions of Organic Acids in Liquid Hydrocarbons at Solid Surfaces", Research in Surface Forces, ed. B. V. Deryagin, Vol.1, p.79, 1960.

38 **G.I. Fuks,** "The Polymolecular Component of the Lubricating Boundary Layer", ibid, Vol.2, p.159, 1964.

39 **J.W. Hoyt,** and **A.G. Fabula,** "The Effect of Additives on Fluid Friction", U.S. Naval Ordnance Test Station Report, 1964

40 **W.M. Vogel,** and **A.M. Patterson,** "An Experimental Investigation of the Effect of Additives Injected into the Boundary Layer of A Underwater Body", Pacific Naval Lab., Defence Research Board of Canada, Report 64-2.

41 **A. C. Eringen,** "Simple Microfluids", Int. J. Engng. Sci., Vol. 2, pp.205-217, 1964.

42 **A.C. Eringen,** "Mechanics of Micromorphic Materials", Proc. XI, Int. Cong. of Appl. Mech.,Springer-Verlag, 1965.

43 **A.C. Eringen,** "Theory of Micropolar Continua", Dev. in Mech., Vol. 3, pp.23-40, Pt.1, 1965.

44 **A.C. Eringen,** "Linear Theory of Micropolar Elasticity", J. Math. Mech., Vol.15, No.1, pp.909-923, 1965.

45 **A.C. Eringen,** "Theory of Micropolar Fluids", J. Math. Mech., Vol.16, No.1, pp.1-18, 1966.

46 **T. Ariman,** and **A.S. Cakmak,** "Couple Stresses in Fluids", J. Phy. Fluids, Vol.10, No.11, pp.2497-2499, Nov. 1967.

47 **S.J. Allen,** and **K.A. Kline,** "Lubrication Theory for Micropolar Fluids", J .Appl. Mech., Trans. ASME, Ser.E, Vol.38, No.3, pp.646-650, Sept. 1971.

48 **A.B. Datta,** "Pivoted Slider Bearing with Convex Pad Surface in Micropolar Fluid", Jap. J Appl. Phys., Vol.11, No.1, pp.98-102, Jan. 1972.

49 **V.K. Agrawal; K.L. Ganju,** and **S.C. Jethi,** "Squeeze Film and Externally Pressurized Bearings Micropolar Fluid Lubricated", Wear, Vol.19, pp.259-265, 1972.

50 **M. Balaram,** "Micropolar Squeeze Films", J. Lub. Technol., Trans. ASME, pp.635-637, Oct. 1975.

51 **J. Prakash,** and **H. Christensen,** "Rheological Anomalies in Thin Hydrodynamic Films — A Microcontinuum View", Symposium on Lubricant Properties in Thin Lubricating Films, American Chem. Soc., NY Meet., pp.79-90, Apr. 4-9, 1976.

52 **J. Prakash,** and **P. Sinha,** "Lubrication Theory for Micropolar Fluids and Its Application to a Journal Bearing", Int. J. Engng. Sci., Vol.13, pp.217-232, 1975.

53 **J. Prakash,** and **P. Sinha,** "Squeeze Film Theory for Micropolar Fluids", Trans. ASME, Lub. Div., Joint Fluids Engng. and Lub. Conf., May 5-7, 1975, Minneapolis, Minn., Paper No.75- LubS-5, May 5-7, 1975, J. Lub. Technol. Trans. ASME, Vol.98, pp.139, 1976.

54 **J. Prakash,** and **P. Sinha,** "A Study of Squeezing Flow in Micropolar Fluid Lubricated Journal Bearings", Wear, Vol.38, pp.17-28, 1976.

55 **J. Prakash,** and **P. Sinha,** "Cyclic Squeeze Films in Micropolar Fluid Lubricated Journal Bearings", J. Lub. Technol., Trans. ASME, 76-Lub-E, 1975.

56 **Kh. Zaheeruddin,** and **Md. Isa,** "Micropolar Fluid Lubrication of One-Dimensional Journal Bearings", Wear, Vol.50, pp.211-220, 1978.

57 **N. Tipei,** "Lubrication with Micropolar Liquids and Its Application to Short Bearings", J. Lub.Technol., Trans. ASME, Vol.101, pp.356-363, Jul. 1979.

58 **Kh. Zaheeruddin,** "The Dynamic Behavior of Squeeze Films in One-Dimensional

Porous Journal Bearings Lubricated by a Micropolar Fluid", Wear, Vol.71, pp.139-152, 1981.

59 **C. Singh,** and **P. Sinha,** "The Three-Dimensional Reynolds Equation for Micropolar Fluid Lubricated Bearings", Wear, Vol.76, No.2, pp.199-209, 1982.

60 **T-W. Huang; C-I Weng,** and **C-K. Chen,** "Analysis of Finite Width Journal Bearings with Micropolar Fluids", Wear, Vol.123, pp.1-12, 1988.

61 **M.M. Khonsari,** and **D.E. Brewe,** "On the Performance of Finite Journal Bearings Lubricated with Micropolar Fluids", STLE, Tribology Trans., Vol.32, No.2, pp.155-160, 1989.

62 **T-W. Huang,** and **C-I. Weng,** "Dynamic Characteristics of Finite-Width Journal Bearings with Micropolar Fluids",Wear,Vol.141, No.1, pp.23-33, 1990.

63 **P. Chaturani,** and **S. Narasimman,** "Numerical Solution of a Micropolar Fluid Flow between Two Rotating Coaxial Disks", Acta Mech., Vol.89, No.1-4, pp.133-145, 1991.

64 **Qiu and Zhang** "Lubrication Theory for Micropolar Fluids and Its Application to a Journal Bearing With Finite Length"

65 **D.A. Boffey,** "The stability of a rigid rotor in a flexibility supported Self-acting Gas Journal Bearings". Univ. Southampton , Gas Bearing Symposium, Paper No.12, 1-15, April 1969.

66 **V. Castelli; C.H. Stevenson,** and **E.J. Gunter,** "Steady-state Characteristics of GaslubricatedSelf-acting Partial-arc Journal Bearings of Finite Width", Trans. ASLE, Vol.7, pp.153-167, 1964.

67 **A.K. Chattopadhyay, S. Karmakar, in 1997** "Non linear analysis of flexibly supported finite turbolent flow oil journal bearings", Applied mechanics and engineering , vol.2, No.4, 557-568.

68 **S. Das, S.K. Guha, and A.K. Chattopadhyay,** "Theoretical analysis of stability characteristic of hydrodynamic journal bearings lubricated with micropolar fluid" Proc. Instn Mech. Engrs., Part J:J.Engineering Tribology, 218,45-56, 2004.

Bibliography:

69 **O. Pinkus,** and **B. Sternlicht,** "Theory of Hydrodynamic Lubrication", *McGraw Hill, NY,1961*

70 **N. Tipei,** "Theory of Lubrication", *Stanford Univ. Press, Stanford, 1962.*

Appendix-1

Appendix-I Computer Listing for Dynamic Analysis Using Perturbation Technique for Aligned Hydrodynamic Journal Bearings Lubricated With Micropolar Fluids

```
C
      DOUBLE COMPLEX P1(55,15),P2(55,15),TERM11
            DOUBLE COMPLEX TERM21,SPO1,SPO2,SPN1,SPN2
            DOUBLE COMPLEX AM11,AM12,AM21,AM22,F11(55),F12(55),F21(55),F22(55)
            DOUBLE COMPLEX CA15,CA25,WDX1,WDY1,WDX2,WDY2,DEV1,DEV2
            INTEGER PRECAV
            DOUBLE PRECISION REAL LM,LM2,LR,LR2,MP,LR2NEW,MPNEW,MPINCR,L2INCR
            DOUBLE PRECISION REAL PHI,KS,ERR1,ERR2
            DIMENSION P(55,20),PP1(55),PP2(55),THETA(55),HH0(55),RLD(5)
      DIMENSION RLM(10),RDS(10),RKS(10),RZ(10),CC1(55),CC2(55),CC3(55)
            OPEN(7,FILE='VALZ.DAT')
            OPEN(6,FILE='VALKS.DAT')
            OPEN(5,FILE='VALDS.DAT')
            OPEN(4,FILE='DATA.DAT')
            OPEN(3,FILE='RESULT.DAT')
            OPEN(2,FILE='VALR.DAT')
            OPEN(1,FILE='VALLM.DAT')
C
            PI=4.0*ATAN(1.0)
            WRITE(*,*)'IPT = ? (=44), JPT = ? (=12)'
            READ(*,*)IPT,JPT
C           WRITE(*,*)'GIVE VALUES FOR: LR (=WHIRL RATIO) (Given as 1.0)'
C           READ(*,*)LR
C           WRITE(*,*)'MICROPOLAR CHARACTERISITCS LM, AN2 (=N2)'
C           READ(*,*)LM,AN2
C           WRITE(*,*)'GIVE VALUES FOR: EPH0'
C           READ(*,*)EPH0
C           WRITE(*,*)'MICROPOLAR CHARACTERISITCS AN2 (=N2)'
C           READ(*,*)AN2
C           WRITE(*,*)'GIVE VALUES FOR: R (=SLENDERNESS RATIO)'
C           READ(*,*)R
C           WRITE(*,1000)
C1000    FORMAT('FOR SUPPORT: STIFFNESS COEFFICIENT, KS = ?'/13X,
C     #'DAMPING COEFFICIENT, DS = ?')
C           READ(*,*)KS,DS
C           WRITE(*,*)'MASS RATIO = ?'
```

```
C       READ(*,*)Z
        WRITE(*,*)'GIVE VALUE FOR: ORF (1.03/1.05)'
        READ(*,*)ORF
C
        KNT=1
        AN2=0.5
        READ(1,*)(RLM(ILM),ILM=1,8)
        READ(2,*)(RLD(IR),IR=1,5)
        READ(5,*)(RDS(IDS),IDS=1,6)
        READ(6,*)(RKS(IKS),IKS=1,6)
        READ(7,*)(RZ(IZ),IZ=1,5)
570     IF(AN2.GT.0.5) GOTO 180
        ILM=1
550     IF(ILM.GT.8) GOTO 560
        LM=RLM(ILM)
        WRITE(3,1510)LM,AN2
1510  FORMAT(5X,/'MICROPOLAR FLUID CHARACTERISTICS:'/5X,'NON-DIMENSIONAL
   # CHARACTERISTICS LENGTH, LM =',F10.3,3X,'COUPLING NUMBER, N² =',
   #F10.3/)
C
        LR=1.0
        MP=1.0
        IZ=1
        Z=RZ(IZ)
530     IF(IZ.GT.1) GOTO 540
        IKS=1
        KS=RKS(IKS)
510     IF(IKS.GT.1) GOTO 520
        IDS=1
490     IF(IDS.GT.1) GOTO 500
        DS=RDS(IDS)
        IR=1
470     IF(IR.GT.1) GOTO 480
        R=RLD(IR)
        EPH0=0.1
C
        WRITE(3,1520)DS,KS,Z
1520  FORMAT(5X,'EXTERNAL SUPPORT CHARACTERISTICS :'/5X,'NON-DIMENSIONAL
   # DAMPING COEFF. DS =',F10.5/5X,'NON-DIMENSIONAL STIFFNESS COEFF.
   #KS =',F10.5/5X,'MASS RATIO, Z =',F10.3/)
```

```
C
      WRITE(3,1530)LR,MP
1530  FORMAT(5X,'LR =',F7.4,5X,'MP =',F7.4/)
      WRITE(3,1010)
1010  FORMAT(3X,'L/D',2X,'EPH0',1X,'ITER',6X,'SS LOAD',6X,'ATT ANGLE',
     #3X,'IP1',1X,'IP2',8X,'SRR',11X,'SPR',11X,'DRR',11X,'DPR',11X,
     #'SRP',11X,'SPP',11X,'DRP',11X,'DPP',4X,'STABILITY',4X,'WH RATIO',
     #7X,'MASS PARA',13X,'SN'/)
450   IF (EPH0.GE.1.0) GOTO 460
C
      WRITE(*,1220)KNT,LR,LM,AN2,R,EPH0
1220  FORMAT(/4X,'KNT=',I8,4X,'LR=',F4.2,3X,'LM=',F7.2,3X,
     #'AN2=',F6.3,3X,'R=',F3.1,3X,'EPH0=',F5.2)
C
     I5=IPT+2
      I6=I5+1
      I4=I5-1
      I3=I4-1
      I2=I3-1
      J5=JPT+2
      J6=J5+1
      J4=J5-1
      J3=J4-1
      J2=J3-1
      AI3=I3
      AJ3=J3
C
      DELTH=2.0*PI/AI3
      DELZ=1.0/AJ3
      DELTH2=DELTH*DELTH
      DELZ2=DELZ*DELZ
      DELR2=DELTH2/DELZ2
C
      RR=1.0/R
      RR2=RR*RR
      LM2=LM*LM
      AN=SQRT(AN2)
      AN3=AN2*AN
      DENO=2.*(1.0+RR2*DELR2)
C
```

```
      ITER=1
      SPO=0.
      SPO1=CMPLX(0.,0.)
      SPO2=CMPLX(0.,0.)
C
C     CALCULATION OF FILM THICKNESS AND THE FUNTIONS F1=COTH(N*LM*H0/2)
C     AND F2={COSECH(N*LM*H0/2)}^2
C
    DO 10 I=2,I5
      AI=I-2
      THETAI=AI*DELTH
      THETA(I)=THETAI
      H0=1.0+EPH0*COS(THETAI)
      HH0(I)=H0
      A=0.5*AN*LM*H0
      TANHA=TANH(A)
      COTHA=1.0/TANHA
      SINHA=SINH(A)
      CSCHA=1.0/SINHA
      CSCHA2=CSCHA*CSCHA
      H02=H0*H0
      H03=H02*H0
      CC1(I)=H02/4.+1./LM2-AN*H0*COTHA/LM+AN2*H02*CSCHA2/4.
      CC2(I)=H03/12.+H0/LM2-0.5*AN*H02*COTHA/LM
      CC3(I)=H0/2.+AN2*H0*CSCHA2-AN*COTHA/LM-AN3*LM*H02*CSCHA2*COTHA/4.
10    CONTINUE
C
C     INITIALISATION OF PRESSURE
C
      DO 20 I=1,I6
      DO 20 J=1,J6
      P(I,J)=0.0
      P1(I,J)=CMPLX(0.,0.)
      P2(I,J)=CMPLX(0.,0.)
20    CONTINUE
C
C     SETTING OF BOUNDARY CONDITIONS
C
70    DO 30 I=2,I5
      P(I,J5)=0.0
```

```
      P(I,1)=P(I,3)
30    CONTINUE
C
C     SOLUTION OF REYNOLDS' EQUATION
C
      DO 40 J=2,J4
      DO 40 I=2,I5
      THETAI=THETA(I)
C
      CC1I=CC1(I)
      CC2I=CC2(I)
      CC3I=CC3(I)
      CA=0.5*CC1I*EPH0*DELTH*SIN(THETAI)/CC2I
      CA1=(1.0-CA)/DENO
      CA2=(1.0+CA)/DENO
      CA3=RR2*DELR2/DENO
      CA4=CA3
      CA5=0.5*EPH0*DELTH2*SIN(THETAI)/(CC2I*DENO)
      TERM=CA1*P(I+1,J)+CA2*P(I-1,J)+CA3*P(I,J+1)+CA4*P(I,J-1)+CA5
      ERR=TERM-P(I,J)
C
      P(I,J)=P(I,J)+ORF*ERR
      IF(P(I,J).LT.0.0) P(I,J)=0.0
      IF(I.EQ.I5) THEN
      P(I5,J)=P(2,J)
            ELSEIF(I.EQ.I4) THEN
            P(1,J)=P(I4,J)
                  ELSE
                  GOTO 40
      ENDIF
40    CONTINUE
C
C     TEST FOR CONVERGENCE
C
      SPN=0.0
      DO 50 J=2,J5
      DO 50 I=2,I5
      SPN=SPN+P(I,J)
50    CONTINUE
      ERR=1.0-SPO/SPN
```

```
      IF(ABS(ERR).LE.0.001.OR.ITER.GE.1000) GOTO 60
      ITER=ITER+1
      SPO=SPN
      GOTO 70
60    IF(ITER.GE.1000) THEN
      GOTO 80
            ELSE
            GOTO 90
      ENDIF
80    WRITE(*,*)'GIVE NEW VALUE FOR: ORF test1'
      READ(*,*)ORF
      ITER=1
      GOTO 70
C
C     TEST FOR CAVITATION
C
90    I=5
130   IF(P(I,2))100,100,110
110   IF(I.EQ.I5) GOTO 120
      I=I+1
      GOTO 130
120   WRITE(*,*)'NO CAVITATION IN THE BEARING'
100   NCAVI=I
      PRECAV=NCAVI-1
      THETA0=(NCAVI-2)*360.0/AI3
C
C     EVALUATION OF LOAD AND ATTITUDE ANGLE
C
      DO 140 J=2,J4
      PP1(J)=0.0
      PP2(J)=0.0
      DO 140 I=2,PRECAV,2
      IF(I.EQ.PRECAV) GOTO 150
      AI=I-2
      TH1=AI*DELTH
      TH2=TH1+DELTH
      TH3=TH2+DELTH
      TERM1=P(I,J)*COS(TH1)+4.*P(I+1,J)*COS(TH2)+P(I+2,J)*COS(TH3)
      TERM2=P(I,J)*SIN(TH1)+4.*P(I+1,J)*SIN(TH2)+P(I+2,J)*SIN(TH3)
      PP1(J)=PP1(J)+TERM1*DELTH/3.
```

```
      PP2(J)=PP2(J)+TERM2*DELTH/3.
      GOTO 140
150   M=PRECAV-1
      AI=M-2
      TH1=AI*DELTH
      TH2=TH1+DELTH
      TH3=TH2+DELTH
      TERM1=-P(M,J)*COS(TH1)+8.*P(M+1,J)*COS(TH2)+5.*P(M+2,J)*COS(TH3)
      TERM2=-P(M,J)*SIN(TH1)+8.*P(M+1,J)*SIN(TH2)+5.*P(M+2,J)*SIN(TH3)
      PP1(J)=PP1(J)+TERM1*DELTH/12.
      PP2(J)=PP2(J)+TERM2*DELTH/12.
140   CONTINUE
C
      WX=0.0
      WY=0.0
      DO 160 J=2,J4,2
      IF(J.EQ.J4) GOTO 170
      TERM1=PP1(J)+4.*PP1(J+1)+PP1(J+2)
      TERM2=PP2(J)+4.*PP2(J+1)+PP2(J+2)
      WX=WX+TERM1*DELZ/3.
      WY=WY+TERM2*DELZ/3.
      GOTO 160
170   M1=J4-1
      TERM1=-PP1(M1)+8.*PP1(M1+1)+5.*PP1(M1+2)
      TERM2=-PP2(M1)+8.*PP2(M1+1)+5.*PP2(M1+2)
      WX=WX+TERM1*DELZ/12.
      WY=WY+TERM2*DELZ/12.
160   CONTINUE
      W=2*SQRT(WX*WX+WY*WY)
      ATTRAD=ATAN(-WY/WX)
      ATT=ATTRAD*180./PI
      SN=1./(PI*W)
      PHI=ATTRAD
C
      NOPT=2
      IF(NOPT-2)180,190,80
190   ITERP1=1
C
240   DO 200 I=1,I6
      P1(I,1)=P1(I,3)
```

```
200     CONTINUE
C
        DO 210 J=2,J4
        DO 210 I=2,PRECAV
        THETAI=THETA(I)
        CC1I=CC1(I)
        CC2I=CC2(I)
        CC3I=CC3(I)
C
C   CALCULATION OF THE COEFFICIENTS RELATED WITH THE EXPRESSION OF
C   THE PERTURBED FILM PRESSURE, P1
C
        CAA=(COS(THETAI)-0.5*DELTH*SIN(THETAI))*CC1I/CC2I
        CAB=(COS(THETAI)+0.5*DELTH*SIN(THETAI))*CC1I/CC2I
        CAC=0.5*CC3I*EPH0*DELTH*SIN(THETAI)*COS(THETAI)/CC2I
        CAD=0.5*DELTH2/(CC2I*DENO)
        CA=0.5*CC1I*EPH0*DELTH*SIN(THETAI)/CC2I
        CA6=(1.0-CA)/DENO
        CA7=(1.0+CA)/DENO
        CA8=RR2*DELR2/DENO
        CA9=CA8
        CA10=-CC1I*COS(THETAI)/CC2I
        CA11=(CAA-CAC)/DENO
        CA12=(CAB+CAC)/DENO
        CA13=CC1I*RR2*DELR2*COS(THETAI)/(DENO*CC2I)
        CA14=CA13
        CA15A=SIN(THETAI)
        CA15B=-2.*LR*COS(THETAI)
        CA15=CAD*CMPLX(CA15A,CA15B)
C
C   CALCULATION OF PERTURBED FILM PRESSURE, P1
C
        TERM11=CA6*P1(I+1,J)+CA7*P1(I-1,J)+CA8*P1(I,J+1)+CA9*P1(I,J-1)+
   #CA10*P(I,J)+CA11*P(I+1,J)+CA12*P(I-1,J)+CA13*P(I,J+1)+CA14*
   #P(I,J-1)+CA15
        DEV1=TERM11-P1(I,J)
        P1(I,J)=P1(I,J)+ORF*DEV1
        IF(I.EQ.2) THEN
        P1(I5,J)=P1(2,J)
                ELSEIF(I.EQ.I4) THEN
```

```
                P1(1,J)=P1(I4,J)
                    ELSE
                    GOTO 210
        ENDIF
210     CONTINUE
C
C       TEST FOR CONVERGENCE OF P1
C
        SPN1=CMPLX(0.,0.)
        DO 220 J=2,J4
        DO 220 I=2,NCAVI
        SPN1=SPN1+P1(I,J)
220     CONTINUE
        DEV1=1.-SPO1/SPN1
        IF((CDABS(DEV1).LE.0.001).OR.ITERP1.GE.250) GO TO 230
        ITERP1=ITERP1+1
        SPO1=SPN1
        GOTO 240
230     IF(ITERP1.GE.250) THEN
        GOTO 80
                ELSE
                GOTO 245
        ENDIF
245     ITERP2=1
250     DO 260 I=1,I6
        P2(I,1)=P2(I,3)
260     CONTINUE
C
        DO 270 J=2,J4
        DO 270 I=2,PRECAV
        THETAI=THETA(I)
        CC1I=CC1(I)
        CC2I=CC2(I)
        CC3I=CC3(I)
C
C    CALCULATION OF THE COEFFICIENTS RELATED WITH THE EXPRESSION OF
C    THE PERTURBED FILM PRESSURE, P2
C
    CBA=(SIN(THETAI)+0.5*DELTH*COS(THETAI))*CC1I/CC2I
        CBB=(SIN(THETAI)-0.5*DELTH*COS(THETAI))*CC1I/CC2I
```

```
      CBC=0.5*CC3I*EPH0*DELTH*SIN(THETAI)*SIN(THETAI)/CC2I
      CBD=-0.5*DELTH2/(CC2I*DENO)
      CA=0.5*CC1I*EPH0*DELTH*SIN(THETAI)/CC2I
      CA16=(1.0-CA)/DENO
      CA17=(1.0+CA)/DENO
      CA18=RR2*DELR2/DENO
      CA19=CA18
      CA20=-CC1I*SIN(THETAI)/CC2I
      CA21=(CBA-CBC)/DENO
      CA22=(CBB+CBC)/DENO
      CA23=CC1I*RR2*DELR2*SIN(THETAI)/(DENO*CC2I)
      CA24=CA23
      CA25A=COS(THETAI)
      CA25B=4.*LR*SIN(THETAI)
      CA25=CBD*CMPLX(CA25A,CA25B)
C
C    CALCULATION OF PERTURBED FILM PRESSURE, P2
C
      TERM21=CA16*P2(I+1,J)+CA17*P2(I-1,J)+CA18*P2(I,J+1)+CA19*P2(I,J-1)
     #+CA20*P(I,J)+CA21*P(I+1,J)+CA22*P(I-1,J)+CA23*P(I,J+1)+CA24*
     #P(I,J-1)+CA25
      DEV2=TERM21-P2(I,J)
      P2(I,J)=P2(I,J)+ORF*DEV2
      IF(I.EQ.2) THEN
      P2(I5,J)=P2(2,J)
            ELSEIF(I.EQ.I4) THEN
            P2(1,J)=P2(I4,J)
                  ELSE
                  GOTO 270
      ENDIF
270   CONTINUE
C
C     TEST FOR CONVERGENCE OF P2
C
      SPN2=CMPLX(0.,0.)
      DO 280 J=2,J4
      DO 280 I=2,NCAVI
      SPN2=SPN2+P2(I,J)
280   CONTINUE
      DEV2=1.-SPO2/SPN2
```

```
      IF((CDABS(DEV2).LE.0.001).OR.ITERP2.GE.250) GO TO 290
      ITERP2=ITERP2+1
      SPO2=SPN2
      GOTO 250
290   IF(ITERP2.GE.250) THEN
      GOTO 80
            ELSE
            GOTO 300
      ENDIF
C
C     EVALUATION OF STIFFNESS
C
300   DO 310 J=2,J6
      F11(J)=CMPLX(0.,0.)
      F12(J)=CMPLX(0.,0.)
      F21(J)=CMPLX(0.,0.)
      F22(J)=CMPLX(0.,0.)
      IF(NCAVI.EQ.I5) THEN
      NMOD=I3
            ELSE
            NMOD=PRECAV
      ENDIF
      DO 310 I=2,NMOD,2
      IF(I.EQ.PRECAV) GOTO 320
      AI=I
      TH1=(AI-2.0)*DELTH
      TH2=TH1+DELTH
      TH3=TH2+DELTH
C
      AM11=P1(I,J)*COS(TH1)+4.*P1(I+1,J)*COS(TH2)+P1(I+2,J)*COS(TH3)
      AM12=P1(I,J)*SIN(TH1)+4.*P1(I+1,J)*SIN(TH2)+P1(I+2,J)*SIN(TH3)
      F11(J)=F11(J)+AM11*DELTH/3.0
      F12(J)=F12(J)+AM12*DELTH/3.0
C
   AM21=P2(I,J)*COS(TH1)+4.*P2(I+1,J)*COS(TH2)+P2(I+2,J)*COS(TH3)
      AM22=P2(I,J)*SIN(TH1)+4.*P2(I+1,J)*SIN(TH2)+P2(I+2,J)*SIN(TH3)
      F21(J)=F21(J)+AM21*DELTH/3.0
      F22(J)=F22(J)+AM22*DELTH/3.0
      GOTO 310
C
```

```
320     M=PRECAV-1
        AI=M-2
        TH1=AI*DELTH
        TH2=TH1+DELTH
        TH3=TH2+DELTH
C
        AM11=-P1(M,J)*COS(TH1)+8.*P1(M+1,J)*COS(TH2)+5.*P1(M+2,J)*COS(TH3)
        AM12=-P1(M,J)*SIN(TH1)+8.*P1(M+1,J)*SIN(TH2)+5.*P1(M+2,J)*SIN(TH3)
        F11(J)=F11(J)+AM11*DELTH/12.
        F12(J)=F12(J)+AM12*DELTH/12.
C
        AM21=-P2(M,J)*COS(TH1)+8.*P2(M+1,J)*COS(TH2)+5.*P2(M+2,J)*COS(TH3)
        AM22=-P2(M,J)*SIN(TH1)+8.*P2(M+1,J)*SIN(TH2)+5.*P2(M+2,J)*SIN(TH3)
        F21(J)=F21(J)+AM21*DELTH/12.
        F22(J)=F22(J)+AM22*DELTH/12.
310     CONTINUE
C
        WDX1=CMPLX(0.,0.)
        WDY1=CMPLX(0.,0.)
        WDX2=CMPLX(0.,0.)
        WDY2=CMPLX(0.,0.)
C
        DO 330 J=2,J4,2
        IF(J.EQ.J4) GOTO 340
        AM11=F11(J)+4.*F11(J+1)+F11(J+2)
        AM12=F12(J)+4.*F12(J+1)+F12(J+2)
        WDX1=WDX1+AM11*DELZ/3.0
        WDY1=WDY1+AM12*DELZ/3.0
C
        AM21=F21(J)+4.*F21(J+1)+F21(J+2)
        AM22=F22(J)+4.*F22(J+1)+F22(J+2)
        WDX2=WDX2+AM21*DELZ/3.0
        WDY2=WDY2+AM22*DELZ/3.0
        GOTO 330
C
340     M1=J4-1
        AM11=-F11(M1)+8.*F11(M1+1)+5.*F11(M1+2)
        AM12=-F12(M1)+8.*F12(M1+1)+5.*F12(M1+2)
        WDX1=WDX1+AM11*DELZ/12.0
        WDY1=WDY1+AM12*DELZ/12.0
```

```
C
      AM21=-F21(M1)+8.*F21(M1+1)+5.*F21(M1+2)
      AM22=-F22(M1)+8.*F22(M1+1)+5.*F22(M1+2)
      WDX2=WDX2+AM21*DELZ/12.0
      WDY2=WDY2+AM22*DELZ/12.0
330   CONTINUE
C
C     TOTAL DYNAMIC LOAD FOR PERTURBED PRESSURES P1 AND P2
C
      WDX1=2.*WDX1
      WDY1=2.*WDY1
      WDX2=2.*WDX2
      WDY2=2.*WDY2
C
C   STIFFNESS AND DAMPING COEFFICIENTS FOR THE PERTURBED FILM
C   PRESSURE, P1
C
      SRR=-2.0*REAL(WDX1)
      SPR=-2.0*REAL(WDY1)
      WDX1A=AIMAG(WDX1)
      WDY1A=AIMAG(WDY1)
      DRR=-2.0*WDX1A/LR
      DPR=-2.0*WDY1A/LR
C
C   STIFFNESS AND DAMPING COEFFICIENTS FOR THE PERTURBED FILM
C   PRESSURE, P2
C
      SRP=-2.0*REAL(WDX2)
      SPP=-2.0*REAL(WDY2)
      WDX2A=AIMAG(WDX2)
      WDY2A=AIMAG(WDY2)
      DRP=-2.0*WDX2A/LR
      DPP=-2.0*WDY2A/LR
C
C     CALCULATION OF WHIRL RATIO AND CRITICAL MASS PARAMETER
C
350   ITERNR=1
C
C     WRITE(*,*)'TEST 1'
      X=((SRR+SRP*PHI)*DSIN(PHI)+(SPR+SPP*PHI)*DCOS(PHI))*EPH0/KS
```

```
      Y=((SRR+SRP*PHI)*DCOS(PHI)-(SPR+SPP*PHI)*DSIN(PHI))*EPH0/KS
C
      A0=(X*DSIN(PHI)+Y*DCOS(PHI))
      B0=(Y*DSIN(PHI)-X*DCOS(PHI))
C     WRITE(*,*)'TEST 2'
C     WRITE(*,*)'X =',X,' Y =',Y,' A0 =',A0,' B0 =',B0
C
C     COEFFICIENTS OF MBAR IN REAL EQ.: A4 FOR MBAR^4, A3 FOR MBAR^3,
C    A2 FOR MBAR^2, A1 FOR MBAR AND A0 IS CONSTANT
C
      LR2=LR*LR
      C1=SPP+SRR
      C2=SPR+SRP
      C3=DPP+DRR
      C4=DPR+DRP
      C5=SPR*SRP-SPP*SRR
      C6=DPR*DRP-DPP*DRR
      C7=DRP*SPR-DRR*SPP+DPR*SRP-DPP*SRR
360   C8=KS**2-LR2*DS**2
C     WRITE(*,*)'C1 =',C1,' C2 =',C2,' C3 =',C3,' C4 =',C4
C     WRITE(*,*)'C5 =',C5,' C6 =',C6,' C7 =',C7,' C8 =',C8
C
      CRM4=-EPH0*((W*LR2)**4)*(Z**2)
C
      CRM3=((W*LR2)**3)*Z*(A0*KS+EPH0*(C1*(1.+Z)+2.*KS)+W*Z*DCOS(PHI))
C
      CRM2=-((W*LR2)**2)*(EPH0*(-C5+C1*KS+LR2*(C6-C3*DS))*(1.+2.*Z)+
     #((A0*SRR-B0*SPR)*KS+W*Z*(SRR*DCOS(PHI)-SPR*DSIN(PHI)))*(1.+Z)+
     #EPH0*(C8-(Z**2)*(C5-LR2*C6))+A0*(KS**2)+2.*KS*W*Z*DCOS(PHI))
C
      CRM1=-W*LR2*(EPH0*(2.*((C5*KS-LR2*(C6*KS+C7*DS))*(1.+Z)+
     #LR2*C3*DS*KS))-(C1*EPH0+W*DCOS(PHI))*C8+((B0*SPR-A0*SRR)*KS-
     #(B0*DPR-A0*DRR)*LR2*DS)*KS-W*((SRR*KS-LR2*DRR*DS)*DCOS(PHI)-
     #(SPR*KS-LR2*DPR*DS)*DSIN(PHI))*(1.+2.*Z))
C
      CRM0=-2.*LR2*(EPH0*C7+W*(DPR*DSIN(PHI)-DRR*DCOS(PHI)))*DS*KS+
     #(EPH0*(C5-LR2*C6)+W*(SPR*DSIN(PHI)-SRR*DCOS(PHI)))*C8
C
      CIM3=EPH0*((W*LR2)**3)*Z*(C3*(1.+Z)+2.*DS)
C
```

```
      CIM2=((W*LR2)**2)*(EPH0*(C7*(1.+Z)**2-(DS*C1+KS*C3)*(1.+2.*Z))-
     #(A0+2.*EPH0)*DS*KS-KS*(A0*DRR-B0*DPR)*(1.+Z)-2.*W*DS*Z*DCOS(PHI)+
     #W*(DPR*DSIN(PHI)-DRR*DCOS(PHI))*Z*(1.+Z))
C
      CIM1=LR2*W*(2.*EPH0*(-DS*C5-KS*C7+LR2*DS*C6)*(1.+Z)+
     #2.*(EPH0*C1+W*DCOS(PHI))*DS*KS+EPH0*C3*C8+((A0*SRR-B0*SPR)*DS+
     #(A0*DRR-B0*DPR)*KS)*KS+W*((DS*SRR+KS*DRR)*DCOS(PHI)-
     #(DS*SPR+KS*DPR)*DSIN(PHI))*(1.+2.*Z))
C
      CIM0=((EPH0*C7+W*(DPR*DSIN(PHI)-DRR*DCOS(PHI)))*C8+2.*(EPH0*
     #(C5-LR2*C6)+W*(SPR*DSIN(PHI)-SRR*DCOS(PHI)))*DS*KS)
C     WRITE(*,*)'TEST 3'
C     WRITE(*,*)'CRM4 =',CRM4,' CRM3 =',CRM3,' CRM2 =',CRM2,
C    #' CRM1 =',CRM1,' CRM0=',CRM0
C     WRITE(*,*)'CIM4 =',CIM4,' CIM3 =',CIM3,' CIM2 =',CIM2,
C    #' CIM1 =',CIM1,' CIM0=',CIM0

C
C     ********************************************
C     SIMULTANEOUS SOLUTION BY NEWTON RAPHSON-METHOD
C     ********************************************
C
C     WRITE(*,*)'LAMDA,MASS_PARA,'
C     READ(*,*)LR,MP
C
C     COMPUTED VALUES OF REAL PART (FR) AND IMEGINARY PART (FI)
C
      FR=CRM4*MP**4+CRM3*MP**3+CRM2*MP**2+CRM1*MP+CRM0
      FI=(CIM3*MP**3+CIM2*MP**2+CIM1*MP+CIM0)*SQRT(LR2)
C
C     COEFFICIENTS REAL AND IMEGINARY EQ. AFTER PARTIAL DIFFERENTIATION
C     WITH RESPECT TO LR
C
      DLR2DLR=2.*LR
C
      DCRM4DL2=4.*CRM4/LR2
C
      DCRM3DL2=3.*CRM3/LR2
C
      DCRM2DL2=2.*CRM2/LR2-EPH0*((W*LR2)**2)*(C6*(1.+Z)**2-
```

```
     #(C3*(1.+2.*Z)+DS)*DS)
C
          DCRM1DL2=CRM1/LR2-LR2*W*(-2.*EPH0*(C6*KS+C7*DS)*(1.+Z)+
     #(C1*EPH0+W*DCOS(PHI))*DS*DS+(2.*EPH0*C3+A0*DRR-B0*DPR)*DS*KS+
     #W*DS*(DRR*DCOS(PHI)-DPR*DSIN(PHI))*(1.+2.*Z))
C
          DCRM0DL2=-2.*(EPH0*C7+W*(DPR*DSIN(PHI)-DRR*DCOS(PHI)))*DS*KS-
     #EPH0*C6*((KS**2)-LR2*(DS**2))-(EPH0*(C5-LR2*C6)+
     #W*(SPR*DSIN(PHI)-SRR*DCOS(PHI)))*(DS**2)
C
          DCIM3DL2=3.*CIM3/LR2
C
          DCIM2DL2=2.*CIM2/LR2
C
          DCIM1DL2=CIM1/LR2+EPH0*W*LR2*(2.*C6*(1.+Z)-C3*DS)*DS
C
          DCIM0DL2=-(EPH0*C7+W*(DPR*DSIN(PHI)-DRR*DCOS(PHI)))*DS*DS-
     #2.*EPH0*C6*DS*KS
C
C    1st ORDER PARTIAL DERIVATIVES OF FR & FI WITH RESPECT TO MP & LR
C
          DFRDMP=4.*CRM4*MP**3+3.*CRM3*MP**2+2.*CRM2*MP+CRM1
C
          DFRDL2=DCRM4DL2*MP**4+DCRM3DL2*MP**3+DCRM2DL2*MP**2+DCRM1DL2*MP+
     #DCRM0DL2
C
          DFIDMP=3.*CIM3*MP**2+2.*CIM2*MP+CIM1
C
          DFIDL2=FI/(DLR2DLR*SQRT(LR2))+(DCIM3DL2*(MP**3)+DCIM2DL2*(MP**2)+
     #DCIM1DL2*MP+DCIM0DL2)*(SQRT(LR2))
C
C         IF(ITER.NE.1) GO TO 20
C         WRITE(*,*) 'REAL TERM=',FR,'IMAGINARY TERM=',FI
C         WRITE(*,*)'WANT TO FURTHER INITIALIZE? IF YES PRESS 1'
C         READ(*,*) LOGIC
C         IF(LOGIC.EQ.1) GO TO 401
          DEN=(DFIDMP*DFRDL2-DFRDMP*DFIDL2)
          MPINCR=(FR*DFIDL2-FI*DFRDL2)/DEN
          L2INCR=-(FR*DFIDMP-FI*DFRDMP)/DEN
          MPNEW=MP+MPINCR
```

```
      LR2NEW=LR2+L2INCR
C
      ERR1=DABS((MPNEW-MP)/MP)
      ERR2=DABS((LR2NEW-LR2)/LR2)
      IF(((ERR1.GT.1.0E-03).AND.(ERR2.GT.1.0E-03)).OR.
     #(ITERNR.GT.250)) THEN
            IF(ITERNR.GT.1000) THEN
                  WRITE(*,*)'MODIFY THE INITIAL VALUES AS ITER IS >1000'
                  MP=MP+2.0
                  GO TO 350
            ENDIF
            MP=MPNEW
            LR2=LR2NEW
            LR=SQRT(LR2)
            ITERNR=ITERNR+1
            WRITE(*,*)'ITERNR =',ITERNR,' LR2=',LR2,' MP=',MP
            GO TO 360
            ELSE
            MP=MPNEW
            LR2=LR2NEW
            LR=SQRT(LR2)
      ENDIF

      IF(LR2) 370,370,380
370   WRITE(3,1020)R,EPH0,ITER,W,ATT,ITERP1,ITERP2,SRR,SPR,DRR,DPR,SRP,
     #SPP,DRP,DPP
1020  FORMAT(F7.5,1X,F4.2,1X,I4,2X,E13.6,2X,E13.6,1X,I3,1X,I3,1X,E13.6,
     #1X,E13.6,1X,E13.6,1X,E13.6,1X,E13.6,1X,E13.6,1X,E13.6,1X,E13.6,2X,
     #'INFINITE')
      GO TO 390
C
380   LR=SQRT(LR2)
      WRITE(3,1030)R,EPH0,ITER,W,ATT,ITERP1,ITERP2,SRR,SPR,DRR,DPR,SRP,
     #SPP,DRP,DPP,LR,MP,SN
1030  FORMAT(F7.5,1X,F4.2,1X,I4,2X,E13.6,2X,E13.6,1X,I3,1X,I3,1X,E13.6,
     #1X,E13.6,1X,E13.6,1X,E13.6,1X,E13.6,1X,E13.6,1X,E13.6,1X,E13.6,4X,
     #'FINITE',2X,E13.6,3X,E13.6,4X,E13.6)
C
390   KOUNT=3
      IF(KOUNT-2)180,420,430
```

```
C
420     WRITE(*,*)'NEW VALUE OF ORF = test2'
        READ(*,*)ORF
        ITER=1
C
        DO 440 J=1,J6
        DO 440 I=1,I6
        P1(I,J)=CMPLX(0.,0.)
        P2(I,J)=CMPLX(0.,0.)
440     CONTINUE
        SPO1=CMPLX(0.,0.)
        SPO2=CMPLX(0.,0.)
        GO TO 240
C
430     EPH0=EPH0+0.1
        KNT=KNT+1
        GOTO 450
460     IR=IR+1
        GOTO 470
480     IDS=IDS+1
        GOTO 490
500     IKS=IKS+1
        GOTO 510
520     IZ=IZ+1
        GOTO 530
540     ILM=ILM+1
        GOTO 550
560     AN2=AN2+0.2
        GOTO 570
180     WRITE(*,*)'PROGRAM TERMINATED'
        STOP
        END
```